The Thesis Committee for Litan Li
Certifies that this is the approved version of the following thesis:

Experimental Studies on the Use of Chemical Additives for Steam-assisted Gravity Drainage

APPROVED BY
SUPERVISING COMMITTEE:

Quoc P. Nguyen, Supervisor

Matthew T. Balhoff

Experimental Studies on the Use of Chemical Additives for Steam-assisted Gravity Drainage

by

Litan Li

Thesis

Presented to the Faculty of the Graduate School of

The University of Texas at Austin

in Partial Fulfillment

of the Requirements

for the Degree of

Master of Science in Engineering

The University of Texas at Austin

December 2017

Dedication

To all the people who made this work possible.

Acknowledgements

My deep thanks go out to the host of people who have made this journey possible. First, I am very grateful to Dr. Nguyen who gave me an opportunity to engage in this work. I have learned so much from him not only on the technical side, but also and perhaps more importantly from his guidance over the last three years in times of difficulty and in times of success. My thanks go out to Tyler, Vence, Bi, and Sean, whose partnership throughout the course of this project was instrumental. I would like to thank Gary, Glen, and Daryl for their expertise and help. To Jeremy and Emily, thank you for your hard work during your time in the SURI program. I wish you the best and your futures are bright. My gratitude goes out to Dr. Balhoff for reading this work and providing his insights. To my parents and church family who have supported me all along this journey, this work would not have been possible without all of you. Finally, my thanks go out to the Heavenly Father, who became flesh to dwell among us.

Abstract

Experimental Studies on the Use of Chemical Additives for Steam-assisted Gravity Drainage

Litan Li, M.S.E.

The University of Texas at Austin, 2017

Supervisor: Quoc P. Nguyen

Steam-assisted gravity drainage (SAGD) is a mature technique for bitumen recovery from oil sand reservoirs; however, it is an energy intensive process that requires large amounts of steam to heat and mobilize the bitumen. The purpose of this work was to find ways to improve SAGD performance using chemical additives. Key mechanisms were identified, a suite of high-temperature additive characterization tests was developed, and promising additives were tested in porous media. Based on the results, experimenters concluded that oil-water interfacial tension reduction held the most potential for improved recovery. A preliminary field-scale study was attempted using numerical simulation, which showed that wettability alteration and oil-water interfacial tension reduction had a positive impact on SAGD performance.

Table of Contents

List of Tables

List of Figures

Chapter 1 Introduction

This chapter provides relevant background information on steam-assisted gravity drainage and the motivation towards improving the process. The chapter continues by stating the objective of this work and providing a list of components to be executed. Finally, an overview of the remaining chapters is given.

1.1 MOTIVATION

The world's energy demand is steadily rising. The United States Energy Information Administration (EIA) predicts a 37% increase in world energy consumption from 2012 to 2040 based on conservative estimates. Strong economic growth from developing nations, rise in global population, and increases in the standard of living all lead to an increase in energy consumption. Petroleum liquids have been the source of one-third of the world's energy demand since 1990 and has been the largest single source of energy in front of coal power, natural gas, renewable energies, and nuclear power. Forecasts by the EIA show that this trend will continue into the coming decades, with petroleum liquids accounting for 30% of the world's total energy consumption in 2040 (U.S. Energy Information Administration, 2016). As proven reserves are exploited, more attention has been given to unconventional resources. As of 2014, Alberta, Canada has 166 billion barrels of proven bitumen reserves (Alberta Energy Regulator, 2015). Bitumen is a highly viscous hydrocarbon composed of a complex soup of chemical species, including long-chain hydrocarbons, metals, resins, and asphaltenes (Pedersen *et al.*, 2014). Bitumen is produced from oil sands through surface mining and *in-situ* thermal methods. Surface mining, performed on a large scale in Alberta, targets shallow oil sands. *In-situ* thermal techniques such as cyclic steam stimulation (CSS), SAGD, and *in-situ* combustion (ISC)

target bitumen situated at depths not accessible by surface mining. Production by *in-situ* techniques in Alberta surpassed that of surface mining in 2012 and is expected to reach 60% of total bitumen production by 2024 (Alberta Energy Regulator, 2015).

At typical oil sand reservoir temperatures (4 to 38 °C), bitumen is highly viscous and practically immobile (Dusseault, 2001). To reduce its viscosity, solvents and a source of heat can be used. For the latter, steam is typically used due to its price, availability, and high heat of condensation. In SAGD, steam is injected at high temperature and pressure underground into the oil sands reservoir through sets of horizontal wells. The injected steam propagates in the formation and forms a steam chamber. At the edge of the steam chamber, steam condenses, liberating its heat, and causes a reduction in bitumen's viscosity which allows the oil to gravity-drain along with condensed water into the production wells. The production wells are sets of horizontal wells situated parallel and approximately five meters below the steam injection wells. The steam chamber grows over time as more bitumen is recovered (Fig. 1.1).

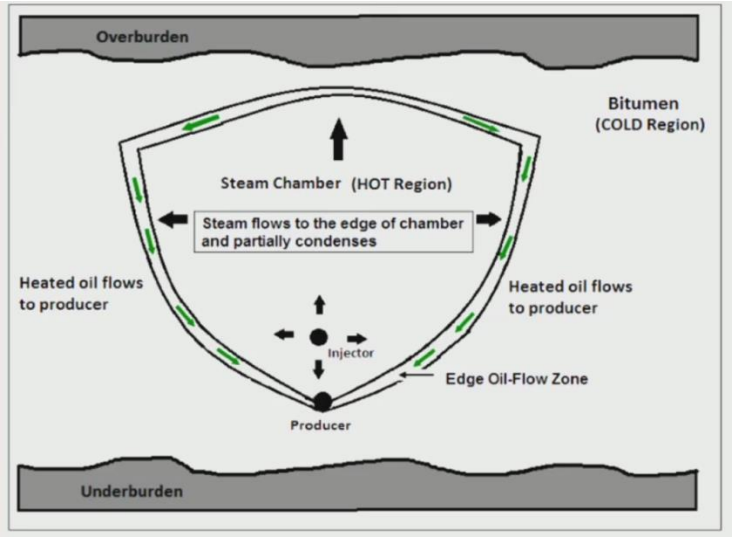

Figure 1.1: Schematic of the SAGD process (Ghasemi and Whitson, 2015).

The fact that large quantities of water and natural gas is needed for steam generation and the associated unwanted CO_2 emissions from SAGD operation provide motivations to improve the efficiency of the SAGD. A common indicator of the performance of SAGD projects is the cumulative steam-to-oil ratio (cSOR), which is the total volume of steam injected to the total volume of bitumen produced at any given time. Chemical additives have the potential to improve the efficiency and the performance of SAGD projects.

1.2 Research Objectives

The purpose of this work was to study the potential of using chemical additives to improve the performance of the SAGD process for the recovery of bitumen. The primary metrics to be quantified are the ultimate recovery and the recovery rate of bitumen. To achieve this goal, the following components of work were executed:

1. Propose a list of potential mechanisms for enhanced oil recovery and obtain an inventory of additives for testing.
2. Develop a suite of high-temperature additive characterization tests that can be used to give information about each additive's potential to improve oil recovery.
3. Test the efficacy of promising additives in permeable media using corefloods and sandpack floods at high temperature, which mimic SAGD conditions at the edge of the steam chamber.
4. Develop a preliminary numerical simulation model of a SAGD process to test the effect of selected mechanisms on SAGD performance.

1.3 DESCRIPTION OF CHAPTERS

Chapter 2 provides a review of literature on topics related to steam-assisted gravity drainage, aspects of enhanced oil recovery, and certain mechanisms of enhanced oil recovery.

Chapter 3 lists the hypothesized mechanisms that can improve SAGD, along with information about the additives and bitumen used throughout the course of this study. Furthermore, this chapter provides details on additive characterization tests performed in single or two-phase systems: pH and conductivity measurements, aqueous stability, phase behavior, and a test similar to the phase behavior test but performed in high-temperature visual cells. For each characterization test, the chapter states the materials used, experimental procedures followed, results obtained, and a discussion of the results.

Chapter 4 provides details on additive characterization tests performed in three-phase systems, which are composed of bitumen, additive solution, and a mineral. These experiments test for whether the additives can alter the wettability of the mineral surface or move the contact line between the three phases. For each characterization test, the chapter gives the materials used, experimental procedures followed, results obtained, and a discussion of the results.

Chapter 5 provides details on coreflood and sandpack flood experiments performed using various additives, which were selected based on the results of the additive characterization tests documented in Chapters 3 and 4. This chapter also states the materials and apparatus used to carry out the experiments, as well as the associated step-by-step procedures. The rationale behind the design parameters for each coreflood or sandpack flood will be given. In addition, the results and their relevant discussions are presented.

Chapter 6 provides details on the numerical simulation work undertaken in this study. Experimenters built and ran a preliminary SAGD model in CMG STARS to examine

the effect of oil-water IFT reduction and reservoir rock wettability alteration on SAGD performance metrics, including the ultimate recovery, oil rate, and cumulative steam-to-oil ratio.

Chapter 7 gives the final conclusions and recommendations for improvements and future work.

Chapter 2 Literature Review

This chapter provides a review of literature on topics related to steam-assisted gravity drainage, aspects of enhanced oil recovery, and certain mechanisms of enhanced oil recovery.

2.1 Steam-assisted Gravity Drainage and Its Variations

Steam-assisted gravity drainage was introduced by Roger Butler and his colleagues at Imperial Oil in the 1970s. It was developed as a technique for recovering bitumen (Butler, 1998). Fig. 2.1 below shows a conceptual diagram of the process.

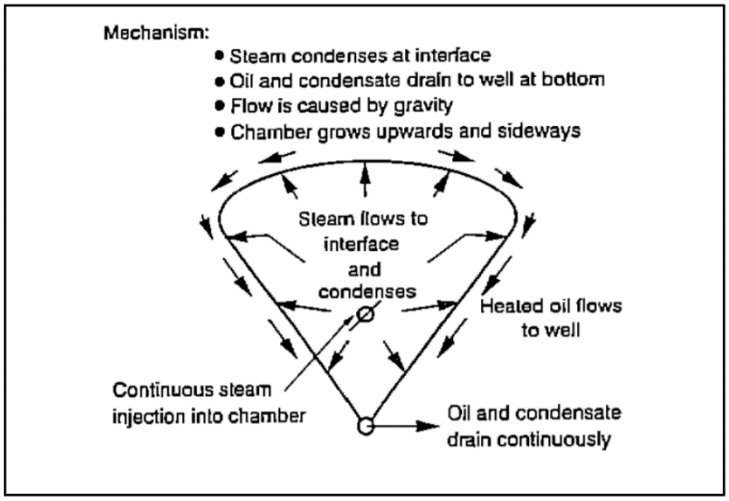

Figure 2.1: Conceptual diagram of the SAGD process (Butler, 1994, modified by author).

Steam is injected at high temperature and pressure underground into the oil sands reservoir through sets of horizontal wells. The injected steam diffuses into the formation and forms a steam chamber. At the edge of the steam chamber, steam condenses, liberating its heat, and causes a reduction in bitumen's viscosity which allows the oil to gravity-drain

along with condensed water into the production wells. The production wells are sets of horizontal wells situated parallel and approximately five meters below the steam injection wells. The steam chamber grows over time as more bitumen is recovered. The use of conventional vertical wells with gravity drainage was not economical. Horizontal wells on the other hand provide a much larger area of coverage. Well pairs of about 500 meters in length were shown to be able to produce bitumen on the order of kilo-barrels per day in Albertan bitumen reservoirs. In fact, Imperial Oil's field pilot test of SAGD in 1978 was one of the first uses of modern horizontal well technology (Butler, 1994).

Since its conception, much effort had been expended to understand and model SAGD, while many innovations have been made to improve the process. Many of these innovations involve the use of solvents. Mokrys and Butler proposed the injection of saturated hydrocarbon vapors at reservoir conditions in a method called "VAPEX" (Mokrys & Butler, 1993). In VAPEX, a solvent close to its dew point at reservoir conditions is injected. The method relies on in-situ upgrading of the bitumen, which was in contact with the solvent and produced at a lower temperature compared to the temperature found in a traditional SAGD steam chamber. An advantage of VAPEX is its potential to produce bitumen at an economic rate in thin reservoirs where excessive heat loss to the overburden and underburden pose a concern. Much effort was made in laboratory-scale VAPEX research starting in the 1990s (James et al., 2008). Despite its applicability to thin and problematic reservoirs, low rates of bitumen production, the high cost of solvents, and other economic factors have hindered field implementation of VAPEX (Haghighat & Maini, 2013). Researchers have also explored various solvent/heat hybrid bitumen recovery methods. Some of these include steam alternating solvent (SAS), expanding solvent steam-assisted gravity drainage (ES-SAGD), N-Solv, and warm VAPEX (Haghighat & Maini, 2013).

More recently, studies done on non-solvent chemistries that possess potential to improve SAGD performance have become available, but are in early (and often laboratory-scale) developmental stages. Some of these chemistries are not just exclusively applicable to SAGD, but to bitumen recovery in general. Oldenburg et al. (2010) studied the possibility of using monofunctional aromatic bases and acids to reduce bitumen viscosity. The principle was to inhibit molecules naturally found in bitumen that may act as links between heavy components such as asphaltenes. Babadagli et al. (2010) explored the use of biodiesel and fatty acid monoglycerides to increase bitumen recovery in in-situ methods by acting as a surfactant. Allenson et al. (2011) demonstrated that the injection of an emulsion viscosity reducer into the borehole can reduce the viscosity of water-in-oil emulsions, which is commonly formed by shear mixing during production in SAGD wells. Water-in-oil emulsions can have very high viscosities which can wear down pumps and reduce production rates. Such a reduction can lead to increased profit. Lu et al. (2014) explored the use of surfactants and nitrogen gas as an insulator, the former of which can form oil-in-water emulsions that lead to reduced residual oil, and the latter can reduce heat loss. Finally, Li et al. (2015) studied the use of foam, showing through numerical simulations that mobility control can provide a more uniform steam chamber growth and reduce heat loss to the overburden. Chemical additives have great potential to improve bitumen recovery, and can be tailored to work for SAGD. However, each new idea poses its own unique challenges.

2.2 Fundamentals of Enhanced Oil Recovery

Enhanced oil recovery (EOR) can be defined as the injection of any materials not natively present in the reservoir for producing oil. In most scenarios, this definition holds.

However, in certain technologies that are also pervasively recognized as EOR processes, what is injected is already present in the reservoir in certain amounts. An example is CO_2 flooding in a reservoir containing native CO_2 (Lake et al., 2014). As such, the question of whether a technology can be classified as an EOR process contains some room for interpretation. An important metric for any EOR process is the recovery factor, defined as

$$E_R = \frac{N_p}{OOIP}$$

where N_p represents the cumulative volume (or mass) of oil produced and *OOIP* represents the original volume (or mass) of oil in place. The recovery factor can be further broken down into the product of the displacement efficiency E_D and the volumetric sweep efficiency E_v. The displacement efficiency is ratio between the amount of oil displaced to the amount of oil contacted by the displacing agent, and the volumetric sweep efficiency is the ratio between the amount of oil contacted by the displacing agent to the OOIP when considering the entire volume of the reservoir. Each of these factors (E_R, E_D, and E_V) can be no less than zero and no greater than one. Another important metric is the oil production rate, which when combined with knowledge about operating costs is important for determining when an EOR project is deemed profitable and when it is not.

EOR is a very rich field, with a great variety of injected materials, targeted reservoir conditions, and targeted hydrocarbon properties. That being said, EOR technologies can be roughly fitted into one or a combination of several categories: chemical EOR (which includes the use of polymers, surfactants, alkalis, foams, and combinations thereof), thermal EOR (SAGD, in-situ combustion, cyclic steam stimulation, etc.), and immiscible and miscible solvent EOR.

2.3 BITUMEN VISCOSITY REDUCTION

Bitumen viscosity reduction is a key mechanism that allows SAGD to work. At typical oil sand reservoir temperatures (4 to 38 °C), bitumen is highly viscous and practically immobile (Dusseault, 2001). Fortunately, the viscosity of low gravity hydrocarbons decreases exponentially with an increase in temperature. Both facts can be seen in Fig. 2.2 below. Notice that the viscosity on the y-axis is on a logarithmic scale, while the temperature on the x-axis is on a linear one. Of course, bitumen viscosity reduction can be achieved with the use of solvents as well, but traditionally SAGD has relied on the latent and sensible heat of steam to dramatically decrease its viscosity. For a qualitative perspective, the viscosity of bitumen at typical reservoir conditions is like that of peanut butter.

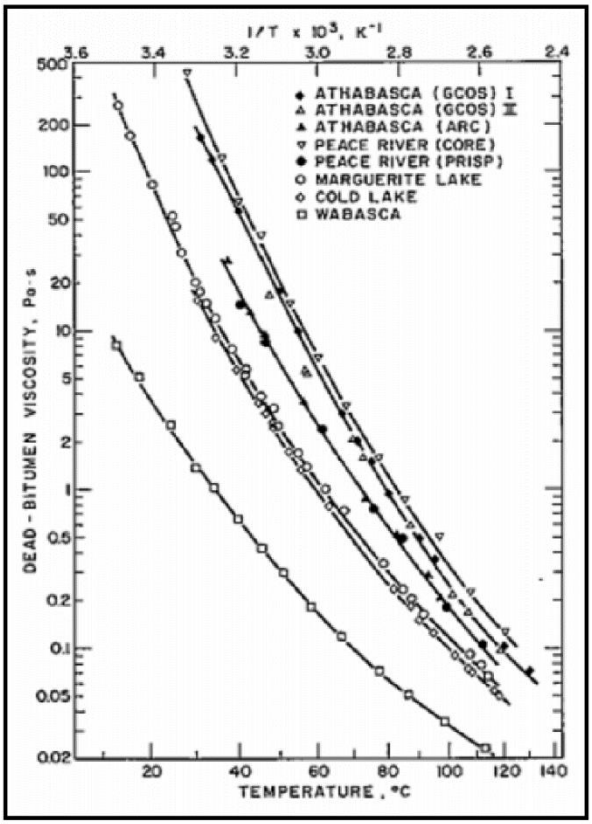

Figure 2.2: Viscosity-temperature relationship for Albertan bitumens (Svrcek & Mehrotra, 1989).

To gain a qualitative understanding of the viscosity-temperature relationship, Eyring et al. (1941) proposed a free volume theory for the viscosity of small or short-length, slender liquid molecules. The predictive power of this model for long-chained hydrocarbons in bitumen is diminished, but a qualitative understanding may still be gained. Liquid molecules at rest vibrate due to thermal energy. The free volume theory describes the liquid molecules as trapped in a "cage" formed by adjacent molecules, which limit the movement of the molecule within the confines of the cage. However, molecules can escape this cage into an adjacent "hole," with an associated molar free energy of activation $\Delta\tilde{G}_0^+$.

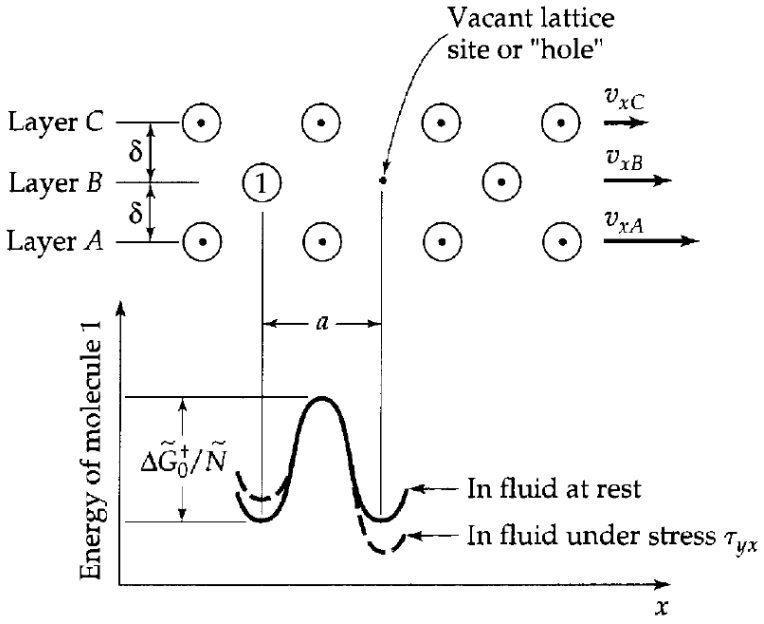

Figure 2.3: Liquid molecules may escape its "cage" by jumping into an adjacent hole (Bird et al., 2002).

The frequency of these jumps ν may be described by an equation reminiscent to the Boltzmann distribution.

$$\nu = \frac{kT}{h}\exp\left(-\Delta\tilde{G}_0^{+}/RT\right) \tag{1}$$

where k is the Boltzmann constant and h is Planck's constant. An applied shear stress by the layer in the lesser y may be thought of as work done on the molecule. Therefore, there is a positive net frequency of jumps in the direction of the applied shear. By relating this model to Newton's Law of Viscosity and using an empirical relationship between $\widetilde{\Delta G}_0^{+}$ and the enthalpy of vaporization $\Delta\widetilde{U}_{vap}$, Eyring derived an equation showing the exponential relationship between viscosity and temperature.

$$\mu = \frac{\tilde{N}h}{\tilde{V}} exp\left(0.408\, \Delta\tilde{U}_{vap}/RT\right) \quad (2)$$

where $\tilde{N}$ is Avogadro's number and $\tilde{V}$ is the molar volume. Thus an intuitive molecular explanation for liquid viscosity as a function of temperature is given. Eq. 3 below gives Darcy's law for the one-dimensional, linear flow of oil in a multi-phase system.

$$q_o = -\frac{kk_{ro}A}{\mu_o}\left(\frac{\partial P_o}{\partial x} + \rho_o \, \mathrm{g} \sin\alpha\right) \quad (3)$$

Here q_o is the volumetric flow rate of oil, k is the permeability, k_{ro} is the relative permeability of oil, A is the cross-sectional area of flow, μ_o is the oil viscosity, P_o is oil-phase pressure, g is the standard acceleration due to gravity, and α is the angle between the flow plane and the horizontal plane. It is evident from Eq. 3 that a decrease in oil viscosity increases the oil drainage rate.

2.4 Oil-water Interfacial Tension Reduction

Capillary forces trap oil in pores, requiring a viscous, buoyancy, or gravity force high enough to move the oil. The Young-Laplace equation for an idealized pore (cylinder) shows that the capillary pressure may be reduced by decreasing the oil-water interfacial

$$P_c = \frac{2\sigma\cos(\theta)}{r} \quad (4)$$

tension (IFT). Here, P_c is the capillary pressure, σ is the interfacial tension, θ is the contact angle measured through the wetting phase, and r represents the radius of the pore throat. Surfactants can reduce capillary forces by decreasing the oil-water IFT. The competition

between capillary forces trapping oil and viscous forces moving oil is represented by the capillary number shown by Eq. 5, which is the ratio of viscous forces to capillary forces.

$$N_{vc} = \frac{\mu u}{\sigma} \tag{5}$$

Here μ is the viscosity of displacing agent, and u is the Darcy velocity. Capillary desaturation curves (CDCs) show that non-wetting (and wetting) phase residual saturation decreases when the local capillary number is sufficiently high.

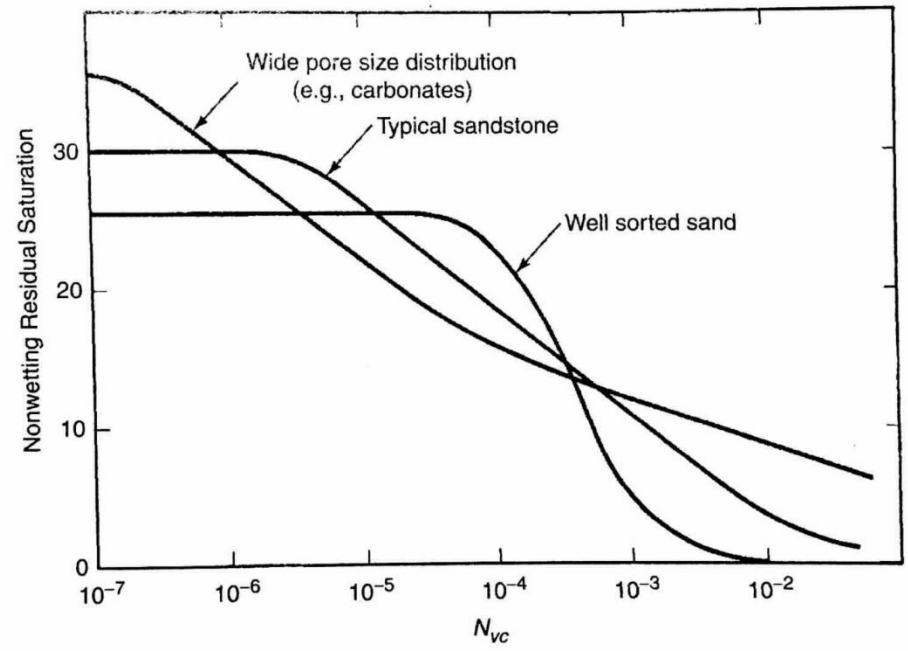

Figure 2.4: A typical CDC (Lake et al., 2014).

To achieve the local capillary numbers needed to decrease residual saturation by increasing injecting fluid viscosity or rate is not feasible; however, IFT can be decreased to a significant degree necessary to decrease residual oil saturation.

Of course, in SAGD there is very little viscous force pushing bitumen to the production well. The process relies on gravity to drain bitumen along the edge of the steam chamber, where the bitumen drains along with condensed steam in the so-called condensate zone. In this zone, one can imagine that some draining bitumen could come to a pore throat too narrow for it to pass, stopped by capillary force. A reduction in oil-water IFT could decrease the capillary pressure enough such that the bitumen drains across the pore throat under the influence of gravity. Based on laboratory-scale experiments and high recovery factors from pilot tests, there are evidences that the residual oil saturation in steam chambers are actually quite low (Walls et al., 2003). Therefore, improving the ultimate recovery of a SAGD project may not be the best goal. However, an increase in the production rate of bitumen could reduce the cumulative steam-to-oil ratio of a project, leading to direct savings from getting more bitumen for the same amount of steam. Bitumen and the mixture of condensed steam and connate water drain along the edge of the steam chamber. Since the aqueous phase is immiscible with bitumen, the two phases compete with each other, which is why the relative permeability of each phase is less than one. Amaefule and Handy (1982) have shown using dilute surfactant solutions that oil-water relative permeabilities increase with decreasing oil-water IFT at the same water saturations, and even become linear as the IFT approaches zero.

Surfactants are the most commonly used agent for reducing oil-water IFT in conventional waterflooding. They are typically injected in slugs. A typical process might also include the injection of a polymer and an alkali, known as alkaline-surfactant-polymer flooding. Surfactants are also used to generate foam, but in those cases the oil-water IFT reduction is usually insignificant. A surfactant is an amphiphilic molecule, and in its most basic form has a polar head group and a non-polar hydrocarbon tail. The molecular structures can get more complicated, such as multiple branching on the tail and different

species of head groups. There are four categories of surfactants: anionic, cationic, nonionic, and amphoteric. Anionic surfactants have a negatively charged head group that is balanced by a positively charged metal cation. Surfactants used for oil-water IFT reduction are most commonly anionic due to their low adsorption on sandstones. Cationic surfactants have a positively charged head group, balanced by an inorganic anion. Nonionic surfactants are neutrally charged and are sometimes used as cosurfactants to tweak the phase behavior of surfactant formulations with native reservoir oil. Finally, amphoteric surfactants have at least both one positive and one negative charge, or vary in charge based on the solution's pH (Lake et al., 2014).

Alkalis are another agent that can be used to reduce oil-water IFT. Alkali can facilitate the generation of natural surfactant from acidic molecules in the oil. Acidic hydrocarbon molecules in the bitumen can partition into the aqueous phase and deprotonate into its anionic form. These molecules have a hydrocarbon tail(s) and an ionic head group, and behave as surfactant molecules do. The molecular structure of these molecules are not known specifically since bitumen contain a complex combination of components; however, it is believed that many of these molecules contain a carboxylic acid head group with hydrocarbon tails. The acid number of a crude oil is defined as the amount of potassium hydroxide needed to neutralize one gram of oil in units of mg KOH/g oil. Crude oils with acid numbers higher than 0.5 mg/g are good candidates for alkali injection (Lake et al., 2014).

2.5 WETTABILITY ALTERATION

The wettability of reservoir rock affects an extensive list of items including the location and flow of individual phases, capillary pressures, relative permeabilities,

waterflood performance, tertiary recovery performance, irreducible water saturation, residual oil saturation, tracer dispersion, and electrical properties (Anderson, 1986).

The wettability of a rock is the tendency of a fluid to spread over or adhere to its surface. In the case of a rock/oil/brine system, it is a measure of the rock's preference for oil or for water (Craig, 1971). For water-wet rocks, water occupies the smaller pores and contacts a majority of the rock surface, while oil presides in larger pores as globules. For oil-wet rocks, oil occupies the smaller pores and contacts a majority of the rock surface while water presides in larger pores as globules (Anderson, 1986). Rocks with no strong preference for either oil or water is said to be of intermediate wettability. The contact of oil with rock surfaces shifts the surfaces' wettability to more oil-wet over time by the adsorption of amphiphilic molecules found in the oil (e.g. asphaltenes) onto the rock. These molecules may even be sufficiently water-soluble to diffuse through a layer of water to reach the rock surface. Another way is by deposition of organic matter onto the rock, coating the rock surface with an organic film (Anderson, 1986). These lead to portions of the reservoir being oil-wet while others remain water-wet, and the reservoir is said to exhibit fractional wettability (Brown & Fatt, 1956). Heterogeneity also plays a big role in determining reservoir wettability since the internal surfaces can be composed of many different minerals, each with unique surface chemistries and adsorption properties. Finally, Salathiel (1973) coined the term "mixed-wet" to describe a specific case of fractional wettability, where the oil-wetting regions form a continuous path in the bigger pores. How mixed-wet conditions develop was not addressed by Salathiel, since there invariably must be a film of water separating rock and oil after the oil moves into the originally water-wet reservoir. As mentioned before, compounds in oil may in some cases diffuse through the water layer to reach the rock surface. Models have shown that the water layer becomes thinner as more oil enters the bigger pores and may rupture when the electrostatic forces

from the electrical double layers are overcome (Hall et al., 1983; Melrose, 1982). When native-state cores are hard to obtain or unavailable, restored-state cores are used in laboratory corefloods. These cores are cleaned using an extensive procedure, saturated with reservoir brine, saturated with oil, and then aged at reservoir temperature for long periods of time in an attempt to obtain original wettability (Anderson, 1986).

Common wettability measurement techniques worth mentioning include the contact angle method, the Amott wettability test, and the United States Bureau of Mines (USBM) wettability method. In the contact angle method, a droplet of oil is placed on a smooth mineral surface, typically calcite or quartz, with both the solid and droplet submerged in brine. The angle between the oil droplet and the mineral surface can be measured using image processing software through the brine phase. Angles between 0° to 60-75°, 60-75° to 105-120°, and 105-120° to 180° indicate water-wet, intermediate-wet, and oil-wet respectively (Anderson, 1986).

An interesting topic of consideration is whether the contact line can move. The contact line is the line where the three phases (oil, brine, and mineral) meet. In porous media, the non-wetting phase occupies the bigger pores in the center of the pore body, while the wetting phase occupy the smaller pores, coats the surface of the grains, and occupies the corners of grain contacts (Peters, 2012). After wettability alteration to a porous media, oil must redistribute inside the pores. One can imagine that the movement of the contact line and a peeling of oil off from the surface of grains or redistribution of the oil must go hand in hand. The water and oil relative permeabilities also are affected by wettability. Oil relative permeability increases with increasing water-wetness while water relative permeability decreases (Peters, 2012).

It is unclear what wettability is best for oil recovery in sandstones and unconsolidated sands. Owens and Archer (1971) showed that the ultimate oil recovery and

oil relative permeability increased with increasing water-wetness in some sandstone cores. Cooke et. al (1974) showed that recovery was better with increasing oil-wetness. Other researchers have shown that neither strongly water-wet nor oil-wet decreases residual oil saturation, as shown in Fig. 2.5 below. I_w is the Amott wettability index, which is a parameter indicating the wettability of core samples. A value of -1 or 1 indicates strongly oil-wet or strongly water-wet. The Amott wettability index is defined as

$$I_w = \delta_w - \delta_o \tag{6}$$

where δ_w represents the displacement-by-water ratio and δ_o the displacement-by-oil ratio as shown below.

$$\delta_w = \frac{V_{osp}}{V_{ot}} \tag{7}$$

$$\delta_o = \frac{V_{wsp}}{V_{wt}} \tag{8}$$

In the above equations, V_{osp} represents the volume of oil that can be displaced by spontaneous imbibition of water and V_{ot} the total volume of oil that can be displaced by spontaneous and forced imbibition of water. Similarly, V_{wsp} stands for the volume of water that can be displaced by spontaneous imbibition of oil and V_{wt} the total volume of water that can be displaced by spontaneous and forced imbibition of oil.

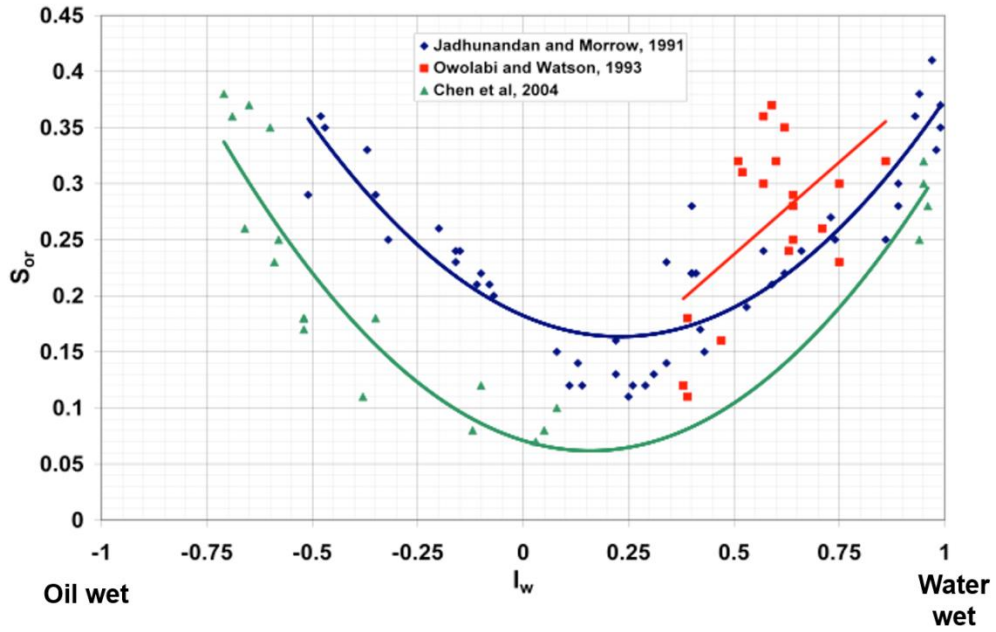

Figure 2.5: Residual oil saturation as a function of wettability (Anderson, 2006).

Lake et. al (2014) suggested that perhaps wettability change is more important than final wettability. When wettability changes, the previously non-wetting fluid migrates to smaller pores and the previously wetting fluids migrate to bigger pores. It is suggested that during this change, the phases become more susceptible to be moved.

Asphaltene precipitation plays an important role in wettability alteration. Qi et al. (2013) showed that higher concentrations of asphaltenes made quartz surfaces more oil-wet in a shorter period of time, where the equilibrium contact angle was achieved in only three days, reaching a maximum of around 100°. An explanation for this phenomenon was given by Gonzalez and Moreira (1991), who suggested that lateral interactions between adsorbed asphaltenes discourage desorption at higher asphaltene concentrations.

2.6 SOLVENTS

A liquid that mixes in all proportions with another liquid is said to be miscible. Solvents may be miscible or partially miscible with oil and improved recovery can be achieved via mass transfer of components of oil into the solvent phase, or via mass transfer of solvent into the oil phase. The diffusion of solvent into bitumen dilutes the latter and decreases its viscosity, which increases oil flow rate based on Darcy's law. This dilution is a dominant mechanism by which solvent processes for bitumen work (James et al., 2008). Further, improved miscibility between the bitumen and aqueous phase decreases oil-water IFT and improves oil relative permeability. This is because the competing flow of the aqueous phase and oil phase is lessened when the IFT is decreased (Amaefule & Handy, 1982).

Solvents tried in SAGD have almost exclusively been hydrocarbons, which in some cases are co-injected with steam to take advantage of the heat to help facilitate diffusion and bitumen viscosity reduction.

There are many variations in the use of hydrocarbon solvents in SAGD, including but not limited to VAPEX, warm-VAPEX, steam alternating solvent (SAS), expanding solvent steam-assisted gravity drainage (ES-SAGD), and N-Solv. The fact that so many variations exist points to the complexity of solvent SAGD strategies.

2.7 CONVECTION AND DISPERSION IN POROUS MEDIA

Chemical species injected into porous media are transported by advection and dispersion (molecular and mechanical dispersion in the porous media). Let C_i and C_j represent the initial and injection additive concentrations (g/mL solution), respectively. The one-dimensional advection-dispersion equation in dimensionless form is

$$\frac{\partial C_D}{\partial t_D} + \frac{\partial C_D}{\partial x_D} - \frac{1}{N_{Pe}} \frac{\partial^2 C_D}{\partial x_D^2} = 0 \tag{9}$$

where C_D, t_D, and x_D represent the dimensionless concentration, time (pore volumes), and distance from the inlet respectively. In addition, N_{Pe} is the Peclet number, which is the ratio of advection to dispersion (Peters, 2012). Eq. 10 shows the definition of C_D.

$$C_D = \frac{C(x,t) - C_i}{C_j - C_i} \tag{10}$$

The solution to Eq. 9 for the dimensionless concentration at the outlet is

$$C_D(1, t_D) = \frac{1}{2} erfc\left[\sqrt{N_{Pe}}\left(\frac{1-t_D}{2\sqrt{t_D}}\right)\right] \tag{11}$$

For a homogenous, isotropic porous media with no additive adsorption, where the injected and displaced fluid has the same density and viscosity, the breakthrough curve looks like the one depicted in Fig. 2.6.

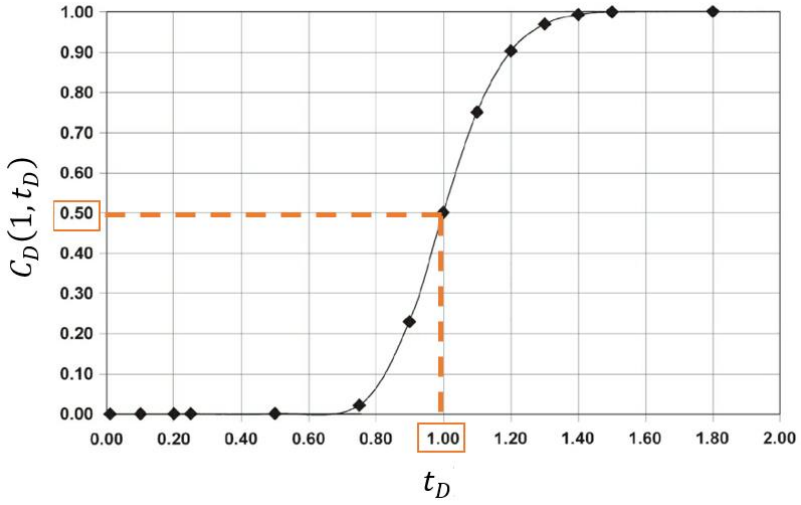

Figure 2.6: Breakthrough curve for idealized water flood (Peters, 2012).

The curve is S-shaped. Additive breaks through before one pore volume due to dispersion and a C_D of 0.5 travels at the advection speed. A concentration C_D of 0.5 measured after one pore volume injected tells experimenters that the additive was detained in some way. A concentration C_D of 0.5 measured before one pore volume injected is most likely due to heterogeneities, such as high permeability channels.

Chapter 3 Additive Characterization in Single or Two-phase Systems

Chapter 3 lists the hypothesized mechanisms that can improve SAGD, along with information about the additives and bitumen used throughout the course of this study. Furthermore, this chapter provides details on additive characterization tests performed in single or two-phase systems: pH and conductivity measurements, aqueous stability, phase behavior, and a test similar to the phase behavior test but performed in high-temperature visual cells. For each characterization test, the chapter states the materials used, experimental procedures followed, results obtained, and a discussion of the results.

3.1 Overview

In order to tackle the challenge of improving SAGD performance via chemical additives, a set of mechanisms was proposed. Table 3.1 shows the list of mechanisms considered and each mechanism's potential impact on petrophysics that can lead to improved SAGD oil recovery. The agent is the additive chemical family that can operate by the associated mechanism. Heat is included in the table since it is the primary agent that makes SAGD work.

Table 3.1: Agents, Mechanisms, and Associated Impact on SAGD Oil Recovery

Agent	Mechanism	Potential Impact
Heat	Reduce bitumen viscosity	Accelerate bitumen drainage
Surfactant	Reduce bitumen-water IFT	Decrease capillary forces that trap oil
	Alter wettability	Increase oil relative permeability, move contact line, peel oil off from surface of grains
Alkali/natural surfactant	Alkali increases aqueous phase pH	Deprotonate natural acids in oil to surfactant form
	Natural surfactant reduces bitumen-water IFT	Decrease capillary forces that trap oil
	Natural surfactant alters wettability	Increase oil relative permeability, move contact line, peel oil off from surface of grains
Solvent	Improve miscibility between additive/aqueous phase and oleic phase	Increase oil relative permeability
	Reduce bitumen viscosity by dilution	Accelerate bitumen drainage

Throughout the course of the study, 26 additives were obtained either from the sponsoring company or from vendors. They are shown in Table 3.2. These include additives in each of the chemical families listed in Table 3.1, in addition to two acids. Additive characterization tests were performed on these additives, and select additives were chosen for core and sandpack flooding experiments.

Table 3.2: List of Additives

Trade Name	Chemical Family	Phase at Room Temperature
TA	Alcohol solvent	Liquid
TB	Non-ionic surfactant	Liquid
TC	Non-ionic surfactant	Liquid
TD[1]	Anionic surfactant	Liquid
TF	Organic alkali	Solid
TG	Inorganic alkali	Solid
TH	Alcohol solvent	Liquid
Organic alkali 1	Organic alkali	Liquid
Organic alkali 2	Organic alkali	Liquid
Organic alkali 3	Organic alkali	Liquid
Organic alkali 4	Organic alkali	Liquid
Organic alkali 5	Organic alkali	Liquid
Organic alkali 6	Organic alkali	Liquid
Organic alkali 7	Organic alkali	Liquid
Organic alkali 8	Organic alkali	Solid
Organic alkali 9	Organic alkali	Liquid
Organic alkali 10	Organic alkali	Solid
Organic alkali 11	Organic alkali	Liquid
Alcohol 1	Alcohol solvent	Liquid
Alcohol 2	Alcohol solvent	Liquid
Acid 1	Organic acid	Liquid
Acid 2	Organic acid	Liquid
Solvent 1	Alcohol solvent	Liquid
Solvent 2	Alcohol solvent	Liquid
Solvent 3	Alcohol solvent	Liquid
Solvent 4	Alcohol solvent	Liquid

[1] TD had an activity of 25 %. All other additives were 100 % active.

The oil used for all experiments except for the phase behavior tests with TA, TB, and TC and the first coreflood was a dewatered bitumen. A bitumen sample diluted with naphtha was used for the phase behavior tests for additives TA, TB and TC and the first coreflood. This was because the diluted bitumen was less viscous and easier to handle.

Once the experimenters gained more experience, the more viscous dewatered bitumen was used for all subsequent experiments. Fig. 3.1 illustrates the density vs. temperature data of the dewatered bitumen.

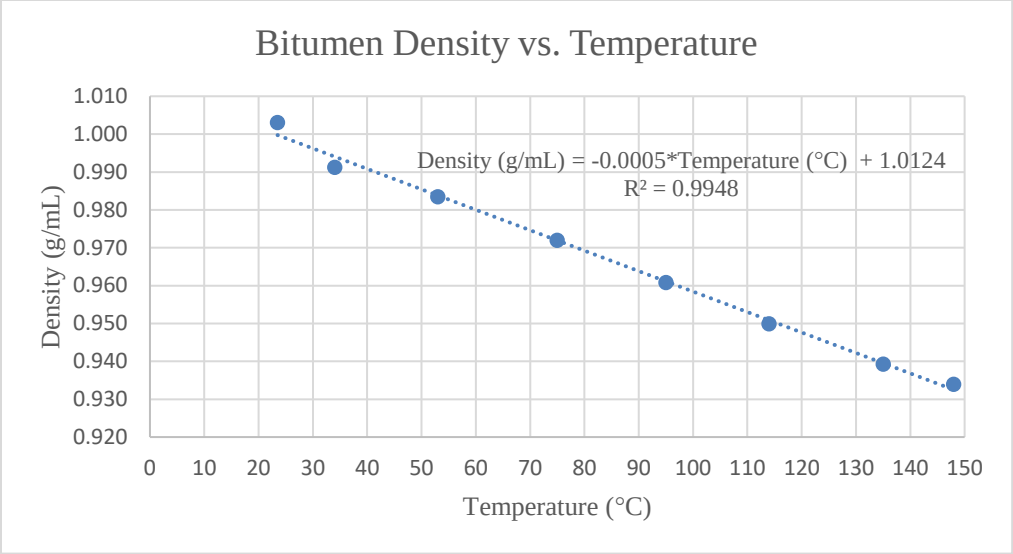

Figure 3.1: Dewatered bitumen density vs. temperature data.

The details, results, and discussion of the characterization tests performed in single and two-phase systems are presented in the following sections. These tests along with the wettability experimenters presented in Chapter 4 serve to find promising additives from the selection pool that might improve oil recovery in a core or sandpack flood mimicking SAGD conditions.

3.2 Conductivity and pH Measurements

3.2.1 Purpose

The purpose of these measurements were three-fold. Measuring the conductivity of aqueous solutions containing additive gave experimenters an idea of the additive's native

salinity, which can be important in interpreting phase behavior results. Measuring the pH of aqueous solutions containing additive gave experiments an idea of the additive's effect on aqueous solution pH. As previously explained, the primary mechanism by which alkali additives work is to extract natural surfactant through increasing the aqueous solution pH. Finally, experimenters performed one coreflood to demonstrate how to measure the dynamic retention characteristics of additives in a core. The pH and conductivity measurements provided a way to estimate additive concentration in the effluent over time. This will be explained in detail in Chapter 5.

3.2.2 Materials

The materials used for pH and conductivity measurements consisted of an analytical balance, 15 mL Fisherbrand polypropylene tubes, additives listed in Table 3.2, disposable Fisherbrand transfer pipettes, a metal spatula, potassium chloride (KCl) obtained from Fisher Scientific, a Hanna Instruments Edge pH meter for measuring pH, a Thermo Scientific Orion 5-Star meter for measuring conductivity, and Kimwipes. In addition, pH 4.01, 7.00, and 10.01 buffer solutions were obtained from Fisher Scientific for calibrating the pH meter before use. Conductivity standards, including the 1413 μS/cm and 12.9 mS/cm solutions, were obtained from Thermo Scientific. The Hanna Instruments Edge is a low-noise pH meter with a temperature sensor that allows for temperature compensation. The Orion 5-Star also contains a built-in temperature sensor that allows for temperature compensation.

3.2.3 Procedure

The following is a prototypical procedure for measuring the pH of several additive solutions. Experimenters first leveled an analytical balance and then placed an empty 15 mL polypropylene tube into a small beaker, which was placed on the scale. The beaker held the tube vertical. The balance was tared, and the additive solution was made by adding an appropriate mass of additive and deionized water into the tube. Solid additives were scooped using a clean metal spatula, while liquids were dispensed using a disposable transfer pipette. Potassium chloride was also added wherever appropriate. Experimenters capped the tubes and gently shook them until the components were dissolved. The above procedure was repeated to make other additive solutions to be measured. Next, the experimenters calibrated the pH meter. First, the pH electrode was thoroughly rinsed with deionized water and gently dabbed dry with a Kimwipe. Then, the electrode was submerged into a 15 mL polypropylene tube containing pH 4.01 buffer solution. Experimenters then gently stirred the solution by moving the electrode in a circular motion until the pH reading stabilized. The above procedure was repeated using pH 7.00 and 10.01 buffers, starting with rinsing the electrode with deionized water. Following calibration, the following steps were taken to obtain pH measurements. The electrode was thoroughly rinsed with deionized water and gently dabbed dry with a Kimwipe. Then, the electrode was submerged into the additive solution and gently moved in a circular motion. The pH value stabilized in less than a minute and the pH value was recorded. The above procedure was repeated to obtain pH measurements for all the additive solutions starting with rinsing the electrode.

The following is a prototypical procedure for measuring the conductivity of several additive solutions. Experimenters first leveled an analytical balance and placed an empty polypropylene tube into a small beaker. The beaker was placed on the scale and held the

tube vertical. The balance was tared, and the additive solution was made by adding an appropriate mass of additive and deionized water into the tube. Solid additives were scooped using a clean metal spatula, while liquids were dispensed using a disposable transfer pipette. Potassium chloride was also added where appropriate. Experimenters capped the tubes and gently shook them until the components were dissolved. The above procedure was repeated to make other additive solutions to be measured. Next, the experimenters calibrated the conductivity meter. First, the probe was thoroughly rinsed with deionized water and gently dabbed dry with a Kimwipe. Then, the probe was submerged into a 15 mL polypropylene tube containing a 1413 μS/cm conductivity standard. Experimenters then gently stirred the solution by moving the probe in a circular motion until calibration step was completed. The above procedure was repeated using a 12.9 mS/cm standard, starting with rinsing the probe with deionized water. After calibration, the following steps were taken to obtain conductivity measurements. The probe was thoroughly rinsed with deionized water, gently dabbed dry with a Kimwipe, submerged into the additive solution, and gently moved in a circular motion. The conductivity value was recorded after the reading stabilized. The above procedure was repeated to obtain conductivity measurements for all the additive solutions starting with rinsing the probe.

3.2.4 Results and Discussion

Fig. 3.2 and 3.3 below show the room temperature pH and conductivities of additives TA through TH and sodium carbonate (Na_2CO_3) at various concentrations in deionized water. TD and TG were slightly basic while TF and Na_2CO_3 were basic with a pH around 11. TD was slightly conductive while TG and Na_2CO_3 were even more

conductive. The conductivity of TD, TG, and Na_2CO_3 solutions varied linearly with additive concentration.

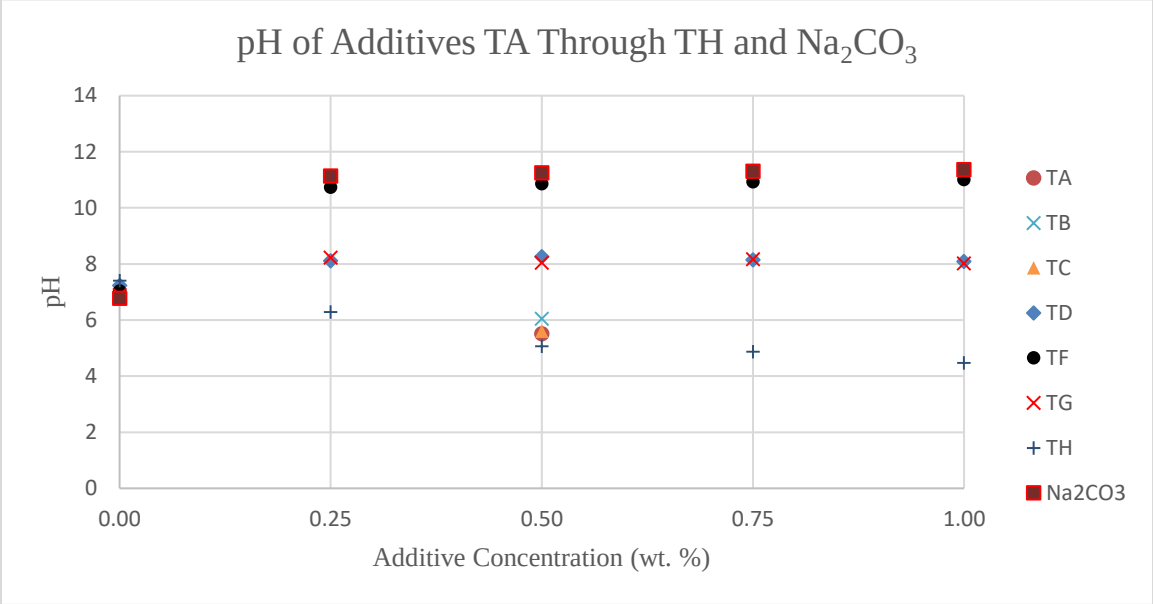

Figure 3.2: pH of additives TA through TH and Na_2CO_3 in aqueous solution.

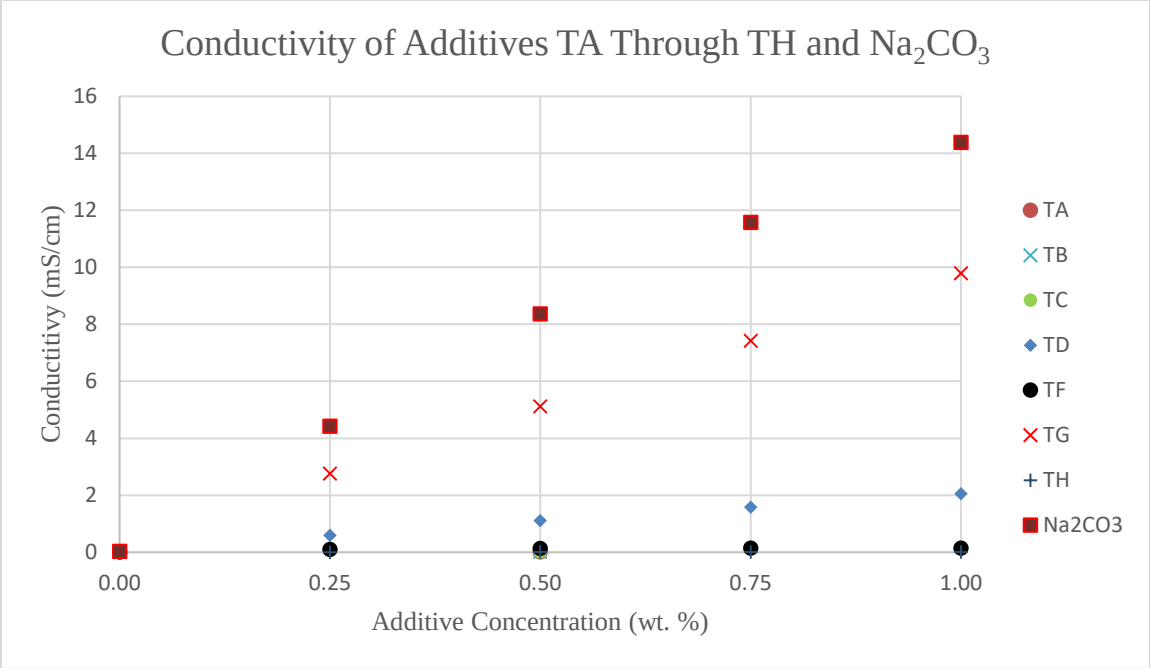

Figure 3.3: Conductivity of additive TA through TH and Na_2CO_3 in aqueous solution.

Fig. 3.4 and 3.5 show the pH and conductivity of solutions of TF and TG in 1 wt. % KCl at various concentrations after being heated to 150 °C and then cooled down to room temperature. This roughly corresponded to what happened in the dynamic additive retention coreflood study, where experimenters injected TF and TG solutions through an Idaho Gray core at 150 °C and measured the pH and conductivity of the effluent at room temperature (the effluent was collected over time, and the additive concentration was represented by the effluent pH and conductivity during periods of injecting TF and TG respectively).

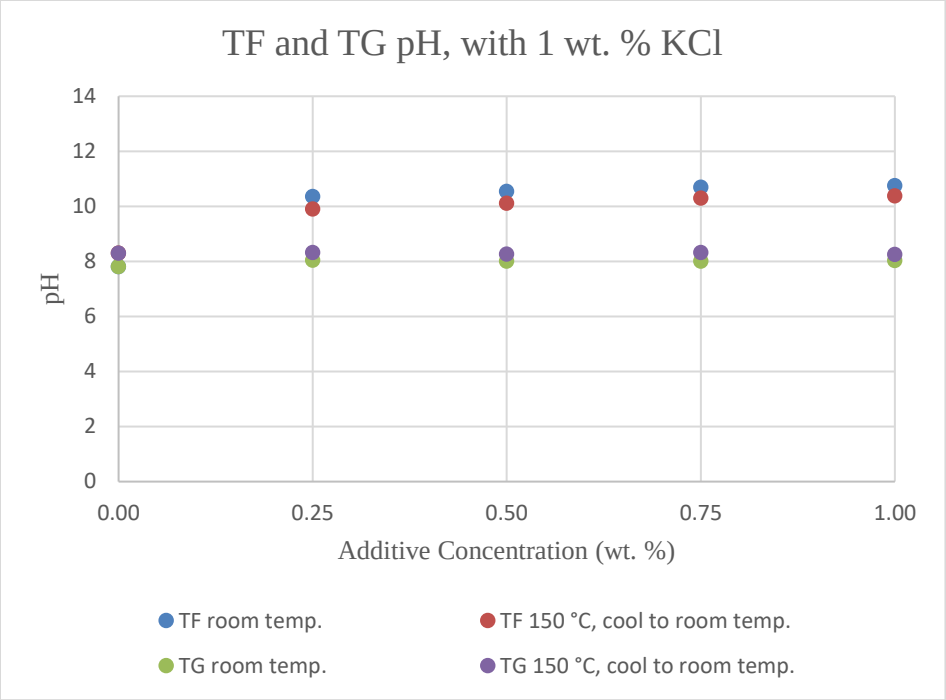

Figure 3.4: pH of TF and TG at various concentrations in 1 wt. % KCl.

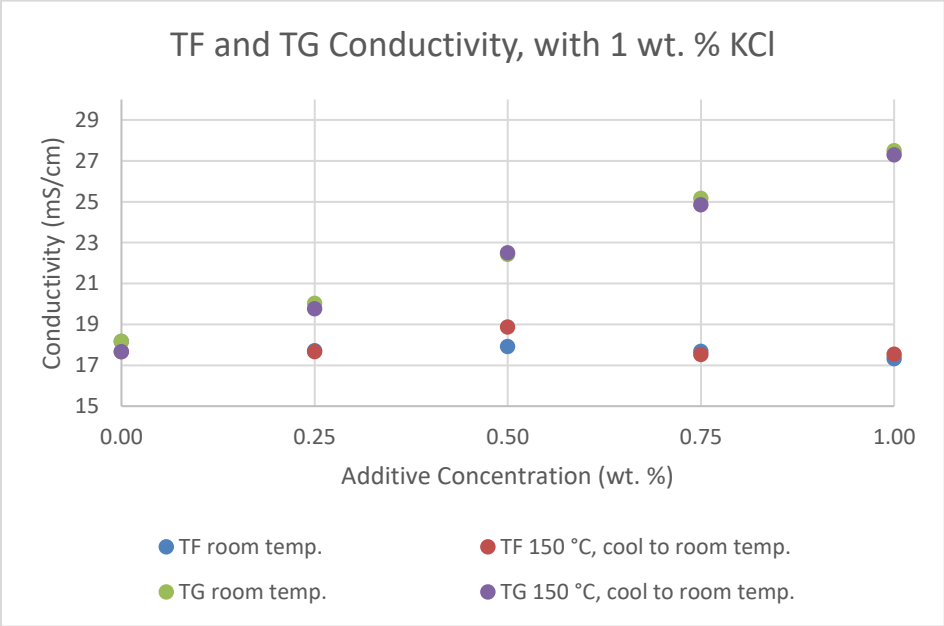

Figure 3.5: Conductivity of TF and TG at various concentrations in 1 wt. % KCl.

Table 3.3 shows the pH and conductivity of Organic alkali 1 through Solvent 4 at 0.2 wt. % and 0.5 wt. % concentration in deionized water. Every organic alkali was able to increase the pH to around 10 to 11 at only 0.5 wt. % concentration. This means that a significant amount of natural surfactant can be extracted from the bitumen using only a small amount of these additives. A stable pH reading was unobtainable for both the alcohols and the solvents, since the solution's ionic strength was low, which is verified by the low conductivity values. The two organic acids lowered aqueous pH to around 3.

Table 3.3: pH and Conductivity of Organic Alkali 1 Through Solvent 4 at 0.2 and 0.5 wt. % Additive Concentration

	0.2 wt. % Additive in Deionized Water		0.5 wt. % Additive in Deionized Water	
Additive	pH	Conductivity (mS/cm)	pH	Conductivity (mS/cm)
Organic alkali 1	11.35	0.809	11.73	1.603
Organic alkali 2	11.31	0.720	11.68	1.327
Organic alkali 3	11.24	0.591	11.62	1.065
Organic alkali 4	11.12	0.345	11.25	0.427
Organic alkali 5	11.4	0.784	11.77	1.413
Organic alkali 6	10.83	0.194	11.01	0.199
Organic alkali 7	11.12	0.382	11.47	0.707
Organic alkali 8	11.18	0.504	11.58	0.943
Organic alkali 9	10.89	0.224	11.24	0.417
Organic alkali 10	10.41	0.079	10.8	0.145
Organic alkali 11	9.82	0.018	10.06	0.033
Alcohol 1	---	0.002	---	0.004
Alcohol 2	---	0.001	---	0.002
Acid 1	3.27	0.165	3.18	0.292
Acid 2	3.71	0.088	3.65	0.102
Solvent 1	---	0.020	---	0.024
Solvent 2	---	0.002	---	0.002
Solvent 3	---	0.011	---	0.024
Solvent 4	---	0.010	---	0.018

[1] --- indicates that the additive did not have enough ionic strength to obtain a pH reading; the pH reading would fluctuate continuously and would not stabilize.

The organic alkalis and acids were all slightly conductive. As mentioned, the alcohols and solvents did not contribute much conductivity to the solution.

3.3 AQUEOUS STABILITY

3.3.1 Purpose

The purpose of the aqueous stability test was to check the miscibility of an additive in aqueous brine solution at various temperatures and salinities. Experimenters looked for cloudiness, precipitates, liquid-liquid segregation, and viscous structures. These can lead to poor transport and higher retention in porous media and thus are unfavorable for corefloods and sandpack floods.

3.3.2 Materials

The materials used in the aqueous stability test consisted of an analytical balance, 50 mL Fisherbrand polypropylene tubes, the additives listed in Table 3.2, a metal spatula, disposable Fisherbrand transfer pipettes, fire safety protective gear, a metal plate, a ring stand, a Benzomatic propane hand torch, tongs, 5 mL Fisherbrand borosilicate glass pipettes, an Eppendorf repeater with 5 mL tip, potassium chloride obtained from Fisher Scientific, weighing paper, a nitrogen accumulator, a metal pipette rack, a convection oven, and a camera.

3.3.3 Procedure

The following is a prototypical procedure for the aqueous stability test. Experimenters first leveled an analytical balance and then placed an empty 50 mL

polypropylene tube into a small beaker, which was placed on the scale. The beaker held the tube vertical. The balance was tared, and the additive solution was made by adding an appropriate mass of additive and deionized water into the tube. Solid additives were scooped using a clean metal spatula, while liquids were dispensed using a disposable transfer pipette. Experimenters capped the tubes and gently shook them until the components were dissolved. The above procedure was repeated to make other additive solutions as needed.

A metal plate was laid on a bench top, and a propane hand torch was placed upright in a ring stand on top of the metal plate, with the flame nozzle pointed downward at a slight angle. Wearing protective gear, the experimenters turned on the flame nozzle, placed the tapered tip of a 5 mL Fisherbrand borosilicate glass pipette into the flame, and rotated the tip for several seconds until the glass began to glow. When the tapered tip was heated, the opening diameter began to shrink until the hole disappeared. After the glass cooled, the bottom tip of the pipette was sealed. The experimenters used tongs to help handle the glass pipette. This procedure was repeated to prepare more bottom-sealed pipettes as needed. The pipettes were placed on a rack. Experimenters then shook the tube containing additive solution to ensure all additives were dissolved as best as possible, and transferred 6 mL of additive solution into a series of pipettes using an Eppendorf repeater. Potassium chloride was used to vary the salinity (although some tubes did not need potassium chloride). Where needed, experimenters weighed out appropriate masses of potassium chloride on a piece of weighing paper, made a crease in the paper, and carefully poured the salt into each pipette. Immediately prior to sealing, nitrogen was blown into the open gas pocket above the liquid meniscus. The pipettes were then sealed by placing the pipette into the flame one inch above the bottom of the liquid meniscus, rotating the pipette until the glass glowed. The

excess glass was slowly pulled away, leaving behind a sealed top. The pipettes were then cooled and placed onto a metal observation rack.

Two types of pictures were taken: one before and one immediately after tilting the pipettes, which is defined as turning the pipettes upside down then right side up 10 times. Experimenters placed the pipettes inside a convection oven at a constant temperature for several days. Afterwards, the experimenters removed the pipette from the oven and took pictures immediately while the pipettes were hot. The pipettes were placed back into the oven for one hour, removed, tilted, and immediately photographed again.

3.3.4 Results and Discussion

Table 3.4 shows the aqueous stability results for 0.2 wt. % additive concentration.

Table 3.4: Aqueous Stability Results for 0.2 wt. % Additive

			Salinity (wt. % Potassium Chloride)					
			0.0		1.0		2.0	
Additive	Additive Conc. (wt. % in deionized water)	Temperature (°C)	Before Tilting	After Tilting	Before Tilting	After Tilting	Before Tilting	After Tilting
Organic alkali 1	0.2	150	C	C	C	C	C	C
Organic alkali 2	0.2	150	C	C	C	C	C	C
Organic alkali 3	0.2	150	C	C	C	C	C	C
Organic alkali 4	0.2	150	C	C	C	C	C	C
Organic alkali 5	0.2	150	C	C	C	C	C	C
Organic alkali 6	0.2	150	C	C	C	C	C	C
Organic alkali 7	0.2	150	C	C	C	C	C	C
Organic alkali 8	0.2	150	C	C	C	C	C	C
Organic alkali 9	0.2	150	C	C	C	C	C	C
Organic alkali 10	0.2	150	C	C	C	C	C	C
Organic alkali 11	0.2	150	C	C	C	C	C	C
Alcohol 1	0.2	150	C	C	C	C	C	C
Alcohol 2	0.2	150	C	C	C	C	C	C
Acid 1	0.2	150	C	C	C	C	C	C
Acid 2	0.2	150	C	C	C	C	C	C
Solvent 1	0.2	150	C	C	C	C	C	C

Table 3.4: Continued

Solvent 2	0.2	150	C	C	C	C	C	C
Solvent 3	0.2	150	C	C	C	C	C	C
Solvent 4	0.2	150	C	C	C	C	C	C

C - miscible, clear
S - liquid-liquid phase separation
T - turbid

At 0.2 wt. % additive concentration, Organic alkali 1 through Solvent 4 were all miscible with water at 150 °C at each of the salinities tested, before and after tilting. Table 3.5 shows the aqueous stability results for 0.5 wt. % additive concentration. All additives were miscible with water at 150 °C at all salinities (before and after tilting) except for TB, TC, Organic alkali 4, Organic alkali 6, and Alcohol 2. Experimenters saw a small volume of a second and less dense liquid phase at 150 °C in the TB solution, both before and after tilting. TC solution was turbid at 150 °C both before and after tilting. Both Organic alkali 4 and 6 solutions had small volumes of a second liquid phase at 150 °C, both before and after tilting. Finally, the Alcohol 2 solutions had a small volume of a second liquid phase at 150 °C before tilting. After tilting, there was also some turbidity. TB and TC are non-ionic surfactants. At 150 °C, the temperature was beyond both additive's cloud point, which is the temperature above which an aqueous solution containing a surfactant becomes turbid. Organic alkali 4 and 6 have longer hydrocarbon chains or hydrocarbon branches, which causes overall hydrophilicity of the molecules to decrease. Alcohol 2 has a longer hydrocarbon chain than Alcohol 1. Organic alkali 7-11 were completely miscible in water.

Table 3.5: Aqueous Stability Results for 0.5 wt. % Additive

			Salinity (wt. % Potassium Chloride)									
			0.0		0.5		1.0		1.5		2.0	
Additive	Add. Conc. (wt. % in deionized water)	Temp. (°C)	Before Tilting	After Tilting	Before Tilting	After Tilting	Before Tilting	After Tilting	Before Tilting	After Tilting	Before Tilting	After Tilting
TA	0.5	150	C	C	C	C	C	C	C	C	C	C
TB	0.5	150	S	S	S	S	S	S	S	S	S	S
TC	0.5	150	T	T	T	T	T	T	T	T	T	T
TD	0.5	150	C	C	C	C	C	C	C	C	C	C
TF	0.5	150	C	C	C	C	C	C	C	C	C	C
TG	0.5	150	C	C	C	C	C	C	C	C	C	C
TH	0.5	150	C	C	C	C	C	C	C	C	C	C
Organic alkali 1	0.5	150	C	C			C	C			C	C
Organic alkali 2	0.5	150	C	C			C	C			C	C
Organic alkali 3	0.5	150	C	C			C	C			C	C
Organic alkali 4	0.5	150	S	S			S	S			S	S
Organic alkali 5	0.5	150	C	C			C	C			C	C
Organic alkali 6	0.5	150	S	S			S	S			S	S
Organic alkali 7	0.5	150	C	C			C	C			C	C
Organic alkali 8	0.5	150	C	C			C	C			C	C
Organic alkali 9	0.5	150	C	C			C	C			C	C
Organic alkali 10	0.5	150	C	C			C	C			C	C

Table 3.5: Continued

Organic alkali 11	0.5	150	C	C			C	C			C	C
Alcohol 1	0.5	150	C	C			C	C			C	C
Alcohol 2	0.5	150	S	S, T			S	S, T			S	S, T
Acid 1	0.5	150	C	C			C	C			C	C
Acid 2	0.5	150	C	C			C	C			C	C
Solvent 1	0.5	150	C	C			C	C			C	C
Solvent 2	0.5	150	C	C			C	C			C	C
Solvent 3	0.5	150	C	C			C	C			C	C
Solvent 4	0.5	150	C	C			C	C			C	C

C - miscible, clear
S - liquid-liquid phase separation
T - turbid

3.4 PHASE BEHAVIOR

3.4.1 Purpose

The purpose of the phase behavior test was to study whether brine and bitumen can form emulsions in the presence of an additive by lowering the oil-water IFT. The additive might act as the surface-acting agent itself, or (in the case of the alkalis) extract natural surfactants found in the bitumen. As shown in Table 3.1, such a reduction in oil-water IFT can decrease the capillary forces that trap oil, which may decrease residual oil saturations or increase the oil production rate in a coreflood or sandpack flood. Thus, additives that cause emulsions to form in aqueous solution were considered attractive candidates for testing in permeable media. Experimenters also looked for any observable changes in the phase behavior pipettes for runs using additives such as the alcohols and solvents, which did not make emulsions but improved miscibility between bitumen and the aqueous phase.

3.4.2 Materials

The materials used in the phase behavior tests consisted of an analytical balance, 50 mL Fisherbrand polypropylene tubes, the additives listed in Table 3.2, a metal spatula, disposable Fisherbrand transfer pipettes, fire safety protective gear, a metal plate, a ring stand, a Benzomatic propane hand torch, tongs, 5 mL and 10 mL Fisherbrand borosilicate glass pipettes, an Eppendorf repeater with 5 mL tip, potassium chloride and sodium carbonate obtained from Fisher Scientific, weighing paper, dewatered bitumen (or the bitumen diluted with naphtha), a piston accumulator for holding the bitumen, a Chandler Engineering QX-6000 Series Pump, a nitrogen accumulator, a metal pipette rack, a convection oven, and a camera.

3.4.3 Procedure

The following is a prototypical procedure for the phase behavior test. Additive solutions and bottom-sealed 5 mL (or 10 mL) Fisherbrand borosilicate glass pipettes were made in the same way as in the aqueous stability tests. The pipettes were placed on a rack. Experimenters then shook the tube containing additive solution to ensure all additives were dissolved as best as possible, and accurately transferred 3.6 mL of additive solution (2.4 mL when using 10 mL glass pipettes) into a series of 5 mL pipettes using an Eppendorf repeater. Potassium chloride was used to vary the salinity (although some tubes did not need potassium chloride). Where needed, experimenters weighed out appropriate masses of potassium chloride on a piece of weighing paper, made a crease in the paper, and carefully poured the salt into each pipette.

Next, 2.4 mL of bitumen (1.6 mL when using 10 mL glass pipettes) was dispensed into each 5 mL pipette, making a total water-to-oil ratio of 1.5 in each pipette. This ratio was kept constant across all phase behavior experiments. To dispense the bitumen, experimenters heated bitumen in a sealed glass container inside a convection oven at 50 °C for around 30 minutes to decrease its viscosity. Bitumen was then added to each pipette using an Eppendorf pipette repeater. An improved method was used later on, where experimenters filled a clean piston accumulator with bitumen and used a QX-6000 Series Pump operating in the constant pressure mode at around 1600 psia to dispense the bitumen through a piece of stainless steel tubing. Since the bitumen was so viscous, it flowed at a reasonable rate despite the large pressure drop. The volume of bitumen dispensed into each pipette was determined by using the volume markings on the side of the glass pipettes. Using the piston accumulator and pump to dispense the bitumen made the process fast, with the added benefit of losing no bitumen and causing no bitumen to stain the upper

sections of the pipette on the inside wall, which precludes sealing later on as the bitumen would burn.

Immediately prior to sealing, nitrogen was blown into the open gas pocket above the liquid meniscus. The pipettes were then sealed by placing the pipette into the flame one inch above the bottom of the liquid meniscus, rotating the pipette until the glass glowed. The excess glass was slowly pulled away, leaving behind a sealed top. The pipettes were then cooled and placed onto a metal observation rack.

Experimenters placed the pipettes inside a convection oven at 150 °C for several days. Since the aqueous additive solution and bitumen interface was small, experimenters removed the pipettes from the oven once per day and tilted them in order to promote additive-bitumen contact. Tilting is defined as turning the pipettes upside down then right side up 10 times. The pipettes were then put back into the oven. Consistent mixing between each pipette was ensured by tilting the whole observation rack that each pipette sits in rather than tilting each pipette individually. Two types of pictures were taken: one before and one immediately after tilting the pipettes. At the end of seven days at 150 °C experimenters removed the pipettes from the oven and took pictures immediately while the pipettes were hot using a white background. The pipettes were placed back into the oven for one hour, removed, tilted, and immediately photographed again using a white background.

Finally, note that additives TA-TH and tests using Na_2CO_3 were performed using 5 mL Fisherbrand borosilicate glass pipettes, with a total liquid volume of 6 mL. Experimenters realized that using 10 mL pipettes allowed for better mixing during the tilt, and therefore switched to using 10 mL pipettes for Organic alkali 1 through Solvent 4. Further, the total volume of liquid was decreased down to 4 mL to conserve bitumen. This should not affect results, since the water-to-oil ratio was kept constant in all tests.

3.4.4 Results and Discussion

Table 3.6 below shows the phase behavior results for additives TA through TH, as well as for various tests done with Na_2CO_3, an inorganic alkali.

Table 3.6: Phase Behavior Results for Na_2CO_3 and TA Through TH at 0.5 wt. % and 150 °C

Additive	Salt	Salinity (wt. % Salt)								
		0.00	0.25	0.50	0.75	1.00	1.25	1.50	1.75	2.00
No additive (base case)[1]	KCl	NE		NE		NE		NE		NE
TA[2]	KCl	NE		NE		NE		NE		NE
TB[2]	KCl	NE		NE		NE		NE		NE
TC[2]	KCl	NE		NE		NE		NE		NE
TD	KCl	NE		NE		NE		NE		NE
TF	KCl	E				E				
TG	KCl	NE		NE		NE		NE		NE
TH	KCl	NE		NE		NE		NE		NE
---	Na_2CO_3	NE	E	E	E	E				
TA	Na_2CO_3	NE	E	E	E	E				
TB	Na_2CO_3	NE	E	E	E	E				
TC	Na_2CO_3	NE	E	E	E	E				
TD	Na_2CO_3	NE	NE	E	E	E				
Na_2CO_3	KCl	E				E				

[1] Same results for naphtha-diluted bitumen and the dewatered bitumen.
[2] The naphtha-diluted bitumen was used for these three runs. Dewatered bitumen was used for all other runs.
E - emulsions formed.
NE - no visible emulsions formed.

No additives above formed visible Winsor Type I (oil-in-water) or Type III (middle phase) emulsions at the temperatures and KCl concentrations tested, except for TF. TF was able to form Type I emulsions with the bitumen. Since TF is an organic alkali, this was

expected. Na_2CO_3 was able to form visible Type I and Type III emulsions with and without additives. This was also expected since Na_2CO_3 is an inorganic alkali. Na_2CO_3 undergoes hydrolysis to form NaOH (strong base) and carbonic acid (weak acid), causing a net increase in aqueous phase pH. TF also increases aqueous solution pH. Experimenters found a pH greater than 11 for a concentration of TF and Na_2CO_3 in deionized water greater than 1 and 0.25 wt. % respectively. Table 3.7 shows the phase behavior results for Organic alkali 1 through Solvent 4.

Table 3.7: Phase Behavior Results for Organic Alkali 1 Through Solvent 4 at 0.5 wt. % Additive and 150 °C

Additive	Salt	Salinity (wt. % Salt)					
		0.00		1.00		2.00	
		Before Tilting	After Tilting	Before Tilting	After Tilting	Before Tilting	After Tilting
No additive (base case)	KCl	NE	NE	NE	NE	NE	NE
Organic alkali 1	KCl	E	E	E	E	E	E
Organic alkali 2	KCl	E	E	E	E	E	E
Organic alkali 3	KCl	E	E	E	E	NE	E
Organic alkali 4	KCl	E	E	E	E	NE	E
Organic alkali 5	KCl	E	E	E	E	E	E
Organic alkali 6	KCl	NE	E	NE	E	NE	E
Organic alkali 7	KCl	E	E	E	E	E	E
Organic alkali 8	KCl	E	E	E	E	E	E
Organic alkali 9	KCl	E	E	E	E	E	E
Organic alkali 10	KCl	E	E	E	E	E	E
Organic alkali 11	KCl	E	E	E	E	E	E
Alcohol 1	KCl	M	M	M	M	M	M
Alcohol 2	KCl	M	M	M	M	M	M
Acid 1	KCl	NE	NE	NE	NE	NE	NE
Acid 2	KCl	NE	NE	NE	NE	NE	NE
Solvent 1	KCl	M	M	M	M	M	M
Solvent 2	KCl	M	M	M	M	M	M
Solvent 3	KCl	M	M	M	M	M	M
Solvent 4	KCl	M	M	M	M	M	M

E - emulsions visible.
M - darker aqueous phase (improved miscibility between bitumen and aqueous phase).
NE - no emulsions visible.

All visible emulsions (E) were oil-in-water emulsions. No emulsions were formed in the base case without any additive, and by the acids. The acids decreased aqueous solution pH, thus no natural soap was expected to have been extracted from the bitumen, which explains the absence of any visible emulsions.

Organic alkali 1 through 11 are organic alkalis. Before tilting, the pipettes were in a state where no disturbance had occurred for at least a day. Before tilting, emulsions were observed in the pipettes containing Organic alkali 1 through 11 except in Organic alkali 3 and 4 at 2 wt. % KCl, and in all pipettes containing Organic alkali 6. Organic alkali 3 and 4 have longer hydrocarbon chains than Organic alkali 1 and 2. This, in combination with a higher salinity at 2 wt. % KCl seemed to have stopped significant oil-in-water emulsions, causing the natural surfactants extracted to not favor the aqueous phase. Organic alkali 6 contains longer hydrocarbon chains, and as such the molecule is more hydrophobic, which can explain the absence of significant visible emulsions in the aqueous phase before tilting. Organic alkali 7 through 11 formed emulsions both before and after tilting. After tilting, significant emulsions were seen for Organic alkali 1 through 11, evidenced by very dark aqueous phases. However, experimenters observed that the dark aqueous phase was darker and remained dark longer for Organic alkali 7 through 11. This indicates improved oil-in-water emulsion formation as evidenced by the smaller oil droplets.

Alcohol 1, Alcohol 2, and Solvents 1 through 4 all caused the aqueous phase to look dark brown. However, this is attributed to improved miscibility between the aqueous and bitumen phase instead of oil-in-water emulsion formation since these molecules do not increase the pH. As with the organic alkali, the aqueous phase was significantly darker after tilting because of the disturbance breaking up the excess bulk bitumen phase. Overall, Organic alkali 7 through 11 show the most promise for improving oil recovery in permeable media as evidenced by strong oil-in-water emulsion formation. Organic alkali 1 through 6 show promise as well, but are ranked behind Organic alkali 7 through 11. Alcohol 1, Alcohol 2, and Solvent 1 through 4 may improve oil recovery by improved miscibility, but are not as promising as Organic alkali 7 through 11. Acids on the other

hand do not show promise to improve oil recovery in porous media based on the phase behavior test.

3.5 Phase Behavior in High-Temperature Visual Cells

3.5.1 Purpose

The purpose of this test was to test whether additives can lower the oil-water IFT. The test was used during the early phase of this study. The hypothesis was that when disturbed, the amount and size of bitumen droplets formed in the aqueous phase should give an indication of the oil-water IFT achieved by the presence of the additive. The smaller and more numerous the droplets, the lower the oil-water IFT achieved. The test was designed to look for additives that only lower the oil-water interfacial tension to non-ultralow values. (additives that do not form stable emulsions). Sapphire glass high-temperature visual cells were used, which were thicker in diameter than the pipettes used in the phase behavior tests. These cells allowed the experimenters to obtain clear pictures of bitumen droplets dispersed into the aqueous phase.

3.5.2 Materials

The materials used in this test consisted of an analytical balance, 50 mL Fisherbrand polypropylene tubes, additives, a metal spatula, disposable Fisherbrand transfer pipettes, high-temperature visual cells, toluene and ethanol obtained from Fisher Scientific, an Eppendorf repeater with 5 mL tip, potassium chloride obtained from Fisher Scientific, dewatered bitumen, a piston accumulator for holding the bitumen, a Chandler Engineering QX-6000 Series Pump, a nitrogen accumulator, a convection oven, and a camera.

3.5.3 Procedure

The following is a prototypical procedure for this test. Experimenters first leveled an analytical balance and then placed an empty 50 mL polypropylene tube into a small beaker, which was placed on the scale. The beaker held the tube vertical. The balance was tared, and the additive solution was made by adding an appropriate mass of additive, KCl, and deionized water into the tube. Solids were scooped using a clean metal spatula, while liquids were dispensed using a disposable transfer pipette. Experimenters capped the tubes and gently shook them until the components were dissolved. The above procedure was repeated to make other additive solutions as needed. A 1 wt. % KCl concentration was chosen for all runs to provide some salinity.

Next, the visual cells were cleaned. First, O-rings were removed and examined for damages. The metal and glass components were taken apart and sequentially cleaned with toluene, ethanol, and deionized water. The metal and glass components were then put into a convection oven and dried at 120 °C for one day to evaporate all liquids that remained from the cleaning process. The parts were then removed from the oven, allowed to cool to room temperature, and assembled with the O-rings.

Experimenters then shook the tubes containing the additive solutions to ensure all additives were dissolved as best as possible, and accurately transferred 9 mL of additive solution into each cell using an Eppendorf repeater. Next, 1 mL of bitumen was dispensed into each visual cell, making a total water-to-oil ratio of 9 (v/v) in each pipette. This ratio was kept constant across all runs. To dispense the bitumen, experimenters heated bitumen in a sealed glass container inside a convection oven at 50 °C for around 30 minutes to decrease its viscosity. Bitumen was then added to each cell using an Eppendorf pipette repeater. An improved method was used later on, where experimenters filled a clean piston accumulator with bitumen and used a QX-6000 Series Pump operating in the constant

pressure mode at around 1600 psia to dispense the bitumen through a piece of stainless steel tubing. Since the bitumen is so viscous, it flowed at a reasonable rate despite the large pressure drop. The volume of bitumen dispensed into each pipette was determined by using the volume markings on the side of the glass. Using the piston accumulator and pump to dispense the bitumen made the process fast, with the added benefit of losing no bitumen.

Immediately prior to sealing the cells, nitrogen was blown into the open gas pocket above the liquid meniscus. Then the cells were sealed, and leak tested by connecting each cell to a small vessel containing pressurized nitrogen at the top through a valve. Once the leak test passed, the pressure was released from the top and the valve was closed. There were no leaks in all runs, evidenced by no salt buildup outside of the cells, and no decrease in the total liquid level. The cells were placed into a convection oven at 150 °C. After one day, the cells were removed from the oven and immediately turned upside down once. Video footage was recorded with a white background. A second upturn was not performed due to bitumen coating the inner surface of the cell during the first, hindering or in some cases precluding observation of the bitumen droplets.

3.5.4 Results and Discussion

Fig. 3.6 below shows the results for this test. Each cell contains dewatered bitumen and an aqueous solution composed of 0.5 wt. % additive and 1 wt. % KCl in deionized water. The total volume of liquid was 10 mL, and the water-to-oil ratio was 9 by volume. Each cell was heated inside a convection oven at 150 °C for 1 day before being photographed. Each picture depicts the cell right after being removed from the oven and immediately turned upside down.

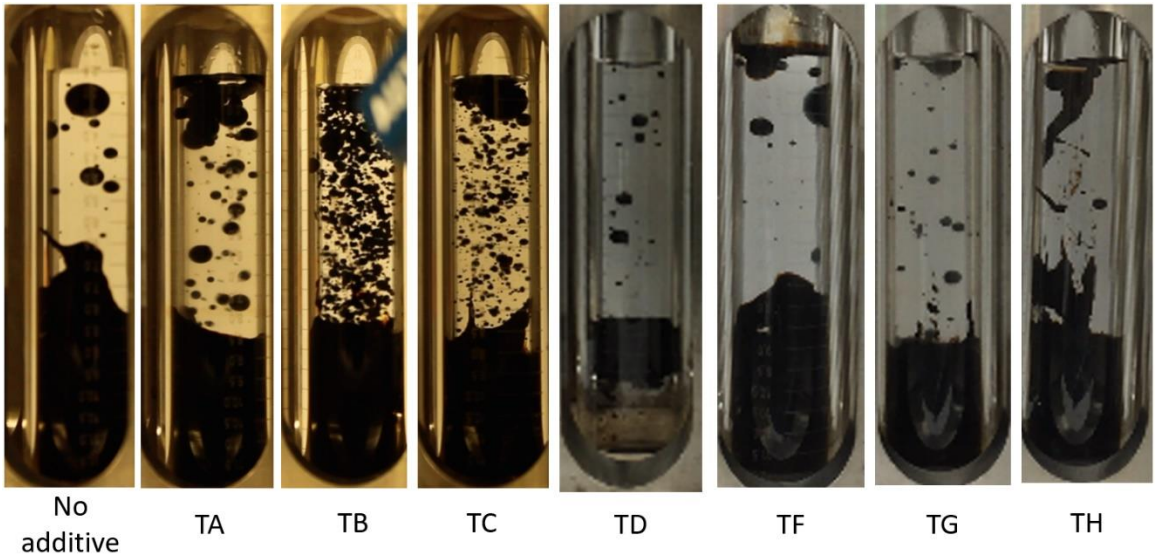

Figure 3.6 Phase behavior in high-temperature visual cells for additives TA through TH.

Experimenters observed significantly more bitumen droplets in the aqueous phase with TB and TC, which were non-ionic surfactants and lowered the oil-water IFT. The phase behavior test did not show this effect, but a clear difference between TB and TC compared to the base case without any additive could be seen in Fig. 3.6. The aqueous stability test showed that 0.5 wt. % TB had some liquid-liquid phase separation at 150 °C, and 0.5 wt. % TC in deionized water was turbid. Both suffer from aqueous stability issues. However, TB and TC were able to lower the oil-water IFT despite that. TF solution was basic, but no emulsions or increased droplet formation was observed. The cells were only heated for one day, and no tilting could be done to help promote additive-bitumen contact prior to the moment the picture was taken, since this would have stained the clean parts of the inner wall of the cell. These two facts best explain why no significant increase in the amount and decrease in the size of bitumen droplets was observed for TF.

Chapter 4 Additive Characterization in Three-phase Systems

Chapter 4 provides details on additive characterization tests performed in three-phase systems, which are composed of bitumen, additive solution, and a mineral. These experiments test for whether the additives can alter the wettability of the mineral surface or move the contact line between the three phases. For each characterization test, the chapter gives the materials used, experimental procedures followed, results obtained, and a discussion of the results.

1.1 Overview

The design of the high-temperature characterization tests discussed in this chapter centers around wettability alteration. Table 3.1 contains a complete list of mechanisms covered by all the characterization tests. The additives used are the ones listed in Table 3.2 of Chapter 3. Experimenters used the dewatered bitumen for all experiments covered in this chapter. The details, results, and discussion of the characterization tests performed in three phase systems are presented in the following sections. Again, these tests along with the tests presented in Chapter 3 serve to find promising additives from the selection pool that might improve oil recovery in a core or sandpack flood mimicking SAGD conditions.

1.2 Wettability Test – Silica and Quartz Grains

4.2.1 Purpose

The purpose of this test was to see whether an additive in aqueous solution can alter the wettability of various silica and quartz grains to more water-wet and peel away bitumen from grains that have been fully coated and aged in bitumen. The aging process makes the surface of the grains more oil-wet by adsorption of molecules from the bitumen phase onto the surface. No contact line should be available at the beginning of the test when the

surfaces of every grain used were covered with bitumen. Successful additives must therefore reach the mineral surface by diffusion or some other means before altering the wettability of the grain surface.

4.2.2 Materials

The materials used in this test include an analytical balance, 50 mL Fisherbrand polypropylene tubes, potassium chloride obtained from Fisher Scientific, a metal spatula, disposable Fisherbrand transfer pipettes, 1/16" – 3/16" diameter quartz grains obtained from Ward's Science, 1.7-1.4 mm diameter silicon dioxide glass spheres obtained from Potters Industries LLC, 140-170 Mesh silica sand obtained from Agsco, a glass petri dish, ethanol obtained from Fisher Scientific, stainless steel high-pressure cells, a nitrogen accumulator, a convection oven, dewatered bitumen, a glass vial, Teflon tape, an Eppendorf repeater with 5 mL tip, and a camera.

.

4.2.3 Procedure

The following is a prototypical procedure for this test. Experimenters first leveled an analytical balance and then placed an empty 50 mL polypropylene tube into a small beaker, which was placed on the scale. The beaker held the tube vertical. The balance was tared and 1 wt. % KCl solution was made by adding an appropriate mass of KCl and deionized water into the tube. Solids were scooped using a clean metal spatula, while liquids were dispensed using a disposable transfer pipette. Experimenters capped the tubes and gently shook them until the components were dissolved. Experimenters found that heating the bitumen-coated grains with 1 wt. % KCl solution containing no additive at 250

°C was hot enough to remove a significant amount of bitumen from the sand grains already. Therefore, no additives were tested.

Next, the experimenters cleaned grains using ethanol and deionized water, and then placed an aliquot of the grains into a glass petri dish and dried it inside a convection oven at 120 °C. The grains used in this test were quartz grains obtained from Ward's Science, glass spheres obtained from Potters Industries LLC, and silica sand obtained from Agsco. The sand was then removed from the oven, allowed to cool, and stirred with an equal mass of dewatered bitumen in a glass vial to fully coat all the grains. The vial was sealed with a cap and Teflon tape, and placed inside a convection oven at 80 °C to age the grains. At the end of seven days, the bitumen-sand mixture was taken out from the oven and allowed to cool to room temperature. After aging, experimenters transferred approximately 6 grams of the bitumen-grain mixture into a stainless steel high-pressure cell and added 50 mL of aqueous solution into the cell using an Eppendorf repeater.

Oxidation of bitumen is known to harden the bitumen and proceeds at a higher rate at higher temperatures (Lamontagne *et al.,* 2001). To minimize bitumen oxidation, experimenters connected a nitrogen accumulator to the middle of the cell and bubbled nitrogen through the aqueous solution for 5 minutes to deoxygenate the solution and displace the air at the top of the cell. The cell was then sealed, and leak tested with nitrogen at high pressure. Experimenters then released the pressure and heated the cells in a convection oven at 250 °C for three days. Afterwards, the cells were removed from the oven and allowed to cool to room temperature. Experimenters then opened the cells and carefully decanted the solutions into 50 mL polypropylene tubes. The sands were removed along with remaining bitumen coated on the sands, placed on a white background, and photographed.

4.2.4 Results and Discussion

Fig. 4.1 shows the results for quartz grains and glass spheres. After heating in the presence of 1 wt. % KCl solution at 250 °C, significant amounts of bitumen were removed from the surface of the siliceous grains even without additive. Some spots of bitumen remain stuck on the grains. In the case of glass spheres, the corners where glass spheres touch helped to retain some of the bitumen but most of the bitumen peeled off. Since bitumen viscosity decreases exponentially with increasing temperature, viscosity was not a deterrent to the bitumen moving.

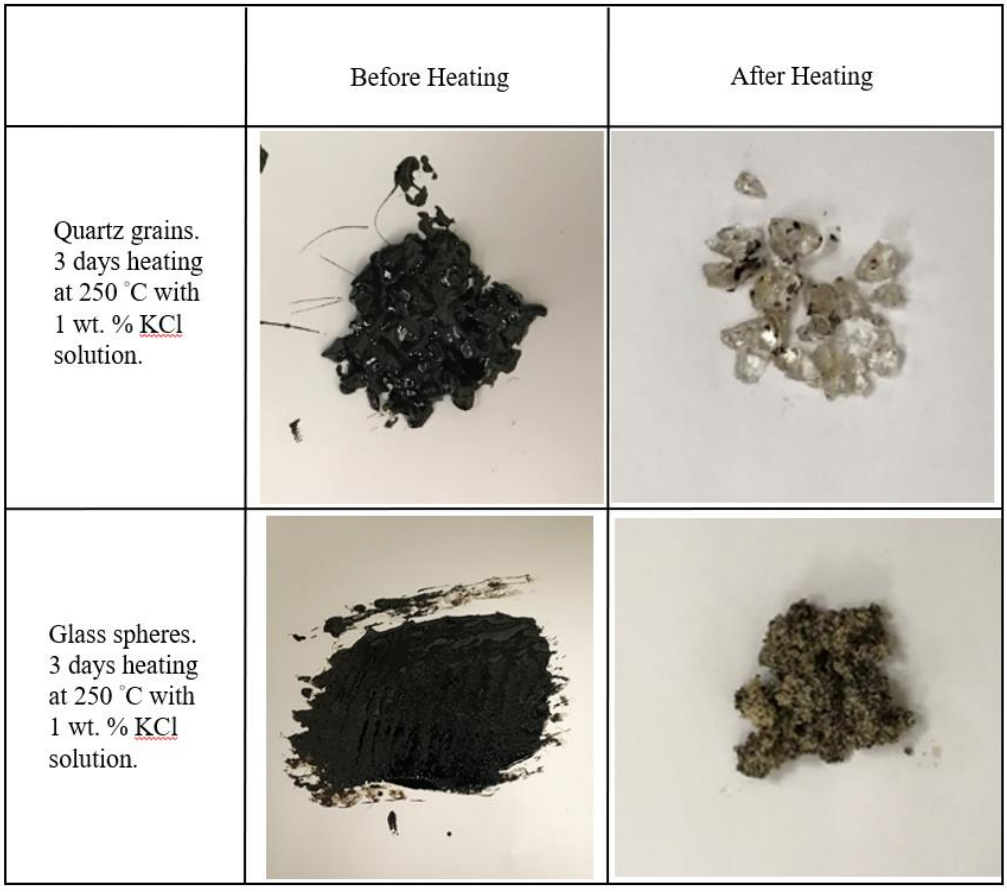

Figure 4.1: Aged bitumen and siliceous grain mixture heated in 1 wt. % KCl solution at 250 °C for three days.

Fig. 4.2 shows the results for silica sand. Again, significant amounts of bitumen were removed from the surface of the silica sand grains as well, so no additives were tested. Arsalan (2011) showed that the surface energy of Ottawa sand and Berea sandstone decreases with increasing temperature, due to the weakening of electrostatic forces as thermal vibrations becomes more energetic. The surface energy can be thought of as the increase in total free energy due to the presence of solid surfaces, which are exposed to the surroundings, and thus in an energetically unfavorable state. A lower surface energy at high temperature then means that a configuration where the surface is covered with the bitumen might be less favorable compared to the case of high surface energy.

	Before Heating	After Heating
Silica sand, 3 days heating at 250 °C with 1 wt. % KCl solution.		
Silica sand, 3 days heating at 250 °C with 1 wt. % KCl solution.		

Figure 4.2: Aged bitumen and silica sand mixture heated in 1 wt. % KCl solution at 250 °C for three days.

4.3 Wettability Test – Quartz Crystals and Berea Core Plugs

4.3.1 Purpose

The purpose of this experiment was to test whether any of the additives can move the contact line (the line where the aqueous, bitumen, and solid phase meet) and thus clean the bitumen off from the mineral surface. Experimenters were also interested in the degree of cleaning. They wanted to have a configuration where a clear contact line was present, so that the additive can have a place to attack the solid mineral surface right from the moment the additive solution was added. To create this clear contact line, experimenters

used slender quartz crystals and small Berea core plugs dipped half way and aged in bitumen.

4.3.2 Materials

The materials used in this test include quartz crystals obtained from Ward's Science, Berea core plugs, ethanol and toluene from Fisher Scientific, a glass petri dish, an analytical balance, a convection oven, dewatered bitumen, glass vials, stainless steel high-pressure cells, the additives listed in Table 3.2, potassium chloride from Fisher Scientific, a nitrogen accumulator with nitrogen gas, Kimwipes, soft cotton swabs, an Eppendorf repeater with 5 mL tip, 50 mL Fisherbrand polypropylene tubes, Teflon tape, a metal spatula, disposable Fisherbrand transfer pipettes, and a camera.

4.3.3 Procedure

The following is a prototypical procedure using slender quartz crystals. Experimenters rinsed the crystals with ethanol and deionized water, then placed them into a glass petri dish and into a convection oven at 120 °C to dry. The crystals were removed, and allowed to cool for one hour. Experimenters then immediately submerged the bottom half of each crystal into dewatered bitumen inside its own glass vial. The vials were capped, placed in a convection oven at 80 °C, and aged for a period of time.

Experimenters prepared stainless steel high-pressure cells for heating the crystals in aqueous solution. The cells were taken apart and thoroughly and sequentially cleaned using toluene, ethanol, and deionized water. The parts were then dried in a convection oven at 120 °C for three hours. Experimenters then removed the parts, allowed them to cool to room temperature, replaced any damaged O-rings, and assembled the cells. The cells were

leak tested at over 900 psig using nitrogen gas by submerging the nitrogen-filled cells under water, making sure that no gas bubbles were escaping. The pressure was released, and the cap was removed.

Next, experimenters removed the vials containing aged quartz crystals from the oven, and allowed them to cool to room temperature. Experimenters then carefully pulled the crystals out of the bitumen, wiped away some excess bitumen using a Kimwipe or soft cotton swab, and photographed the crystals using a white background. The crystals were then placed into the cell. Using an Eppendorf repeater, experimenters added 45 mL of the aqueous solution into the cell, leaving a section of gas at the top to account for the volumetric expansion of the solution at high temperature. Experimenters then connected a nitrogen accumulator to the cell and bubbled nitrogen through the solution for 5 minutes to deoxygenate the solution and displace the air at the top. Experimenters left the pressure inside the cell at atmospheric pressure, since the total pressure will increase to the saturation pressure of water at the set temperature of the oven. The cells were then sealed, and placed inside a convection oven at 250 °C. After three days, experimenters removed the cells from the oven, allowed them to cool to room temperature, and took off the caps. Excess bitumen floating at the top of the solution was dabbed away with a Kimwipe or cotton swab, and the aqueous solution was carefully decanted into a 50 mL polypropylene tube. Experimenters then removed the crystals, and photographed them using a white background.

The experimental procedure used when using Berea core plugs were the same except for the following improvements and modifications. Berea core plugs 1” in diameter and length were each cleaned and dried using the way mentioned above. These plugs were dipped halfway into bitumen and aged. Experimenters found that aging for four days at room temperature created a clear contact line. Once the cells were prepared, the plugs were

placed into the cell with the unaged side on the bottom. These cells were heated at 150 °C. After the heating period, cooling to room temperature, and with the aqueous solution decanted, the cells were opened on the bottom to reduce the risk of inadvertent bitumen staining while removing the plugs.

4.3.4 Results and Discussion

Fig. 4.3 shows the results for quartz crystals that were aged in bitumen at 80 °C, then heated in 1 wt. % KCl aqueous solution at 250 °C for 3 days. The bitumen was completely peeled off from the quartz crystal after heating. In the case of quartz grains and glass spheres, some amount of bitumen remained on the mineral surfaces due to more complex topology. However here, the bitumen was completely peeled off. This was not only due to the smooth topology, but also due to the decrease in surface energy of the quartz surface, and the significant decrease in the viscosity of the bitumen at high temperature. Even when the aging period was lengthened to two months, the quartz crystal was still completely cleaned after heating. Creating a contact line using pure quartz crystals would not work, so experimenters decided to use a real piece of sandstone instead.

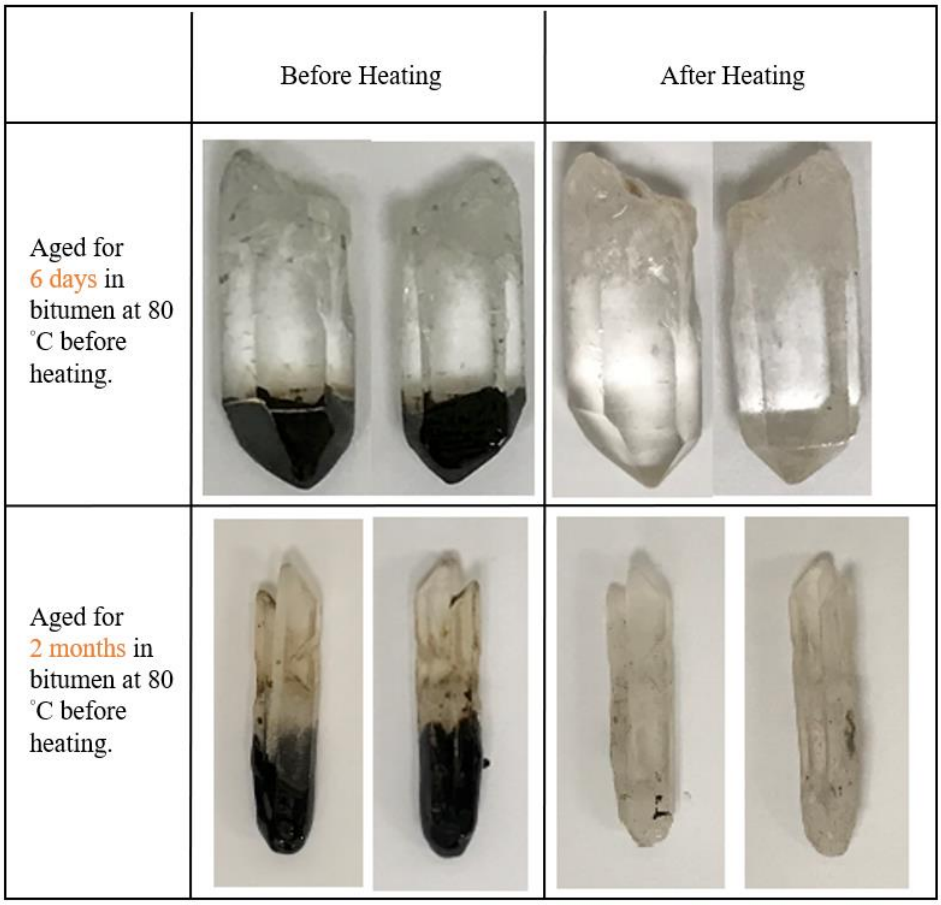

Figure 4.3: Quartz crystals aged in dewatered bitumen, then heated in 1 wt. % KCl for three days at 250 °C.

First, different aging procedures were tested. Fig. 4.4 shows these results. The first row shows pictures of a single Berea core plug that was aged by dipping them halfway into dewatered bitumen, then kept in an oven at 80 °C for seven days. As can be seen in Fig. 4.4, at the end of seven days of aging, the entire plug is dark. No definite contact line can be clearly seen. The bitumen traveled upward by capillary forces and stained the upper half of the plug as well. Even though the native Berea core plug should be more water-wet than oil-wet, bitumen was a more wetting phase than air. After heating in 1 wt. % KCl solution at 150 °C for three days, the plug remained dark. The bitumen did not peel from the Berea

core plug. Likewise, the core plug shown in the second row was aged in the same way, but for a shorter period of time. Still, the entire plug was stained at the end of aging.

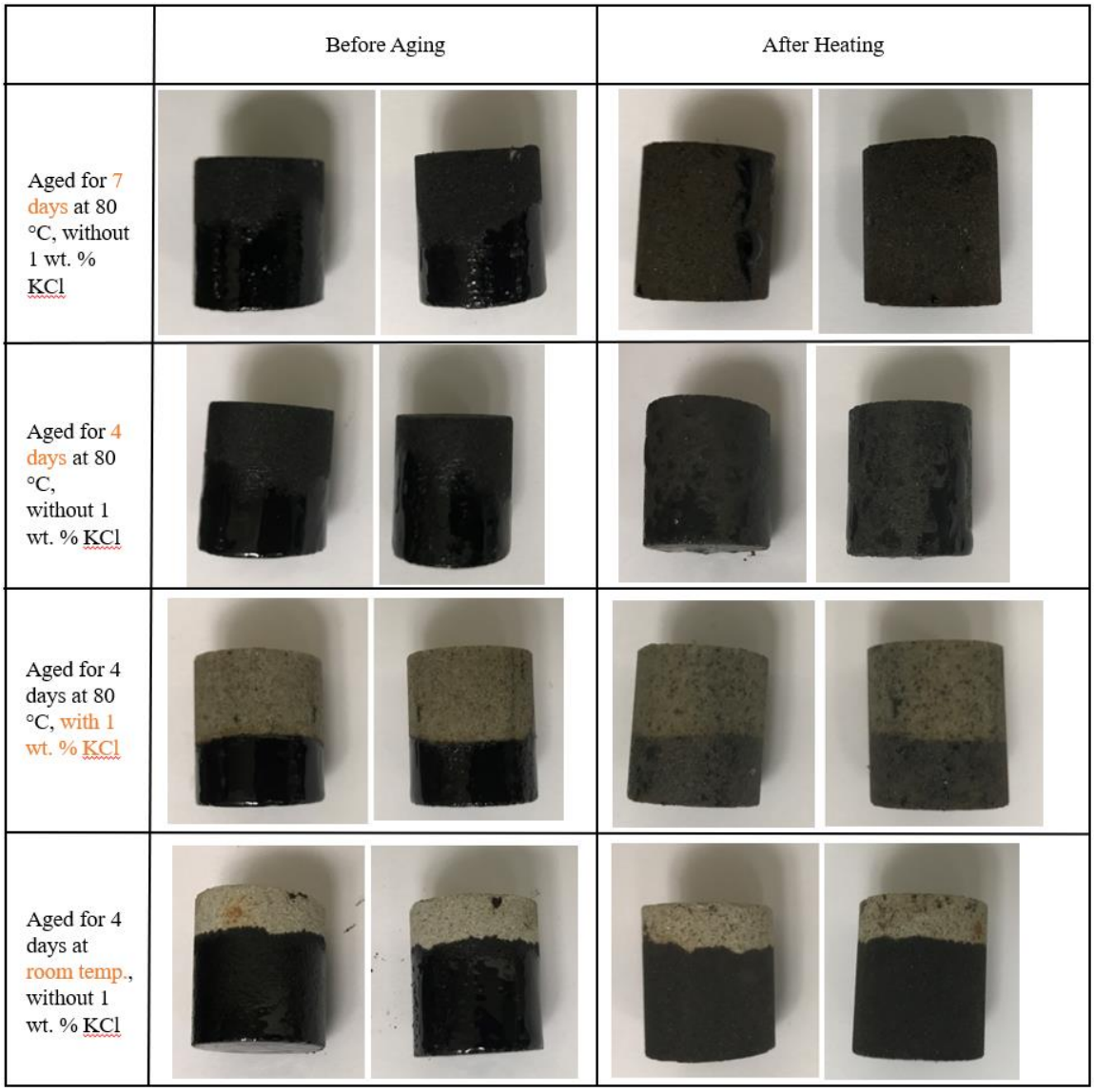

Figure 4.4: Berea core plugs aged using various parameters, then heated in 1 wt. % KCl for three days at 150 °C.

The third row shows a Berea core plug that was aged for four days at 80 °C, but in the presence of deionized water with 1 wt. % KCl. The plug was dipped halfway into bitumen, then the 1 wt. % KCl solution was dispensed into the vial, submerging the upper half of the plug. After aging, a definite contact line was obtained. Water was a more wetting phase than bitumen, and thus prohibited upward bitumen movement. However, after heating the plug in 1 wt. % KCl solution at 150 °C for three days, the stain was significantly lighter than before. The presence of water during the aging process seemed to have limited the process. It is possible that a thin layer of water could have been formed between the bitumen and mineral surface during the course of aging, which would have slowed down the aging process. The Berea core plug aged using the final aging procedure is shown in the fourth row. The core plug was dipped half way into the bitumen, then simply aged at room temperature for four days. The bitumen traveled upward, but the rate of upward movement was significantly decreased compared to aging at 80 °C. A visible contact line was established, and following heating at 150 °C in 1 wt. % KCl solution for three days, the stain remained dark. The latter can be attributed to the fact that no water was used during aging. The aging procedure used on the Berea core plug in the fourth row was then adopted as the standard aging procedure for all the runs using Berea core plugs to follow. The Berea core plug in the fourth row also represents the base case. Neither significant contact line movement nor bitumen peeling was observed.

Using the finalized core plug aging parameters, experimenters tested whether several organic alkalis (Organic alkali 1, 3, 7, and 8) with differing hydrocarbon chain lengths could move the contact line or cause significant amounts of bitumen to peel off. Fig. 4.5 shows the results. In this figure, the plug in each row is different from the others. Each plug was aged and heated at 150 °C for three days in the presence of an additive solution composed of 0.5 wt. % of the indicated additive and 1 wt. % KCl. In each of the

cases, neither significant movement of the contact line nor significant peeling of bitumen was observed. Note that the dark spots in the upper half of the plug in the fourth row was made unintentionally. This happened when the plug contacted some bitumen stuck on the inner walls of cell while being removed after heating. Minor stains can be seen in the plug in the first and third rows as well.

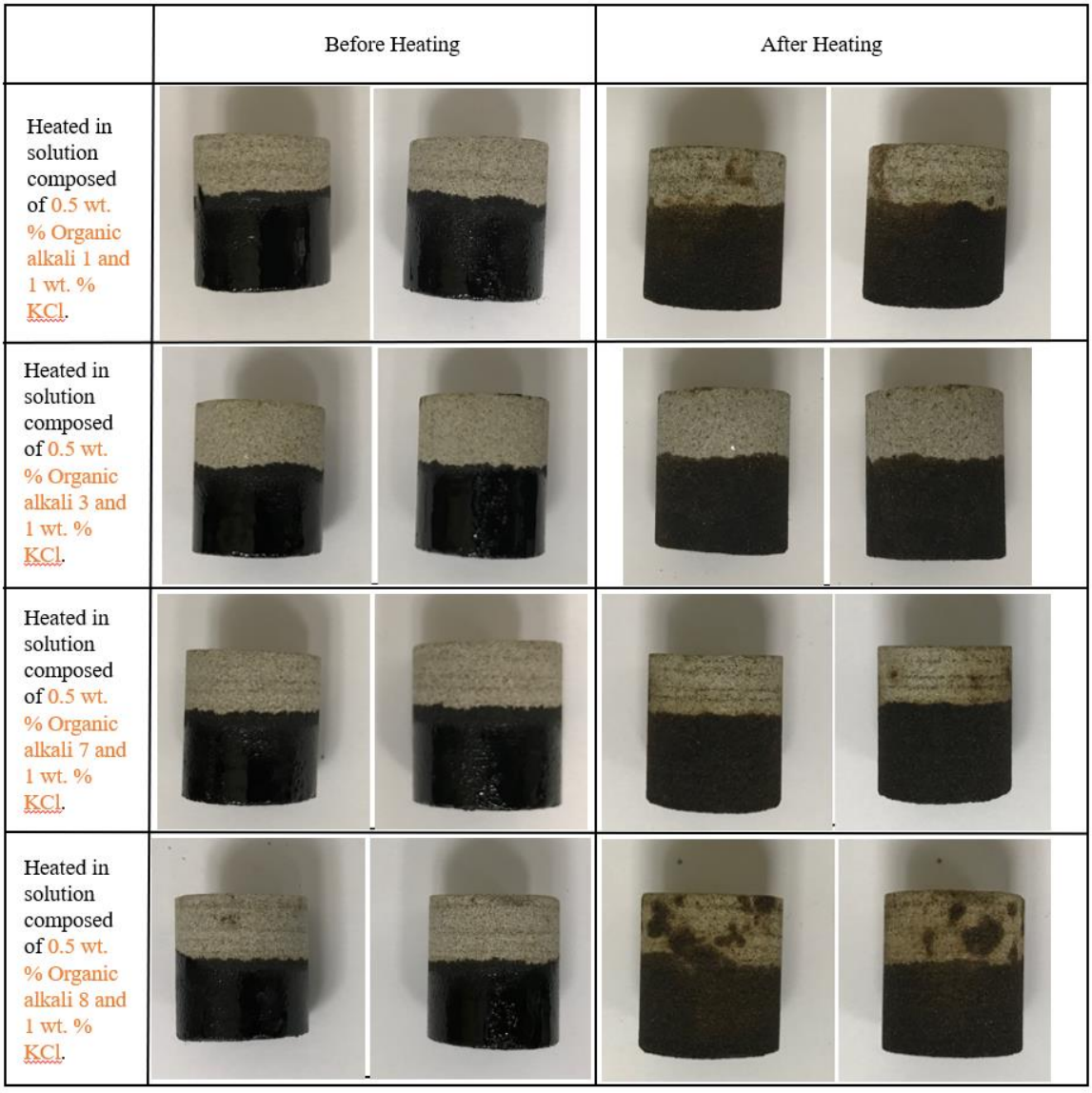

Figure 4.5: Aged Berea core plugs heated at 150 °C for three days in the presence of organic alkalis of various hydrocarbon lengths.

Fig. 4.6 shows the results of Berea core plugs heated in the presence of Na_2CO_3 (first row) and various alcohol solvents (second, third, and fourth row). Again, the core plugs were aged for four days at room temperature to create the distinct contact line prior to heating. Again, in each of the cases, neither significant movement of the contact line nor

significant peeling of the bitumen was observed. Dark spots in the upper half of the plugs were made due to the same reason explained for their counterparts in Fig. 4.5. Presence of the dark spots does not affect the conclusion from the results.

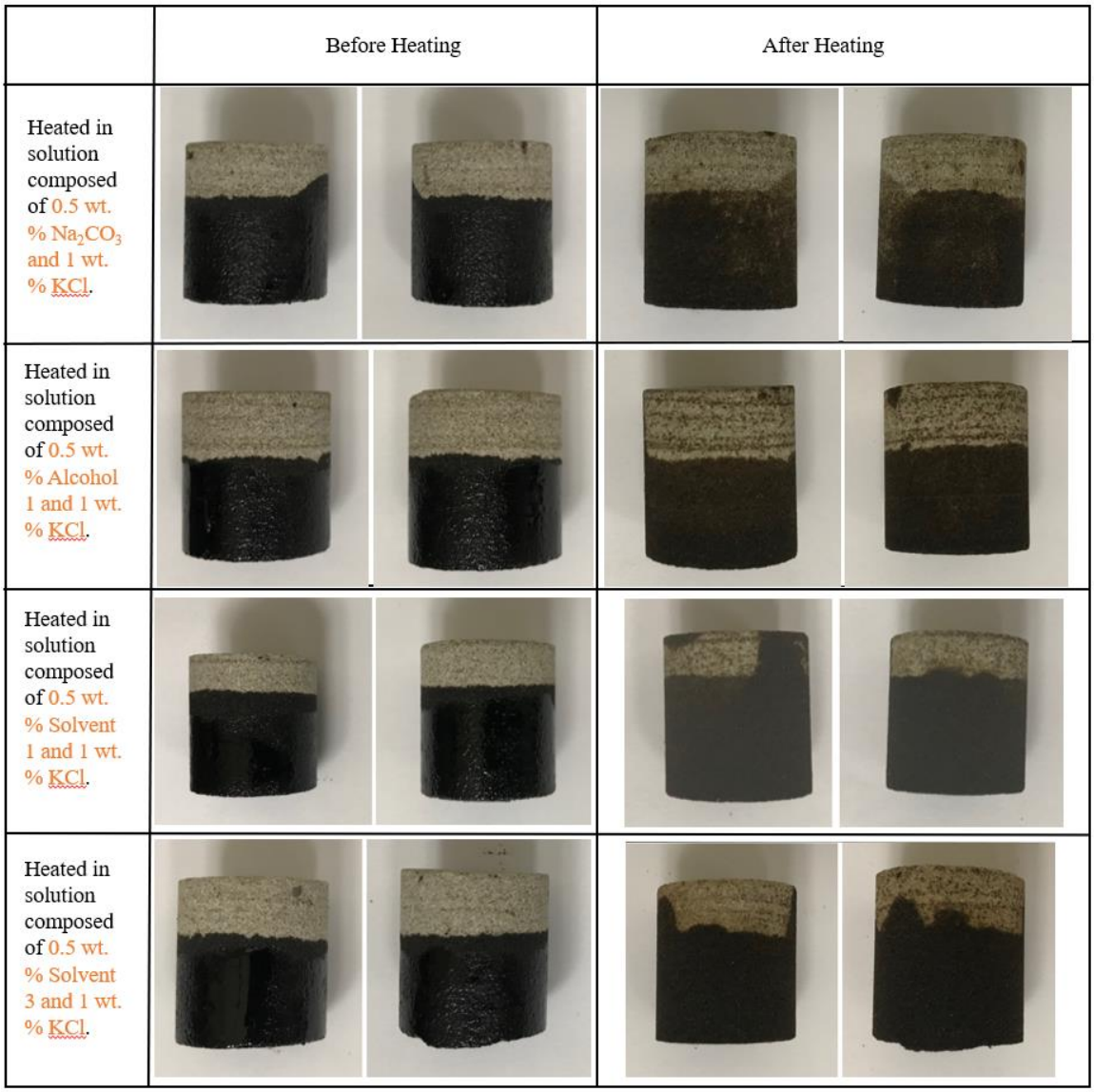

Figure 4.6: Aged Berea core plugs heated at 150 °C for three days in the presence of sodium carbonate, and various alcohol solvents.

Fig. 4.7 shows the results of Berea core plugs heated in the presence of two organic alkali of differing degrees of branching (first and second row) and in an acid (third row). As before, the core plugs were aged for four days at room temperature to create the distinct contact line prior to heating. In each of the cases, the experimenters did not observe any significant movement of the contact line and peeling of the bitumen. The explanation for the dark spots in Fig. 4.6 also applied to their counterparts in this figure.

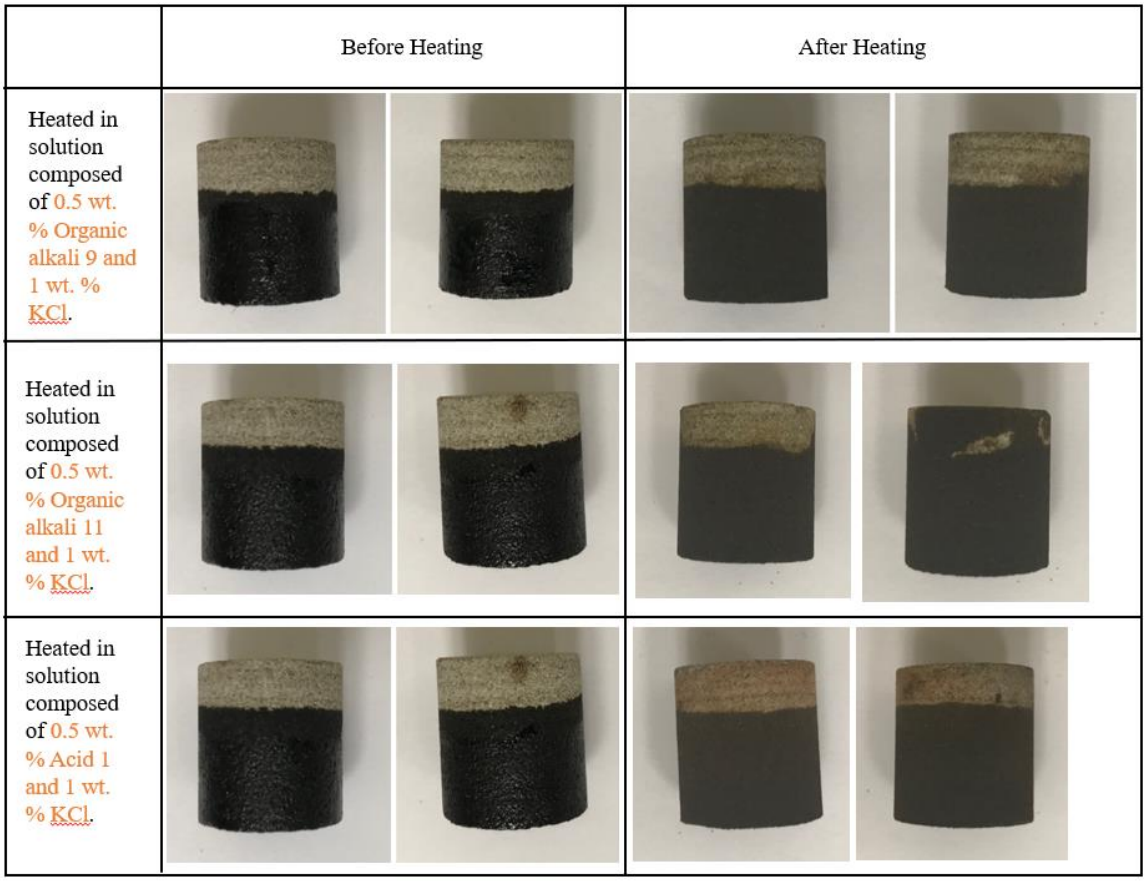

Figure 4.7: Aged Berea core plugs heated at 150 °C for three days in the presence of Acid 1 and organic alkalis of various degrees of branching.

The experiments done using the various siliceous quartz grains and the quartz crystals showed that high temperature experiments using pure quartz minerals was not

conducive to finding out an additive's wettability alteration potential. It was observed that almost all of the bitumen gets peeled off at temperatures at least above 150 °C, even with two months of aging time. These Berea core plugs did not show that the additives tested move the macroscopic contact line downwards appreciably, and no shown signs of significant bitumen removal from the surface of the plugs appeared. Note that at the time these tests using Berea core plugs were conducted, the researchers had moved from the TA through TH series of additives to Organic alkali 1 through Solvent 4, and thus they were not tested. Organic alkali 1 through Solvent 4 were selected to incorporate the most attractive chemical families from TA through TH, and additionally included the acid family. The additives selected from Organic alkali 1 through Solvent 4 for the Berea core plug studies represented the most interesting variation in molecular structure, and encompassed all the chemical families in that additive pool. Thus, not every single additive was tested and needed to be tested to reach the conclusions presented herein.

4.4 WETTABILITY TEST – CALCITE CRYSTALS

4.4.1 Purpose

The purpose of this test was two-fold. First, in similar manner to the experiment detailed in section 4.3, experimenters wanted to test a configuration where a clear contact line (line where the solid, bitumen, and aqueous solution phases meet) was present, which can give additives a location to attack the mineral surface starting at the very beginning of heating. Experimenters wanted to see whether any of the additives can move this contact line, cleaning bitumen off from the mineral surface, and if so how significant the cleaning can be. Secondly, the experimenters used calcite crystals in this test, since carbonate formations are another important type of reservoir that contains viscous oils.

4.4.2 Materials

The materials used in this experiment include Iceland spar calcite crystals obtained from Ward's Science, a metal hacksaw, ethanol and toluene from Fisher Scientific, a glass petri dish, an analytical balance, a convection oven, dewatered bitumen, glass vials, stainless steel high-pressure cells, the additives listed in Table 3.2, potassium chloride from Fisher Scientific, a nitrogen accumulator with nitrogen gas, Kimwipes, soft cotton swabs, an Eppendorf repeater with 5 mL tip, 50 mL Fisherbrand polypropylene tubes, Teflon tape, a metal spatula, disposable Fisherbrand transfer pipettes, and a camera.

4.4.3 Procedure

The following is a prototypical procedure for this test. A large block of calcite crystal was protected with cushioning and secured in a vice. The experimenters then used a metal hacksaw to cut out a small calcite crystal roughly three centimeters in length from the larger mineral block. Calcite crystals have three cleavage planes, so smaller crystals that fit the high-pressure cells and with smooth surfaces were able to be procured this way. The crystal was cleaned with ethanol and deionized water, placed into a glass petri dish, and dried inside a convection oven at 120 °C for one day. They were then removed from the oven and allowed to cool for one hour. Experimenters then immediately submerged the bottom half of each crystal into dewatered bitumen inside separate glass vials. The vials got capped, and the crystals were aged.

Experimenters prepared stainless steel high-pressure cells for heating the crystals in aqueous solution. The cells were taken apart and sequentially cleaned by using toluene, ethanol, and deionized water thoroughly. The parts were then dried in a convection oven

at 120 °C for three hours to evaporate all liquids remaining on the cells. Experimenters then took out the parts from the oven, allowed them to cool to room temperature, replaced any damaged O-rings, and assembled the cells. The cells were leak tested at over 900 psig using nitrogen gas by submerging the nitrogen-filled cells under water, making sure that no gas bubbles were escaping. The pressure was released, and the cap was removed.

The vials containing the aged calcite crystals were removed from the oven and allowed to cool to room temperature. The experimenters carefully pulled each crystal out of the vial, dabbed away excess bitumen with a cotton swab or Kimwipe and photographed the crystals using a white background. The crystals were then placed into the cell. Using an Eppendorf repeater, experimenters added 45 mL of the aqueous solution into the cell, leaving a section of gas at the top to account for the volumetric expansion of the solution at high temperature. Experimenters then connected a nitrogen accumulator to the cell and bubbled nitrogen through the solution for 5 minutes to deoxygenate the solution and displace the air at the top. Experimenters left the pressure inside the cell at atmospheric pressure, since the total pressure will increase to the saturation pressure of water at the set temperature of the oven. The cells were then sealed, and placed inside a convection oven at either 150 °C or 250 °C. After three days, experimenters removed the cells from the oven, allowed them to cool to room temperature, and removed the caps. Excess bitumen floating at the top of the solution was dabbed away with a Kimwipe or cotton swab, and the aqueous solution was carefully decanted into a 50 mL polypropylene tube. Experimenters then removed the crystals from the bottom, and photographed them using a white background.

4.4.4 Results and Discussion

The aged crystals were heated in aqueous solution at either 150 °C or 250 °C for three days. Fig. 4.8 shows the results for the base case. Each black-bordered pane is comprised of four photos of a single calcite crystal on different sides. The left panes show the aged crystal right before heating. The right panes show the crystal after heating. The calcite crystals shown in the first and second row were heated in the presence of 1 wt. % KCl for three days at 150 °C and 250 °C, respectively. Experimenters observed beading up of bitumen droplets and a partial removal of bitumen from the surface at both temperatures. Unlike the quartz crystals, the bitumen was not completely peeled off from the surface of the calcite mineral, even after heating at 250 °C. The calcite surfaces seems to have been much more oil-wet than that of quartz. Successful additives should remove significant amounts of bitumen from the calcite surface, noticeably more than those in the base case. Ideally, additives should be able to completely clean the surface.

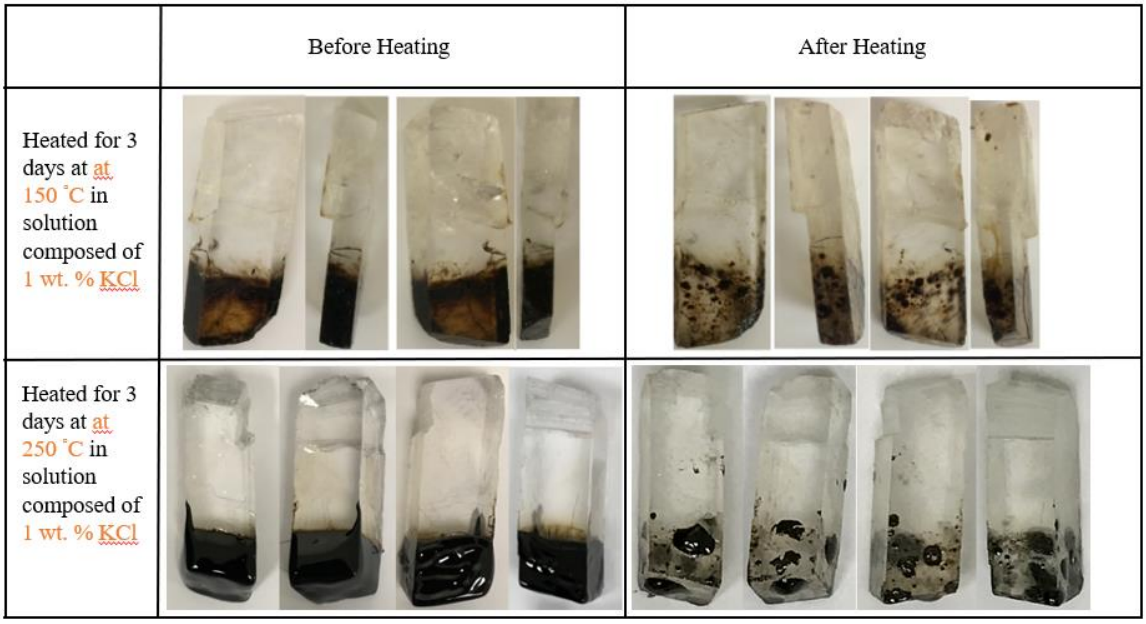

Figure 4.8: Aged calcite crystals heated in the presence of 1 wt. % KCl solution. These are the base case runs.

Fig. 4.9 shows the results for additives TA, TB, and TC. TA is an alcohol solvent, while TB and TC are non-ionic surfactants. The peeling of bitumen and associated movement of the contact lines were not more significant compared to the base case at 250 °C.

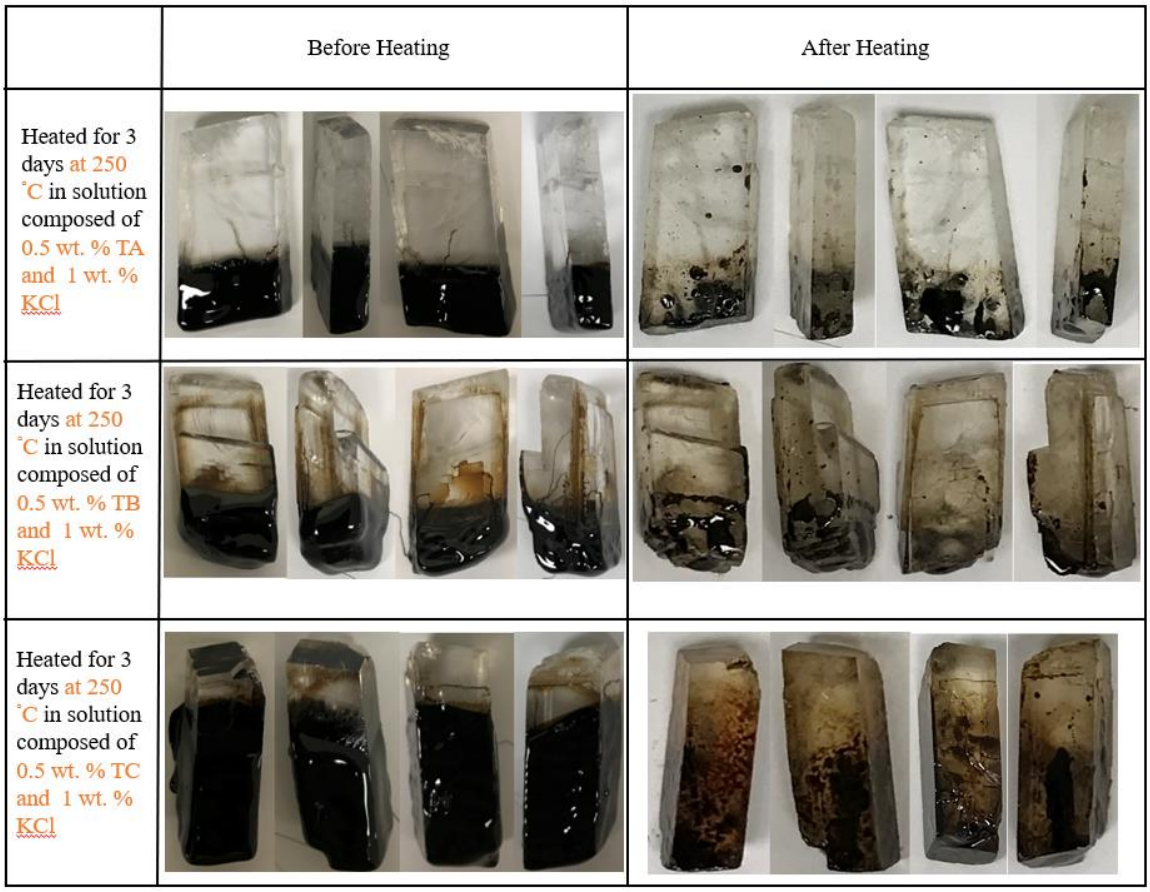

Figure 4.9: Aged calcite crystals heated at 250 °C in the presence of TA, TB, and TC additive solutions.

Following the runs shown in Fig. 4.9, experimenters decided to lower the heating temperature to 150 °C to simulate the conditions at the condensing zone near the edge of the steam chamber more realistically. Fig. 4.10 shows the results for additives TD through TH. TD is an anionic surfactant, TF is an organic alkali, TG is an inorganic alkali, and TH is another alcohol solvent. Again, the degrees of bitumen removal and contact line movement were not deemed more significant as compared to the base case run at 150 °C.

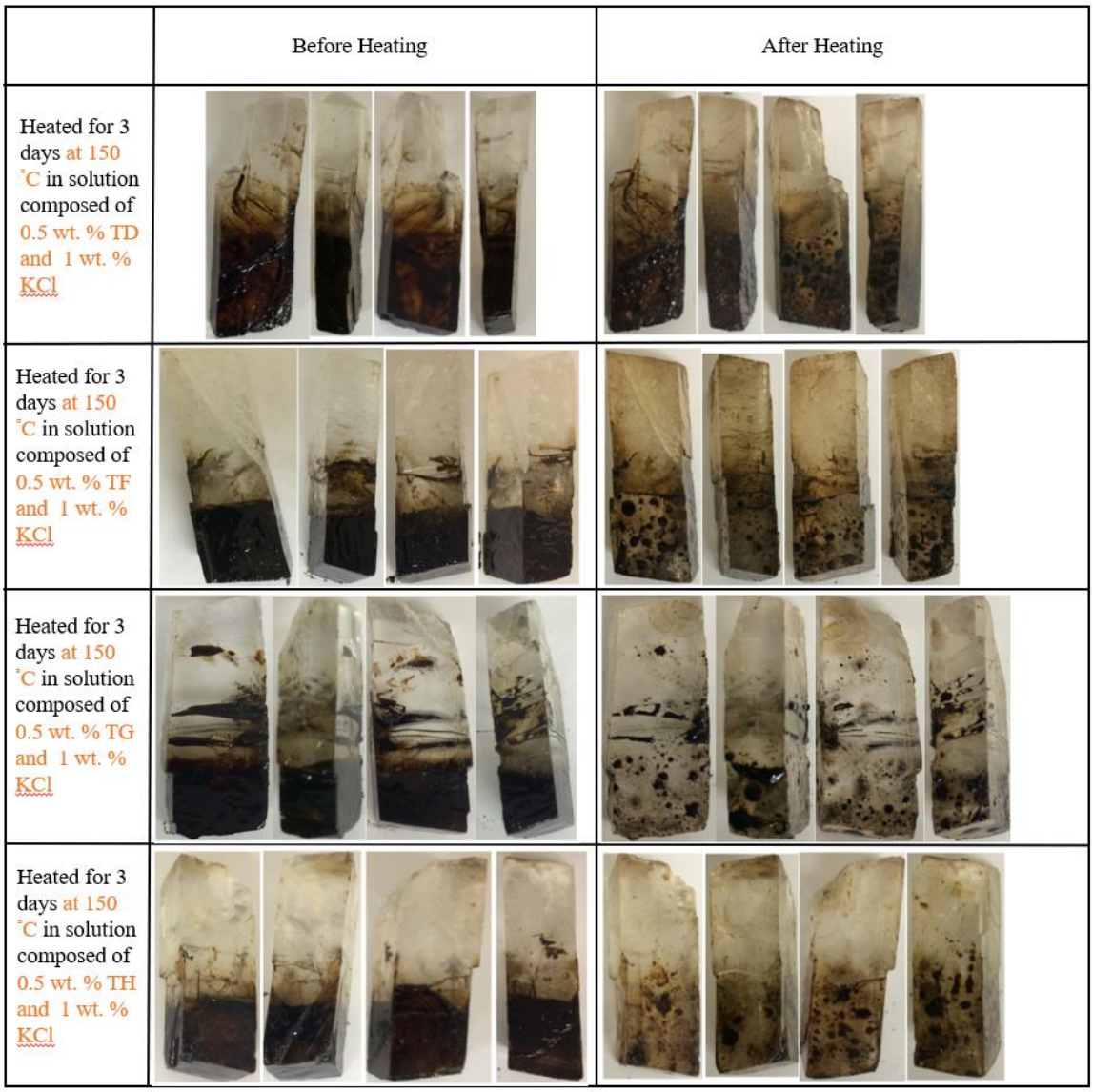

Figure 4.10: Aged calcite crystals heated at 150 °C in the presence of TD, TF, TG, and TH additive solutions.

Moving on to Organic alkali 1 through to the Solvents, Figs. 4.11 and 4.12 show that the degree of bitumen removal and contact line movement using organic alkalis (Organic alkali 1, 3, 7, and 8) were not more significant than the base case.

	Before Heating	After Heating
Heated for 3 days at 150 °C in solution composed of 0.5 wt. % Organic alkali 1 and 1 wt. % KCl	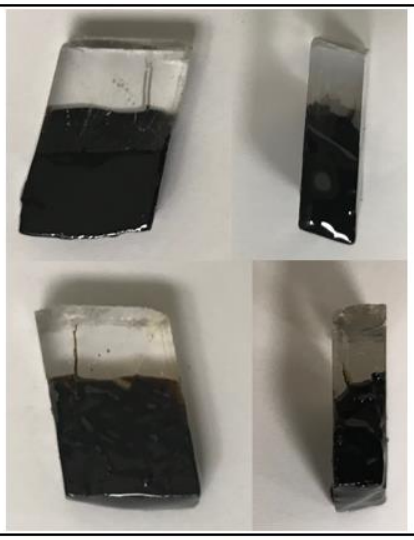	
Heated for 3 days at 150 °C in solution composed of 0.5 wt. % Organic alkali 3 and 1 wt. % KCl	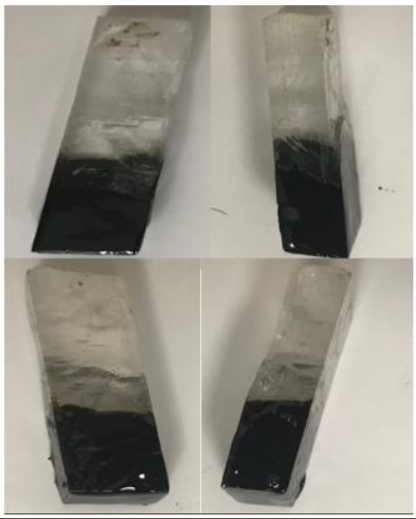	

Figure 4.11: Aged calcite crystals heated at 150 °C in the presence of organic alkali solutions.

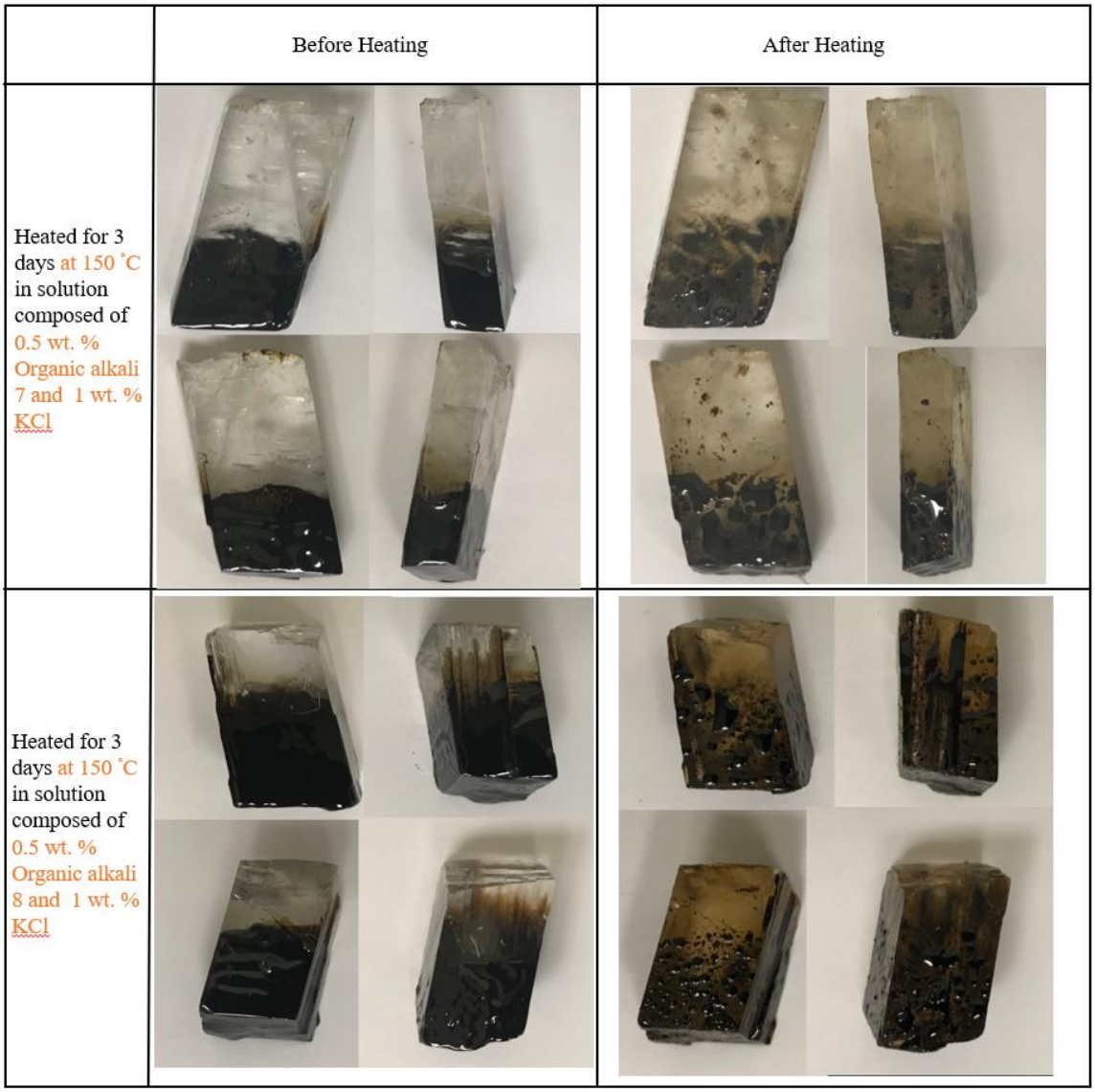

Figure 4.12: Aged calcite crystals heated at 150 °C in the presence of more organic alkali solutions.

Further, Na_2CO_3 and various alcohol solvents did not produce a more significant removal of bitumen and movement of the contact line as compared to the base case. These runs are shown in Figs. 4.13 and 4.14.

	Before Heating	After Heating
Heated for 3 days at 150 °C in solution composed of 0.5 wt. % Na_2CO_3 and 1 wt. % KCl		
Heated for 3 days at 150 °C in solution composed of 0.5 wt. % Alcohol 1 and 1 wt. % KCl	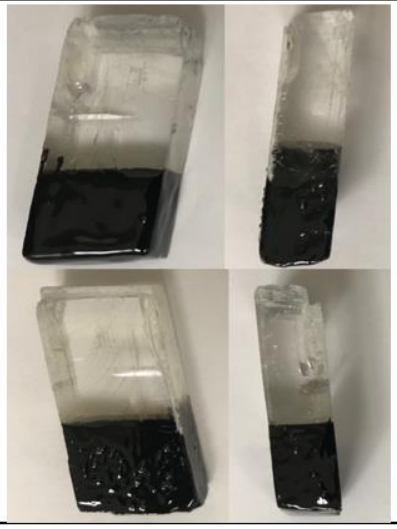	

Figure 4.13: Aged calcite crystals heated at 150 °C in the presence of Na_2CO_3 and Alcohol 1.

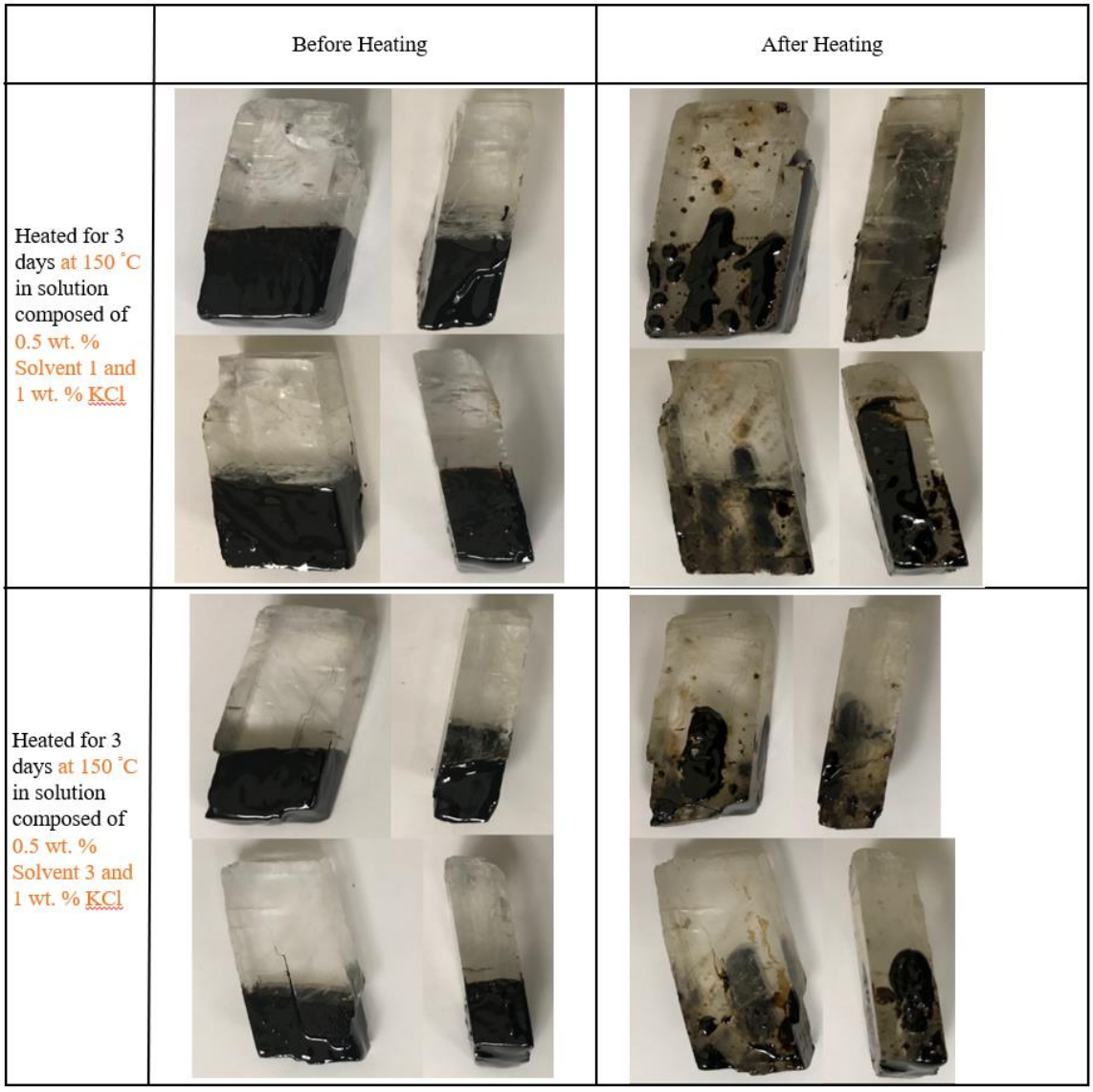

Figure 4.14: Aged calcite crystals heated at 150 °C in the presence of various alcohol.

The effect of an acid (Acid 1) and that of hydrocarbon branching on organic alkalis (Organic alkali 6, 9, and 11) were tested as well, as shown in Figs. 4.15 and 4.16. Bitumen removal and contact movement were not more significant compared to the base case.

	Before Heating	After Heating
Heated for 3 days at 150 °C in solution composed of 0.5 wt. % Organic alkali 6 and 1 wt. % KCl	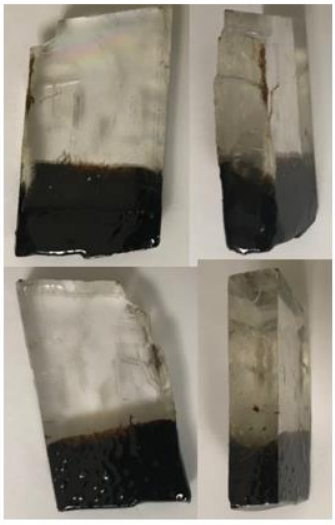	
Heated for 3 days at 150 °C in solution composed of 0.5 wt. % Organic alkali 9 and 1 wt. % KCl	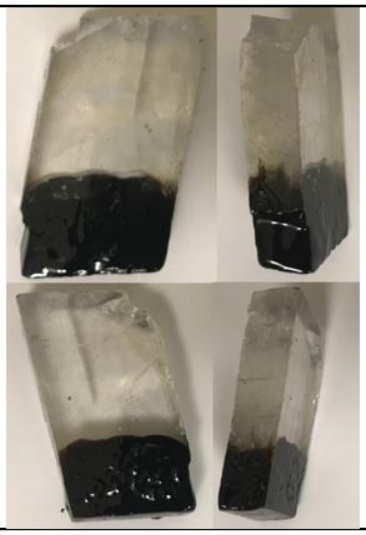	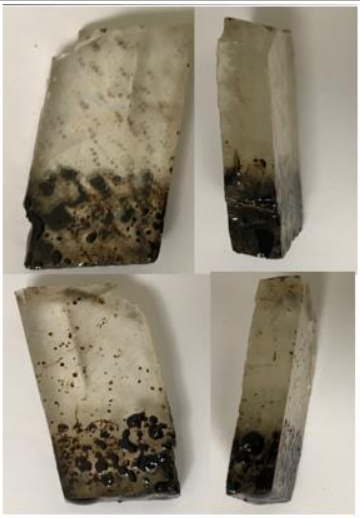

Figure 4.15: Aged calcite crystals heated at 150 °C in the presence of branched organic alkalis (Organic alkali 6 and 9).

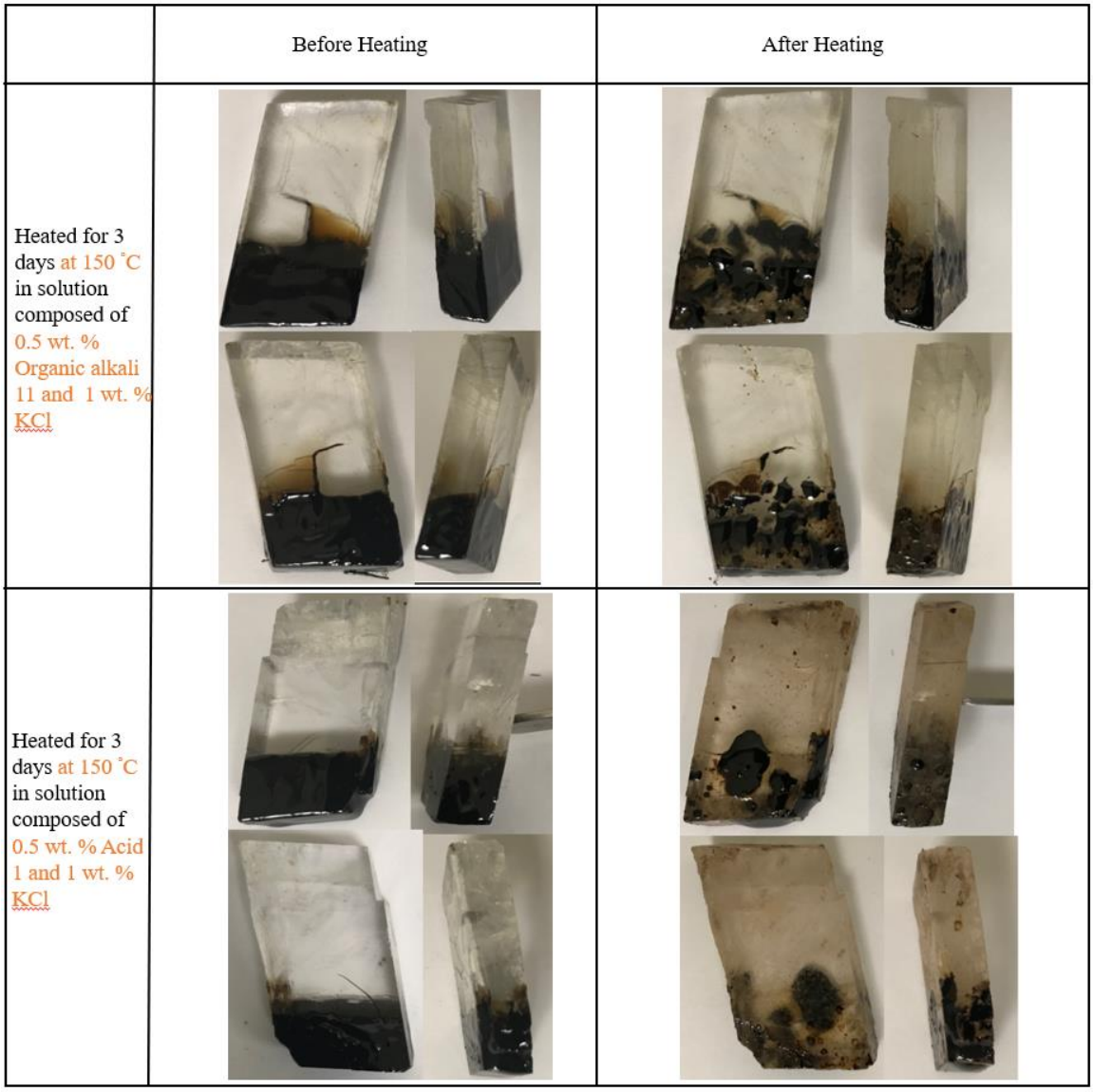

Figure 4.16: Aged calcite crystals heated at 150 °C in the presence of a branched organic alkali (Organic alkali 11) and an organic acid (Acid 1).

Overall, the list of additives in Table 3.2 was not as successful at wettability alteration and contact line movement as compared to oil-water interfacial tension reduction. However, several key pieces of knowledge were gained through these experiments detailed in this chapter. A temperature of 250 °C was too hot for pure quartz

grains and crystals. Lowering the temperature to 150 °C will most likely not change this. Bitumen will not stick to the surface. Any future experiments using new additives must consider using real core plugs as demonstrated, or some other type of siliceous material. The conditions during aging is crucial if a definite contact line is desired. With core plugs, bitumen will travel upward by capillary action if the third phase is air, since air is more non-wetting than the bitumen. If a water phase is introduced, the upward movement of bitumen is stopped completely, but the degree of aging seems to suffer significantly. The best option is to age at a lower temperature without water to slow down the upward capillary action, and make a contact line that does not fade upon heating without additive in the solution. Finally, bitumen tends to stick on calcite crystals much more compared to on quartz. Even when heated to 250 °C, a clean piece of calcite aged in bitumen will not be completely cleaned without an additive in the solution.

Chapter 5 Additive Performance in Porous Media

Chapter 5 provides details on coreflood and sandpack flood experiments performed using various additives, which were selected based on the results of the additive characterization tests documented in Chapters 3 and 4. This chapter also states the materials and apparatus used to carry out the experiments, as well as the associated step-by-step procedures. The rationale behind the design parameters for each coreflood or sandpack flood will be given. In addition, the results and their relevant discussions are presented.

5.1 Overview

Overall structure of the study can be broken down into the following:

1. Propose a list of potential mechanisms for enhanced oil recovery and obtain an inventory of additives for testing.
2. Develop a suite of high-temperature additive characterization tests that can be used to give information about each additive's potential to improve oil recovery.
3. Test the efficacy of promising additives in permeable media using corefloods and sandpack floods at high temperature, which mimic SAGD conditions at the edge of the steam chamber.
4. Develop a preliminary numerical simulation model of a SAGD process to test the effect of selected mechanisms on SAGD performance.

This chapter tells the materials used, procedures followed, and results obtained from coreflood and sandpack flood experiments using additives chosen from their characterization tests. Injection solutions were fed at 150 °C, and back pressure regulators

were used to keep the injection solutions in the liquid state. In each coreflood, the rationale behind the chosen parameters and additives is given. The primary metrics to be quantified are the ultimate recovery and the recovery rate of bitumen.

5.2 Apparatus and Materials

Figs. 5.1, 5.2, and 5.3 show the schematics of the coreflood and sandpack flood setups used throughout the course of this study. Experimenters performed the first coreflood using the setup depicted in Fig. 5.1. Having made modifications and improvements to the first setup, the experimenters performed the second, third, and fourth corefloods using the setup displayed in Fig. 5.2. With experience gained from the first and second setups, experimenters designed and built a sandpack setup capable of operation at 250 °C. The dynamic additive retention study was performed using the setup presented in Fig. 5.2, with only minor modifications.

In Fig. 5.1, the injection system included a deionized water reservoir, a QX-6000 Series pump from Chandler Engineering, a piston accumulator containing injection brine, a piston accumulator containing injection additive solution, and a six feet long coil inside the oven used to preheat the injection fluid before it enters the core. A piston accumulator containing the naphtha-diluted bitumen was placed inside the oven during the oil saturation step only.

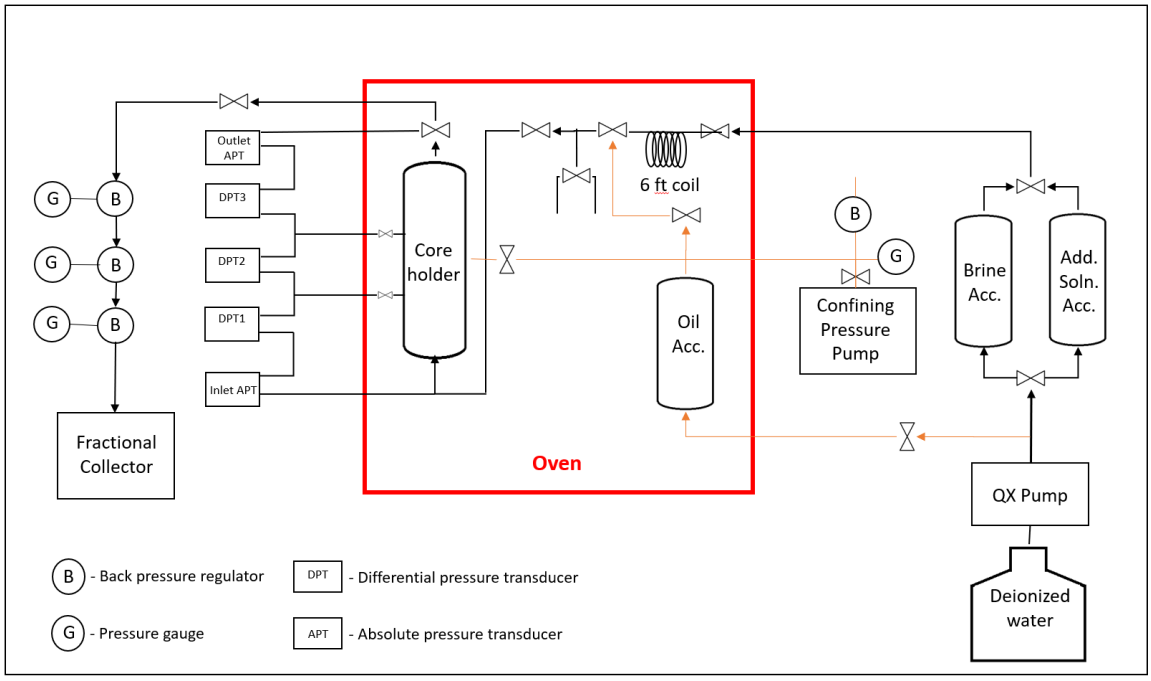

Figure 5.1: Setup used for Coreflood 1.

The QX-6000 series pump is a positive displacement one, which operates by taking in injection liquid, then displacing that trapped volume in a precise manner into the discharge tubing. The pump can operate at very accurate and precise flow rates, and can operate in (but not limited to) a constant rate delivery or constant pressure mode. In order to keep the pump's inner body clean, the injection fluids were not fed through the pump itself. Instead, experimenters injected deionized water into piston accumulators, which contained the injection brine and additive solution injected during the coreflood. The coil was simply a long piece of tubing bent into a coil to conserve space inside the oven. Experimenters performed a test where water was injected at different flow rates into the 6 feet coil, which was situated inside the oven. The back pressure was set to 650 psig to ensure that the water remained in the liquid state. A calibrated thermocouple measured the inline temperature at the end of the coil. The 6-ft. coil was long enough to preheat the

injection fluid to the oven's set temperature up to 15 mL/min, which is much greater than the injection rates used in the coreflood. The core holder is a Hassler type core holder. Radial confining pressure was applied using mineral oil and a hand pump, whereby a rubber sleeve inside the core holder applied confining pressure on the core. Five Rosemount pressure transducers were used to measure pressures. Two absolute pressure transducers measured the inlet and outlet pressures. Three differential pressure transducers measured sectional pressure drops. The experimenters used three backpressure regulators connected in series to keep fluids in the system in the liquid state. A fraction collector automatically positioned 15 mL polypropylene tubes at the outlet on a time basis to collect the effluent.

Fig. 5.2 shows the second setup, which was used for the second, third, and fourth corefloods. Experimenters also performed the additive retention study using this setup, with only minor modifications.

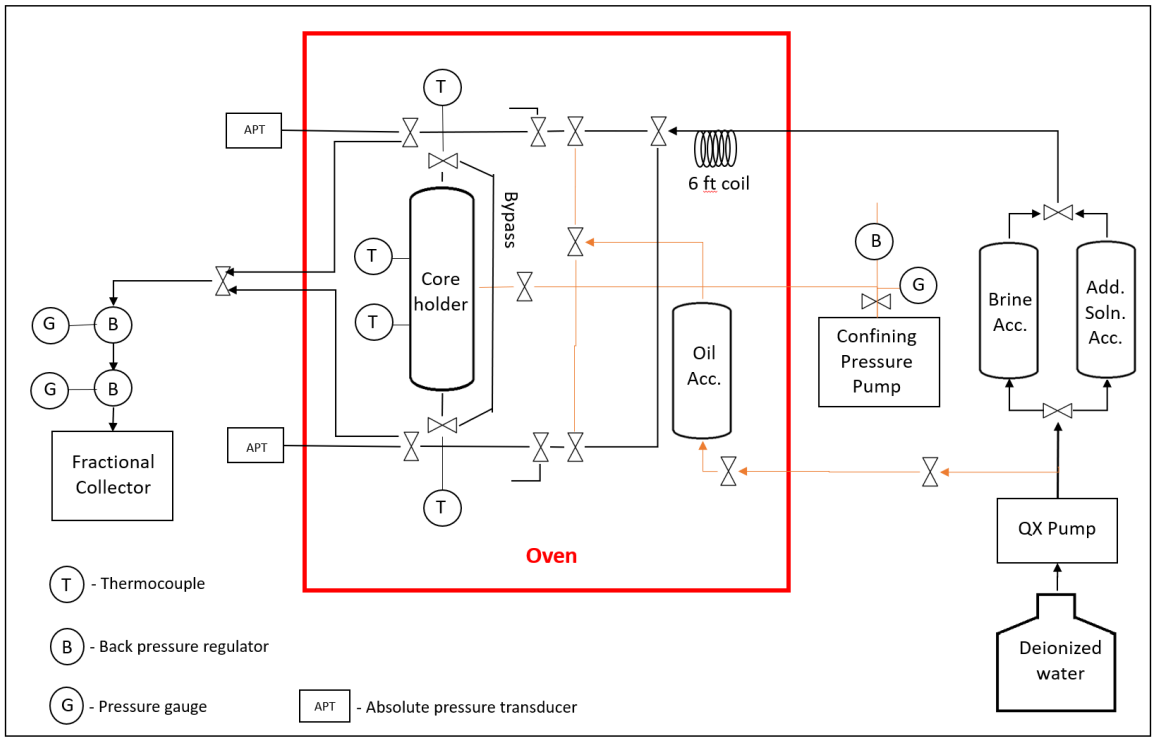

Figure 5.2: Setup used for Coreflood 2, 3, and 4. The additive retention study was also performed using this setup, with only minor modifications.

This setup was similar to the first setup shown in Fig. 5.1, with the following differences and modifications. Four Type J thermocouples were installed to monitor temperatures at the inlet and outlet, and two locations along the core. A bypass line was installed to give the ability to test the injection before injecting into the core. The amount of back pressure regulators at the outlet was reduced from three to two in series, decreasing the tubing volume at the outlet side. Additional valves and tubing were added inside the oven to allow top to bottom injection capability if needed.

Fig. 5.3 shows the sandpack setup. It is capable of experiments at a higher temperature, nitrogen gas injection, and retains support for both injection directions (simply disconnect, reposition, and reconnect the inlet and outlet tubing, and swap the ports on the differential transducers). The Hassler type core holder used in the previous two

setups limited the maximum operating temperature to 150 °C. In addition, valves used inside the oven had a maximum working temperature of 232 °C. A new sandpack and removal of all valves inside the oven allowed for safe operation up to 250 °C and 850 psig in this new setup. Note that the oil accumulator was removed after oil saturation, prior to the oven temperature being raised to the injection temperature. Nitrogen gas injection is supported, which can be used to control the quality of injection steam; however, at this point in the study, steam injection has not yet been attempted. A Jasco PU-2080Plus Intelligent HPLC pump was used to inject additive solution directly. This separate pump can also be used in a steam flood to co-inject additive solution into a nitrogen stream, where after making its way across the coil gets vaporized prior to entering the sandpack.

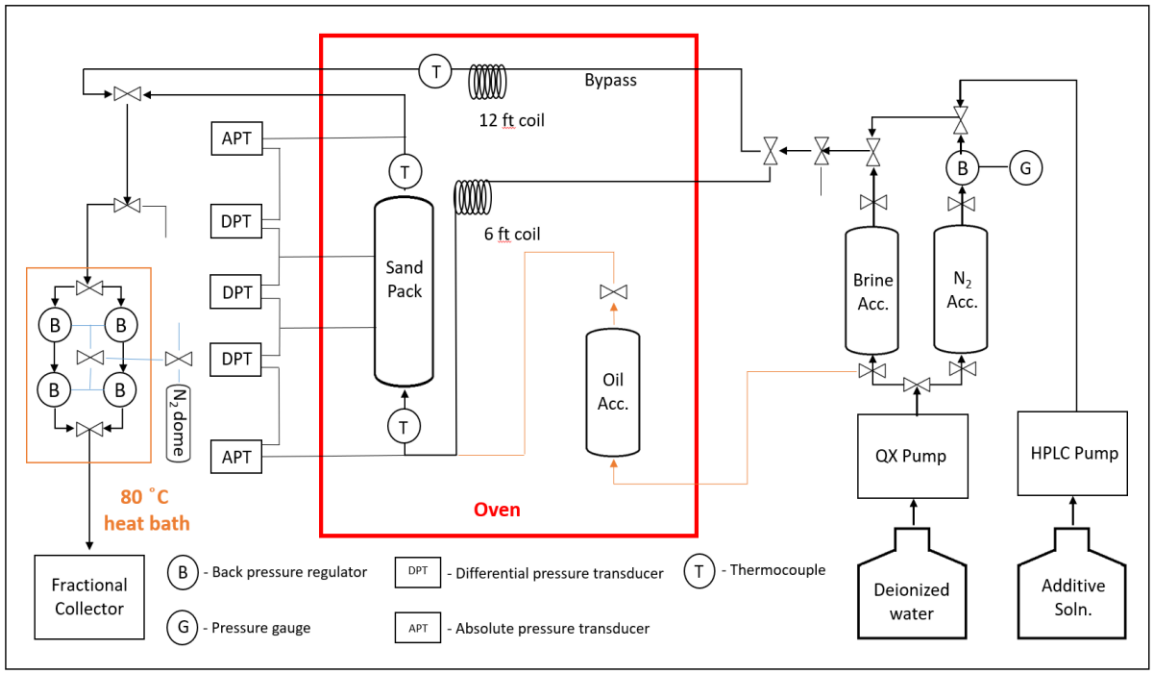

Figure 5.3: Sandpack setup.

Finally, two pairs of back pressure regulators were installed in this setup to allow continuous injection in case one pair failed. The back pressure regulators were submerged in a water bath at 80 °C to help ease the flow of viscous bitumen. The back pressure regulators' dome was connected to a larger volume of nitrogen to minimize pressure fluctuations. All other components of this setup were similar to previous setups.

A list of materials and equipment used in the experiments is given below. Materials used for injection fluid preparation include select additives from Table 3.2, sodium carbonate and potassium chloride obtained from Fisher Scientific, deionized water, an analytical balance, disposable transfer pipettes, and a metal spatula. Injection fluid was stored in 5-gallon glass containers and stirred using a stir bar and benchtop magnetic stirrer during injection. The naphtha-diluted bitumen was used in the first coreflood, while the dewatered bitumen was used in all other corefloods and sandpack floods. One-foot long Idaho gray cores of 1.5" diameter were used for corefloods, bound in a heat shrink wrap and held in a Hassler type 1.5" inner diameter core holder. Sandpacks were made by using a Vibco PJT-100 vibrating table, 1.22" inner diameter 11.45" long cylindrical vessel, Teflon tape, 325 Mesh screens, Teflon washers, Teflon O-rings, and 140-170 Mesh silica sand from Agsco. A desktop PC fitted with LabVIEW was used to record pressure transducer data and thermocouple data, along with data acquisition cards from National Instruments. A hand pump filled with mineral oil was used for applying confining pressure. The rest of the setup included a Chandler Engineering QX-6000 Series Pump, a Jasco PU-2080Plus Intelligent HPLC pump, needle valves from Autoclave Engineers, ball valves from Swagelok, Inconell 600 and 316 stainless steel tubing, a vacuum pump, Teflon tape, digital and analog pressure gauges, piston accumulators for injection fluids and bitumen, absolute and differential pressure transducers from Rosemount, Omega Type J thermocouples, and Equilibar back pressure regulators fitted with Teflon diaphragms. The

effluent collection system consisted of Equilibar back pressure regulators, a metal tray for holding the water heat bath, a fraction collector, Fisherbrand 15 mL polypropylene tubes, a nitrogen accumulator, and a benchtop heater for heating the water bath. Toluene used for cleaning was obtained from Fisher Scientific.

5.3 PROCEDURE

The following presents the procedure for the corefloods. Injection solutions were injected in the liquid state at 150 °C with the use of back pressure regulators. Experimenters calibrated all pressure transducers, thermocouples (if used), and pumps to ensure accurate measurement and flow rate delivery. Setup tubing and the back pressure regulators were cleaned sequentially with toluene and deionized water. Tubing and all other equipment not contacted by bitumen from previous use were rinsed thoroughly with deionized water to remove contaminants. Experimenters then got rid of all liquids using compressed air.

Idaho Gray cores were dried at 150 °C inside a convection oven for one day to get rid of all moisture. Experimenters wrapped a heat shrink wrap around the core and applied heat using a heat gun to shrink the wrap. This protects the core holder's rubber sleeve from fluids inside the core. Experimenters then loaded the core into the core holder and drilled holes approximately one eighth inch deep through taps located one third and two thirds along the length of the core. With the heat shrink penetrated, experimenters injected air at the core holder inlet to confirm communication between the inlet, outlet, and taps. Confining pressure was applied at 300 psia above the back pressure.

Experimenters measured the volume of tubing outside the core holder required for porosity and oil saturation calculations by injecting 1 wt. % KCl into this volume using the volume-dispensed indicator on the QX-6000 pump, which was very accurate. This included

the tubing volume upstream of the core holder inlet, and volume downstream of the core holder. All fed injection fluids contained KCl at 1 wt. % concentration to prevent clay swelling. Experimenters leak tested the core holder using compressed air, pressurizing the core holder, then shutting it in and making sure that the pressure did not drop over time. Later, after the core was saturated with 1 wt. % KCl during porosity and permeability measurement, the whole system was leak tested at a pressure no less than 1000 psig by using the QX-6000 pump in constant pressure mode, and thoroughly checking for water leaks. A series of 15 mL polypropylene tubes were numbered, weighed, and placed into the fraction collector.

Experimenters then measured the core porosity. The core was placed under vacuum by sucking out the air using a vacuum pump, and then closing valves situated downstream and upstream of the core holder. Experimenters injected 1 wt. % KCl solution from bottom to top at 1 mL/min until the pressure inside the core holder reached 100 psig. The slow rate and orientation of injection minimized viscous fingering. The pressure inside the core eventually did reach 100 psig, since some air remained in the core even after vacuuming. Vacuuming the core prior to saturation minimizes the error in porosity measurement associated with trapped air in dead end and small pores. The back pressure regulators at the outlet of the system was set to 100 psig. The outlet valve was opened, then closed, and more solution was injected until the pressure inside the core reached 100 psig again. This process was repeated several times. Finally, the solution was injected until breakthrough and then injected further and collected in a graduated cylinder. The cumulative injected volume indicated on the QX pump was recorded at breakthrough and at several different volumes of effluent collected. Experimenters calculated the pore volume at each step using Eq. 12,

$$V_p = V_c - V_e - V_t \tag{12}$$

$$\phi = \frac{V_p}{V_b} \tag{13}$$

and then used the average pore volume to calculate the porosity. In the above equations, V_p stands for the pore volume (mL), V_c the cumulative volume injected (mL), V_e the effluent volume (mL), V_t the volume of all other spaces that the injection fluid entered as described earlier (mL), and V_b is the bulk volume of the core.

Next, experimenters attempted to measure the absolute permeability of the core to brine at room temperature. Experimenters injected 1 wt. % KCl solution at 10, 20, 30, 40, 30, 20, then 10 cc/min. The pressure drops at each flow rate were recorded using LABVIEW. Experimenters found that the pressure drop was too low to be read accurately even at 40 cc/min for the Idaho Gray core, which indicated that the permeability was quite high. The stable pressure drop value at each flow rate can be used to calculate the absolute permeability k using Darcy's law (rearranged) as shown below.

$$k = -\frac{q\mu_w L}{A\Delta P} \tag{14}$$

Here q is the volumetric injection rate, ΔP represents the pressure drop, L is the length of the core, and A is the cross-sectional area of the core. The final permeability was to be taken as the average of the permeabilities calculated from each injection rate. Note that a permeability was able to be measured for the sandpacks. At the conclusion of permeability measurement, another leak test was conducted by pressuring the entire system to 1000 psig (using 1 wt. % KCl solution) as described earlier.

The next step was to saturate the core with bitumen. Experimenters placed the oil accumulator inside the oven and set the temperature to 50 or 80 °C to decrease the bitumen viscosity. Bitumen discharge due to thermal expansion was collected and saved until the oil accumulator and bitumen inside it reached the set temperature. Bitumen was then injected at 1 mL/min from bottom to top until breakthrough. The volume of bitumen inside the core V_o was calculated using Eq. 15 below.

$$V_o = V_{c,o} - V_{e,o} - V_t \tag{15}$$

Here $V_{c,o}$ is the cumulative volume of bitumen injected (mL) and $V_{e,o}$ is the volume of bitumen in the effluent (mL). The oil accumulator was then removed from the oven.

With the outlet being open and the back pressure being set to prevent water from boiling, experimenters set the oven at an elevated temperature to age the core for a period of time. Bitumen expanded and was collected in the graduated cylinder. The outlet valve was shut after the bitumen reached the steady state temperature and core aging continued. Negligible amounts of water came out during thermal expansion. The system was then heated to 150 °C for four hours before beginning to feed the injection fluid. An assumption was made that V_o remained constant. The original oil in place (OOIP) by mass was then calculated by multiplying V_o by the bitumen density at 150 °C.

Experimenters used different injection fluids in sequential injection periods (one or two periods). The combination of low injection rate and bottom-to-top injection orientation minimized viscous forces and viscous fingering to mimic a gravity-stable process. Experimenters set the back pressure and set the cycle time on the fractional collector. This is the amount of time that each effluent tube collected effluent. Since the mass of bitumen collected was weighed for each effluent tube and used to plot the recovery curves, this

cycle time was the time period between each recovery data point. At the beginning of each injection period, the chosen injection fluid was bled up to a point close to the core holder inlet. Experimenters collected pressure data on LabVIEW and injected fluid at a constant rate. The time taken for the injection fluid to reach the inlet of the core was taken in account and the start time was noted. If using the QX pump, the cumulative injected volume was set to zero at this point. The HPLC pump does not have cumulative volume tracking; therefore, the injection fluid reservoir was weighed for the initial mass when using the HPLC pump. Additives that were not completely miscible in deionized water were continuously stirred inside the additive reservoir and injected via the HPLC pump. Otherwise, they were injected from a piston accumulator using the QX pump. Experimenters also injected 1 wt. % KCl solution during some injection periods for certain corefloods. In such cases the HPLC pump or QX pump (with a piston accumulator holding the solution) was used. The effluent was collected in a series of polypropylene tubes. At the end of the injection period, the end time and cumulative injected volume (or final reservoir mass) were recorded. Additional injection periods were executed in the same manner.

Shutdown procedures were then followed. To separate brine from bitumen in each effluent tube, experimenters first decanted the brine into another tube. To remove brine droplets left behind and any brine trapped in pockets within the bitumen, the experimenters heated the effluent tubes (capped) to 80 °C in a convection oven to decrease bitumen viscosity, and then centrifuged the tubes. The caps were opened and the coalesced brine was removed by tapping the tube. Experimenters then calculated the total mass of bitumen and brine produced from every effluent tube using the initial masses of the effluent and brine tubes respectively. Where significant emulsions were found, a small volume of hydrochloric acid was used to break the emulsions. After oil saturation and core aging,

tubing downstream of the core was filled with bitumen. This mass of bitumen was approximated by multiplying the tubing volume by the density of the bitumen at room temperature, and subtracted from the mass of bitumen in the first effluent vial. Finally, experimenters constructed a production curve, plotting recovery efficiency, remaining oil, and oil cut vs. injected pore volumes. Eq. 16 shows the recovery efficiency E_R by mass,

$$E_R = \frac{Np}{OOIP} \tag{16}$$

where *Np* is the cumulative mass of bitumen produced (g) and *OOIP* represents the original mass of oil inside the core or sandpack (g). Experimenters defined the remaining oil as one subtracted by E_R. The oil cut for each data point is the mass of bitumen to the total mass of liquid in each tube.

Sandpack flood experiments were carried out similarly as the coreflood experiments, but with several key differences. The sandpack was prepared in the manner as follows. Experimenters first dried 140-170 Mesh silica sand obtained from Agsco at 120 °C inside a convection oven to remove moisture. The sandpack was secured to a Vibco PJT-100 vibrating table and the upper cap was removed. Experimenters placed two 325 Mesh screens at the taps. Two 325 Mesh screens and a Teflon washer were placed at the bottom of the sand pack and similarly at the top after the pack was filled. This prevented sand from migrating during liquid injection. The vibrating table was set at an intermediate frequency and sand was added in 10 mL aliquots every minute. Experimenters then lowered the frequency after the sandpack was filled, and allowed shaking to proceed for another 24 hours. If the sand level dipped, more sand was added. Finally, experimenters slightly overfilled the sandpack to ensure that the sand was compact upon placing the cap back on. Once capped, to ensure that no leaks came through the threads, experimenters

pressurized the sandpack with nitrogen to 850 psig and submerged the sandpack underwater. Afterwards, the experimenters released the nitrogen, dried the sandpack, and weighed it. After saturating the sandpack with 1 wt. % KCl solution, the experimenters weighed the sandpack again and multiplied the mass difference by the solution density at room temperature to obtain the pore volume. The sandpacks were not aged over an extended period of time, since the goal of the sandpack flood experiments was to test the oil-water interfacial tension reduction mechanism of the selected additive. Outlet back pressure regulators were submerged in a water bath at 80 °C to ease flow by reducing flowing bitumen viscosity.

The dynamic additive retention study was conducted in a similar manner to the corefloods, except that the bitumen saturation and core aging steps were skipped. After the Idaho Gray core was flushed with 1 wt. % KCl solution, experimenters injected the TG solution (deionized water containing 1 wt. % TG and 1 wt. % KCl). After, another 1 wt. % KCl flush was fed to clear the core of as much TG as possible and to reestablish effluent salinity. Then, the TF solution (deionized water containing 1 wt. % TF and 1 wt. % KCl) was injected. Effluent pH and conductivity values were measured using a pH meter and conductivity meter.

5.4 COREFLOOD 1

Table 5.1 shows the details for Coreflood 1. The goal of Coreflood 1 was to test whether additive TA can improve ultimate recovery. At the time Coreflood 1 was performed, experimenters had additives TA, TB, and TC. The aqueous stability and phase behavior tests were conducted, and it was found that TA exhibited the best miscibility in aqueous solution at elevated temperature. Experimenters selected TA for the first

coreflood, and the naphtha-diluted bitumen was used for its lower viscosity, which made it easier to handle.

Table 5.1: Coreflood 1 Parameters

Temp. (°C)	Fluid Phase in Core	Core	Bitumen	Porosity	Absolute Permeability (D)	OOIP (g)
150	Liquid	Idaho Gray	Naphtha-diluted bitumen	0.37	---	88
First Injection Period	Deionized water containing 1 wt. % KCl			Second Injection Period	Deionized water containing 0.5 wt. % TA and 1 wt. % KCl	
	Bottom to top				Bottom to top	
Injection Rate (PV/day)	2 (0.1576 mL/min)			Injection Rate (PV/day)	2 (0.1576 mL/min)	

Fig. 5.4 and 5.5 show the recovery curves. Experimenters injected a 1 wt. % KCl solution until the oil cut was close to zero, and then injected 0.5 wt. % TA/1 wt. % KCl. Only a four percent incremental increase in E_R was observed over more than six pore volumes of TA solution injected, and no significant increase in the oil cut was observed. Therefore, experimenters conclude that TA did not decrease residual oil saturation.

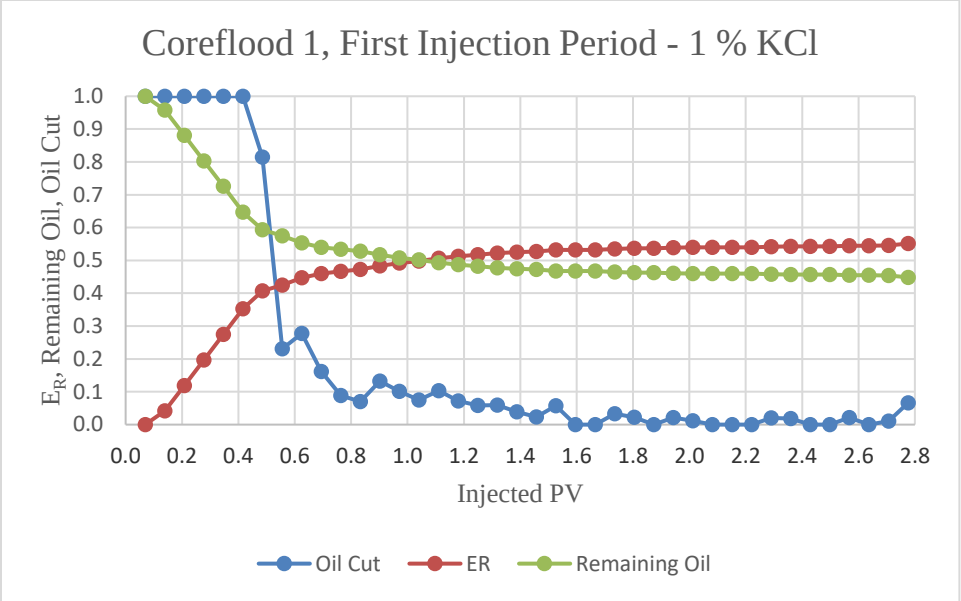

Figure 5.4: Recovery curves for Coreflood 1's first injection period.

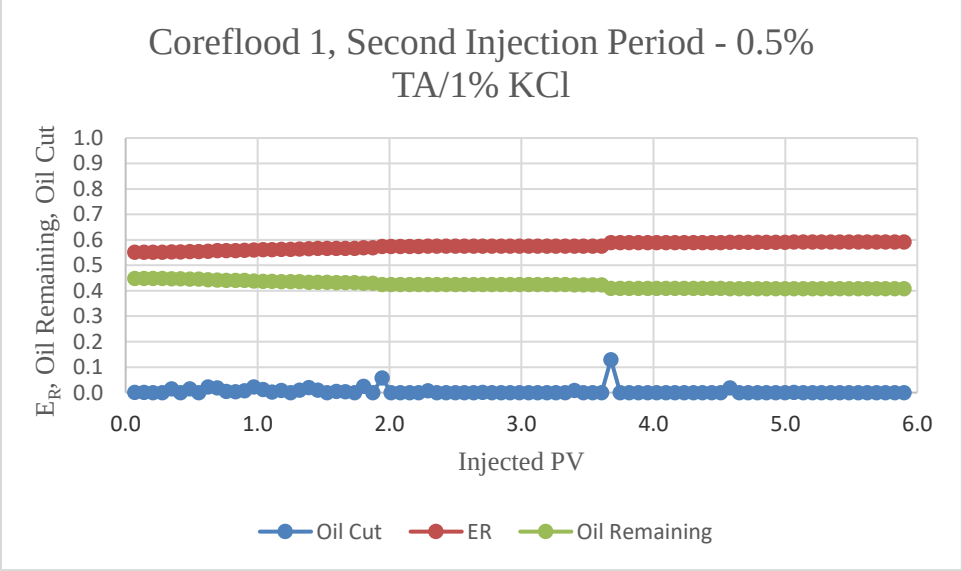

Figure 5.5: Recovery curves for Coreflood 1's second period.

Small amounts of bitumen were produced continually. Experimenters believe that part of this bitumen may be from the bitumen stuck on the inside of the tubing between the fraction collector and the core outlet, as well as from the outlet back pressure regulators.

These would have come out slowly as the injected fluid slowly dragged the bitumen downstream.

5.5 COREFLOOD 2 AND 3

Table 5.2 and 5.3 show the details for Corefloods 2 and 3 respectively. The goal was to test whether additive TC (non-ionic surfactant) could improve the ultimate recovery or increase the oil rate. dewatered bitumen was used for this study, which is more viscous than the naphtha-diluted bitumen. Following Coreflood 1, experimenters conducted the phase behavior test using the visual cells, and found that dewatered bitumen dispersed into much smaller droplets upon perturbation in the presence of TB and TC as compared to the base case. There was a small amount of liquid-liquid phase separation in TB solutions at 150 °C, while TC was turbid. Between TB and TC, since the additive was dispersed more uniformly in the aqueous solution for the latter, experimenters chose TC. In addition, the additive solution was constantly mixed in its container using a stir bar and magnetic stir plate to help the solution remain homogeneous during the course of injection.

Table 5.2: Coreflood 2 Parameters

Temp. (°C)	Fluid Phase in Core	Core	Bitumen	Porosity	Absolute Permeability (D)	OOIP (g)
150	Liquid	Idaho Gray	Reservoir	0.39	---	90
First Injection Period	Deionized water containing 0.5 wt. % TC and 1 wt. % KCl					
	Bottom to top					
Injection Rate (PV/day)	4 (0.3322 mL/min)					

Table 5.3: Coreflood 3 Parameters

Temp. (°C)	Fluid Phase in Core	Core	Bitumen	Porosity	Absolute Permeability (D)	OOIP (g)
150	Liquid	Idaho Gray	Reservoir	0.38	---	93
First Injection Period	Deionized water containing 1 wt. % KCl			Second Injection Period	Deionized water containing 0.5 wt. % TC and 1 wt. % KCl	
	Bottom to top				Bottom to top	
Injection Rate (PV/day)	4 (0.3422 mL/min)			Injection Rate (PV/day)	4 (0.3422 mL/min)	

Figs. 5.6, 5.7, and 5.8 display the recovery curves for Corefloods 2 and 3. Fig. 5.9 shows that TC did not appreciably increase the oil cut obtained in each effluent tube. This means that the oil rate was not appreciably increased. However, during the core aging step in Coreflood 2, the oven broke and the core was aged in UT 1 bitumen for over three weeks at room temperature, making the core more oil-wet. The bitumen migrated into smaller pores, occupying a larger fraction of the smaller pores, and lowering the oil relative permeability. This would have decreased the oil rate and the recovery efficiency for a given pore volume of solution injected. Therefore, experimenters conclude that TC did not increase the oil production rate *significantly*, with the caveat that a small increase may be possible.

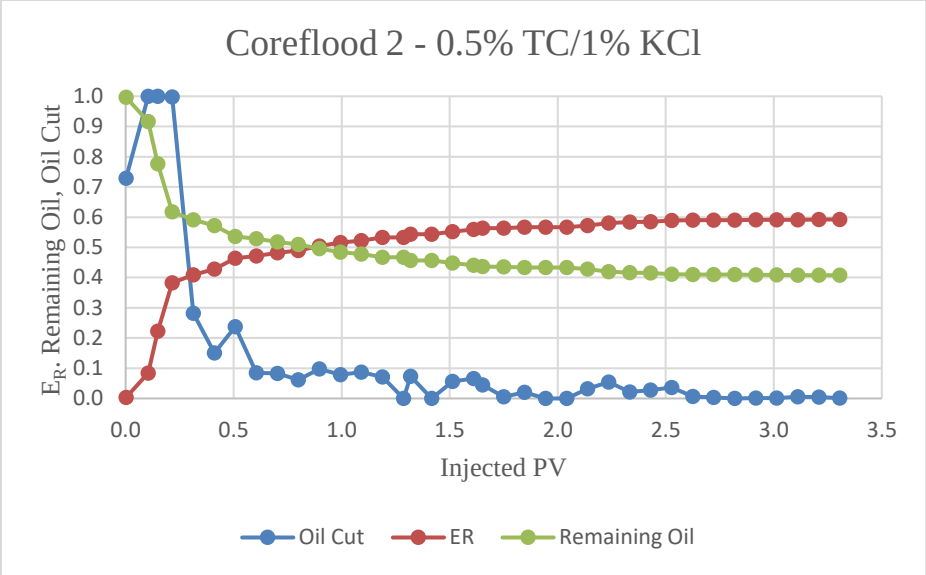

Figure 5.6: Recovery curves for Coreflood 2.

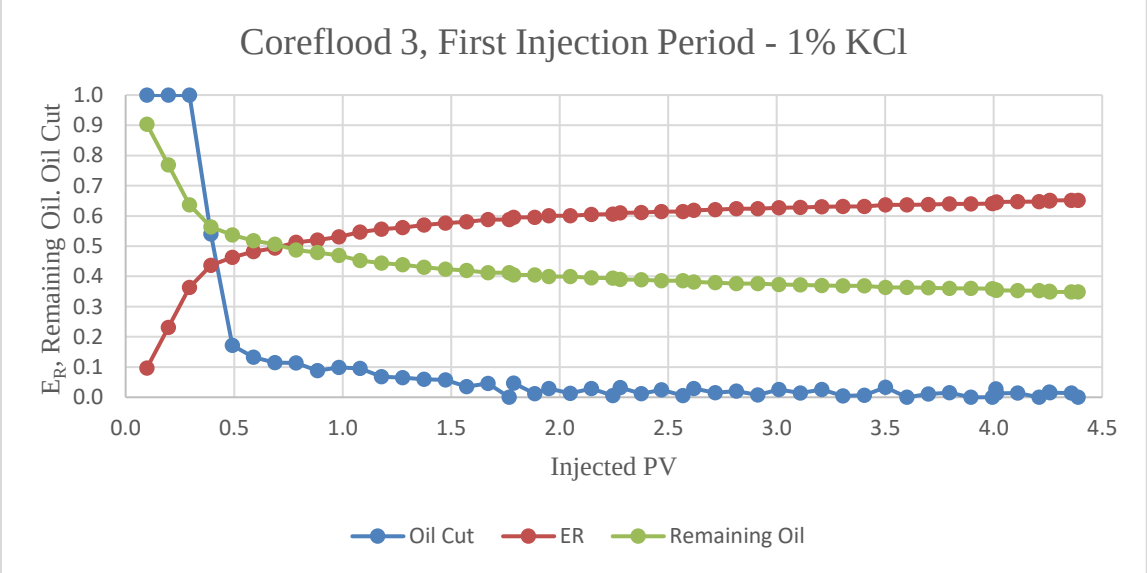

Figure 5.7: Recovery curves for Coreflood 3's first injection period.

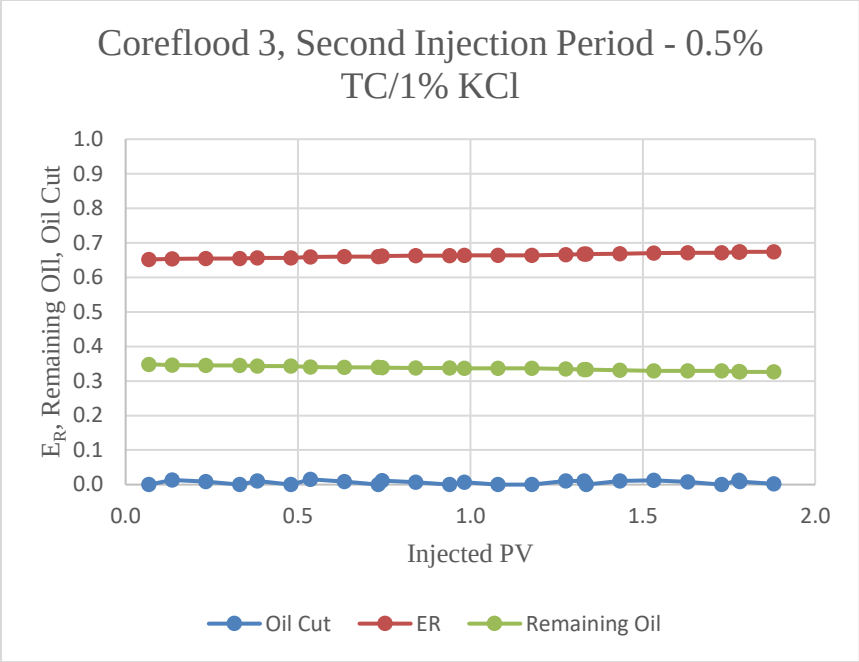

Figure 5.8: Recovery curves for Coreflood 3's second injection period.

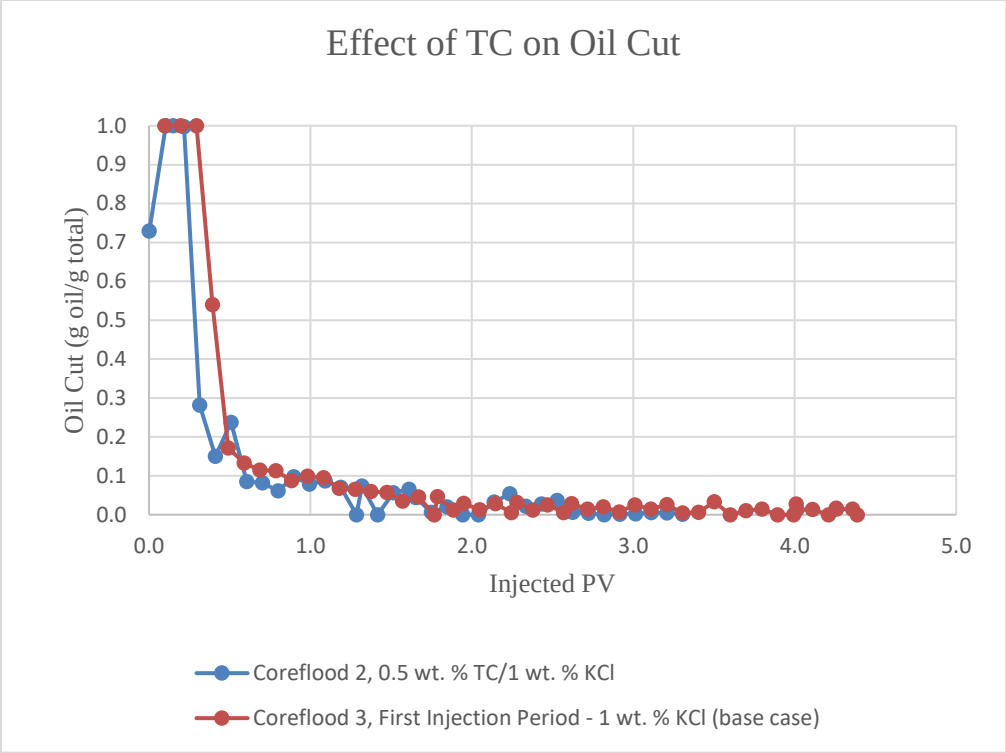

Figure 5.9: Effect of TC on oil cut.

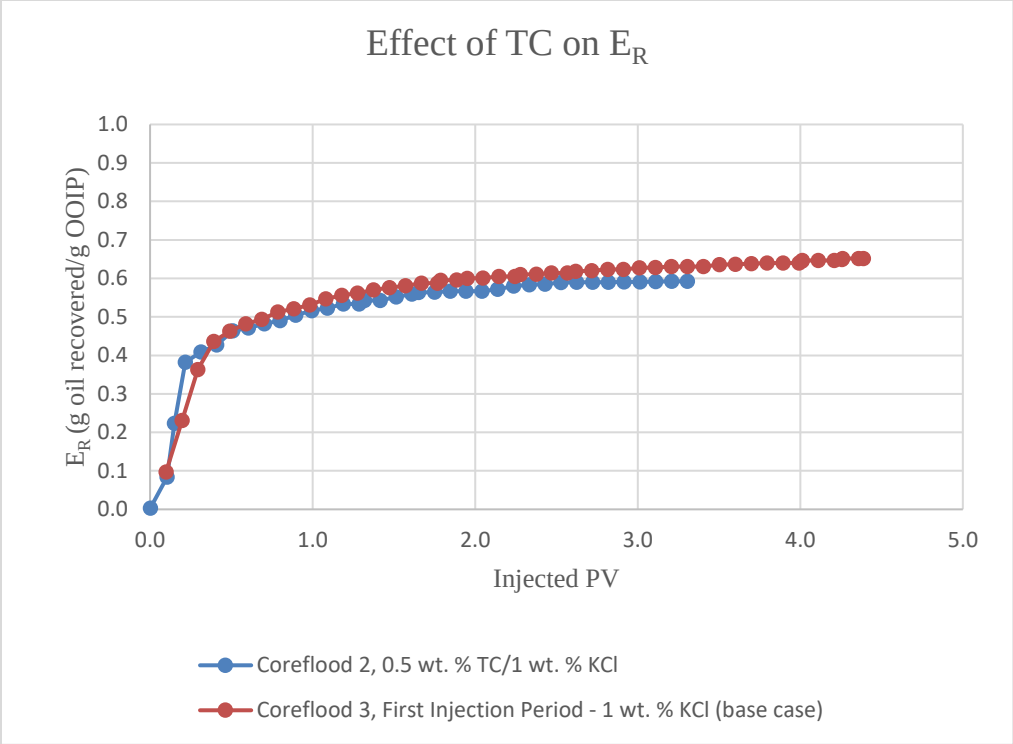

Figure 5.10: Effect of TC on recovery efficiency.

In Coreflood 3, experimenters injected 1 wt. % KCl solution until the oil cut was almost zero for several pore volumes of injection, then switched to the TC solution. Only a two percent increase in ultimate recovery was gained over two pore volumes of injected TC solution. Again, some of this bitumen were bitumen that coated the inner walls of the outlet tubing and outlet back pressure regulators. These slowly came out as the injection fluid dragged it. TC did not appreciably increase the ultimate recovery. A comparison shown in Fig. 5.10 also supports this conclusion. Note that differences in pore structure between cores due to core heterogeneity were unavoidable and affect these comparisons. However, experimenters are more interested in finding significant improvements at the laboratory scale, since implementation at the field scale involves other significant challenges.

5.6 COREFLOOD 4

Table 5.4 shows the details for Coreflood 4. At the time Coreflood 4 was conducted, experimenters had additives TA through TH and did several phase behavior tests using Na_2CO_3 and combinations of Na_2CO_3 with several of the other additives. Phase behavior runs containing Na_2CO_3 showed significant oil-in-water emulsions with the dewatered bitumen. Experimenters decided to combine TC's (non-ionic surfactant) oil-water IFT reduction with Na_2CO_3's ability to extract natural surfactant to test whether an appreciable increase in the ultimate recovery and oil rate was possible. Note that 150 °C, bottom to top injection, and the high permeability of the Idaho Gray core already present fairly favorable conditions for recovery. Potassium chloride was not included in the injection solution since Na_2CO_3 provides some salinity on its own to prevent clays native in the core from swelling.

Table 5.4: Coreflood 4 Parameters

Temp. (°C)	Fluid Phase in Core	Core	Bitumen	Porosity	Absolute Permeability (D)	OOIP (g)
150	Liquid	Idaho Gray	Reservoir	0.35	---	83
First Injection Period	Deionized water containing 0.5 wt. % TC and 0.5 wt. % Na_2CO_3					
	Bottom to top					
Injection Rate (PV/day)	4 (0.3070 mL/min)					

Fig. 5.11 depicts the recovery curve and Fig. 5.12 gives a comparison between Coreflood 4 (0.5 wt. % TC/0.5 wt. % Na_2CO_3), the base case (1 wt. % KCl), and Coreflood 2 (0.5 wt. % TC/1 wt. % KCl). In the latter figure, the curves are close to each other during

the early times before four pore volumes (24 hours). Therefore, the combination of TC and Na_2CO_3 did not appreciably increase the oil rate and recovery efficiency during the early time. However, after four pore volumes (24 hours), a noticeable increase in recovery can be seen in the Coreflood 4 curve. The delay was most likely due to the adsorption of the natural surfactants in the core. Coreflood 2 and the first injection period of Coreflood 3 were stopped because the oil cut was almost zero. Had the trend continued, the TC-Na_2CO_3 curve would have been significantly higher at the end of Coreflood 4. Oil recovery could be appreciably improved at these conditions.

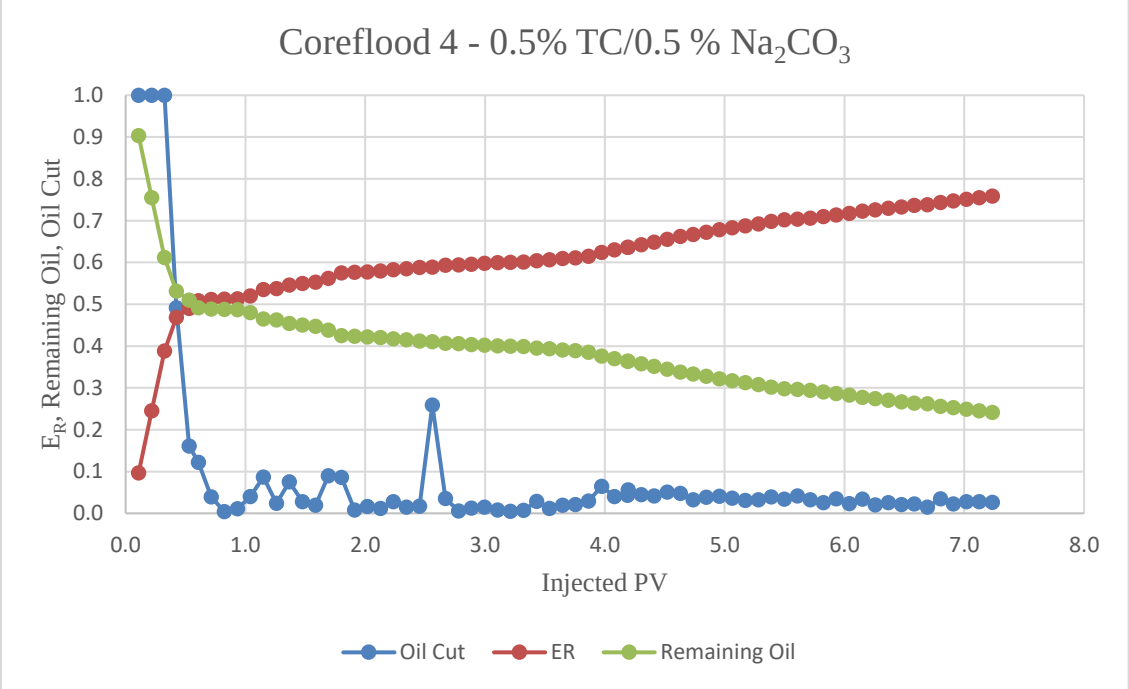

Figure 5.11: Recovery curves for Coreflood 4.

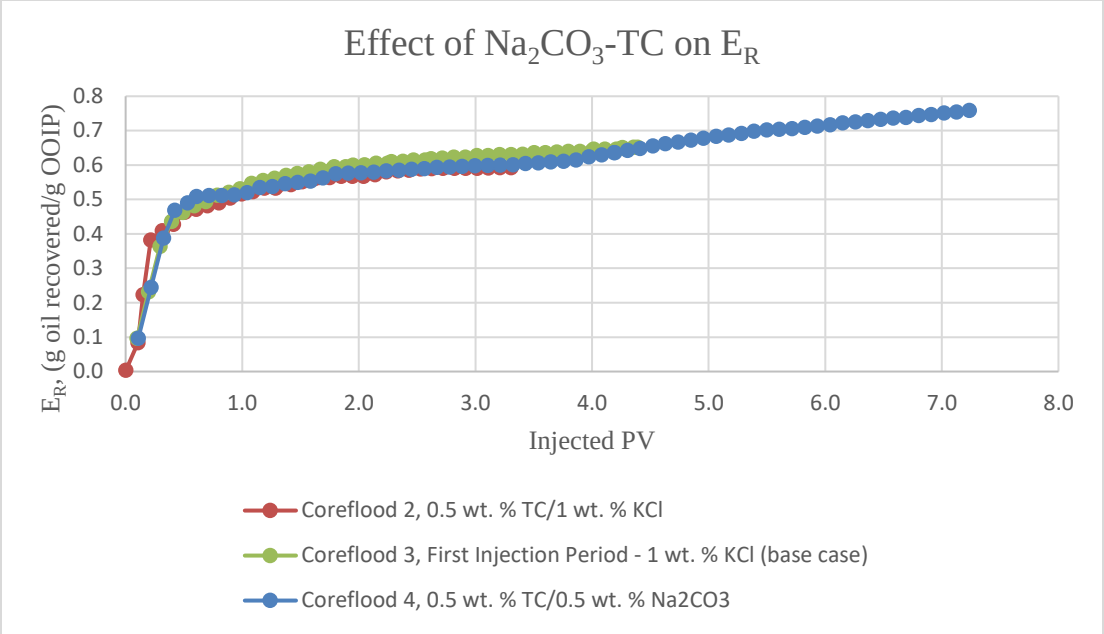

Figure 5.12: Effect of Na_2CO_3 on recovery efficiency.

5.7 SANDPACK FLOOD 1 AND 2

Table 5.5 and 5.6 provide the details for Sandpack Flood 1 and 2 respectively. With the new phase of additives Organic alkali 1 through Solvent 4 came a switch from using Idaho Gray cores to using sandpacks. The permeability was low enough to be measured, and the greater homogeneity of the sandpacks allowed better comparison. The sandpack permeabilities are within the typical Canadian oil sands' range of 0.5 to 5 D (Dusseault, 2001). Further, the replacement of the core holder increased the maximum allowable operating temperatures to 250 °C, which can be useful for future steam floods. Commercial SAGD projects are typically in unconsolidated sandstones. Silica sand (140-170 Mesh) obtained from Agsco was used, but because of this there were no longer any clays. The injection direction was also switched to better mimic the condensate zone at the edge of SAGD steam chambers.

Organic alkali 7 through 11 showed the strongest formation of oil-in-water emulsion, as evidenced by darker emulsions. Further, they were completely miscible in aqueous solution at 150 °C. Experimenters chose to test Organic alkali 7, the lowest in molecular weight of Organic alkali 7 through 11.

Table 5.5: Sandpack Flood 1 Parameters

Temp. (°C)	Fluid Phase in Core	Sandpack	Bitumen	Porosity	Absolute Permeability (D)	OOIP (g)
150	Liquid	140-170 Mesh silica sand	Reservoir	0.36	2.6	73
First Injection Period	Deionized water containing 0.5 wt. % Organic alkali 7 and 1 wt. % KCl					
	Top to bottom					
Injection Rate (PV/day)	2 (0.1108 mL/min)					

Table 5.6: Sandpack Flood 2 Parameters

Temp. (°C)	Fluid Phase in Core	Sandpack	Bitumen	Porosity	Absolute Permeability (D)	OOIP (g)
150	Liquid	140-170 Mesh silica sand	Reservoir	0.38	2.3	75
First Injection Period	Deionized water containing 1 wt. % KCl					
	Top to bottom					
Injection Rate (PV/day)	2 (0.1147 mL/min)					

Fig. 5.13 and 5.14 show the recovery curves for Sandpack Flood 1 and 2 respectively. Fig. 5.15 showed that the recovery was slightly better when using the organic alkali, with a notable increase in recovery starting at four pore volumes. Looking at Fig. 5.16, one could see a noticeable improvement in oil cut between roughly two to seven pore volumes. Since the sandpacks are more homogeneous, the comparison between Sandpacks 1 and 2 should suffer less from difference in pore structure. Therefore, although the recovery improvement was modest, experimenters conclude that Organic alkali 7 was able to improve bitumen recovery and oil rate.

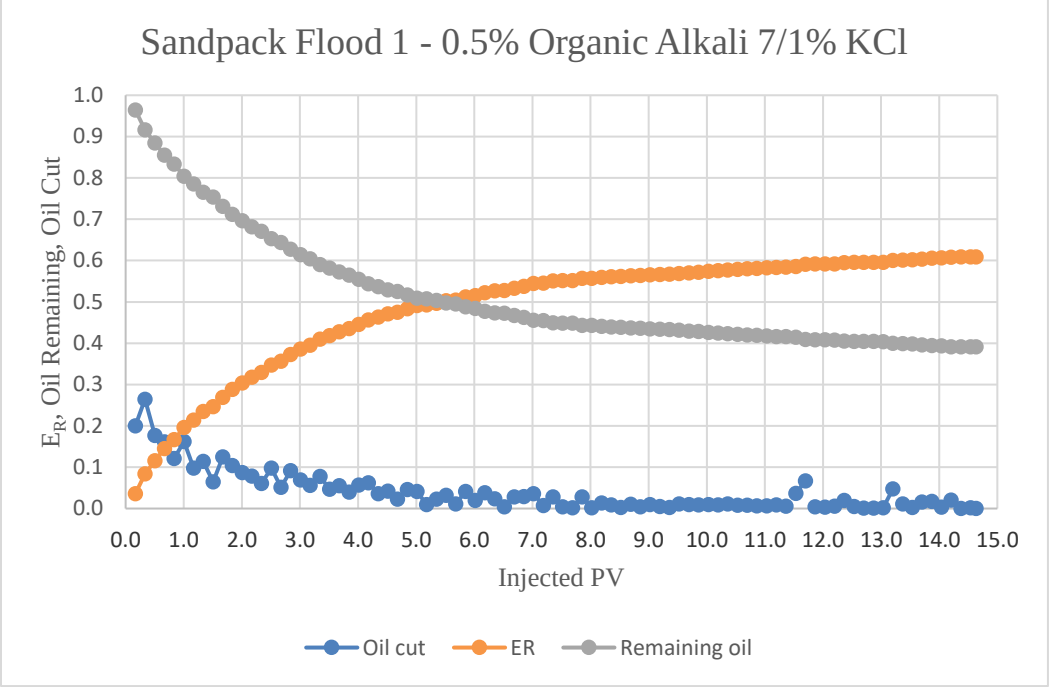

Figure 5.13: Recovery curves for Sandpack Flood 1.

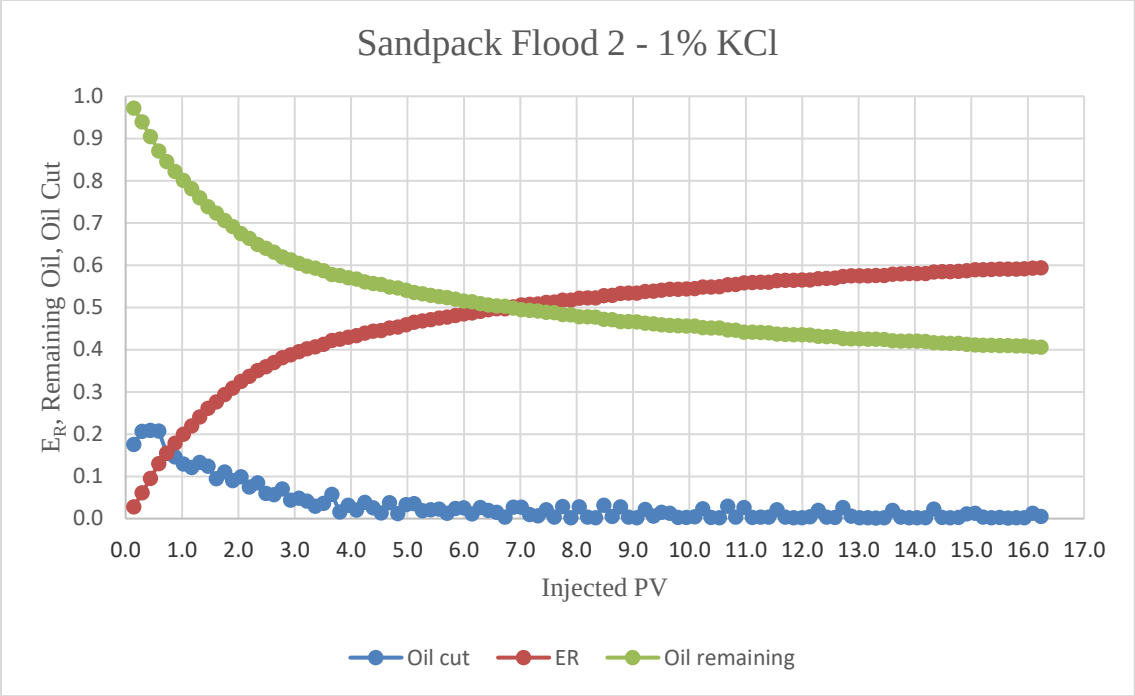

Figure 5.14: Recovery curves for Sandpack Flood 2.

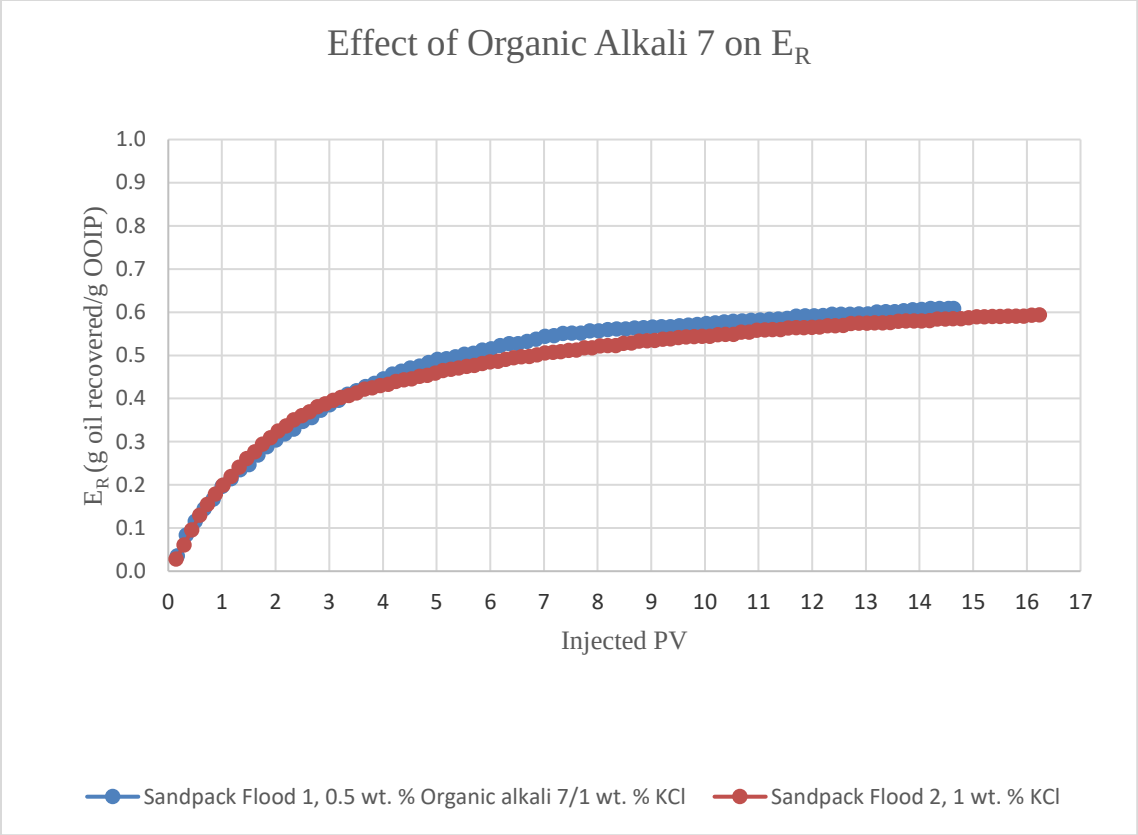

Figure 5.15: Effect of Organic alkali 7 on recovery efficiency.

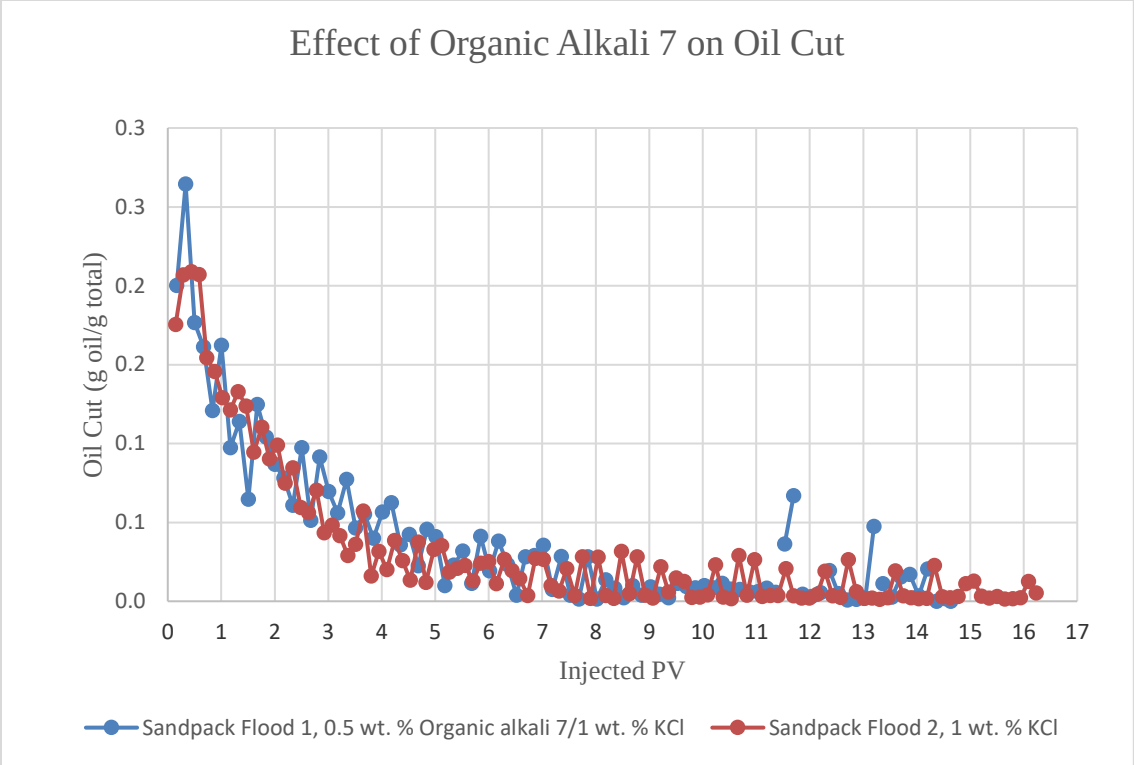

Figure 5.16: Effect of Organic alkali 7 on oil cut.

5.8 Dynamic Additive Retention Study

TF and TG had high pH and conductivity respectively, and were available at the time of this experiment. They were chosen for this core retention study. Table 5.7 provides more details.

Table 5.7: Dynamic Additive Retention Study Parameters

Temp. (°C)	Fluid Phase in Core	Core	Porosity	Absolute Permeability (D)
150	Liquid	Idaho Gray	0.32	---

First Injection Period	1 wt. % KCl flush	Second Injection Period	Deionized water containing 1 wt. % TG and 1 wt. % KCl
	Bottom to top		Bottom to top
Injection Rate (PV/day)	10	Injection Rate (PV/day)	10
Third Injection Period	1 wt. % KCl flush	Fourth Injection Period	Deionized water containing 1 wt. % TF and 1 wt. % KCl
	Bottom to top		Bottom to top
Injection Rate (PV/day)	10	Injection Rate (PV/day)	10

Experimenters injected about six pore volumes of 1 wt. % KCl. The effluent pH and conductivity stabilized. Experimenters then injected 1 wt. % TG/1 wt. % KCl at 10 pore volumes per day until the effluent conductivity stabilized. Next, 1 wt. % KCl was injected until the effluent conductivity was stabilized. Finally, experimenters injected 1 wt. % TF/1 wt. % KCl at 10 pore volumes per day until the effluent pH stabilized. All effluent pH and conductivity measurements were made after the effluent cooled to room temperature. Fig. 5.17 below shows the breakthrough curve.

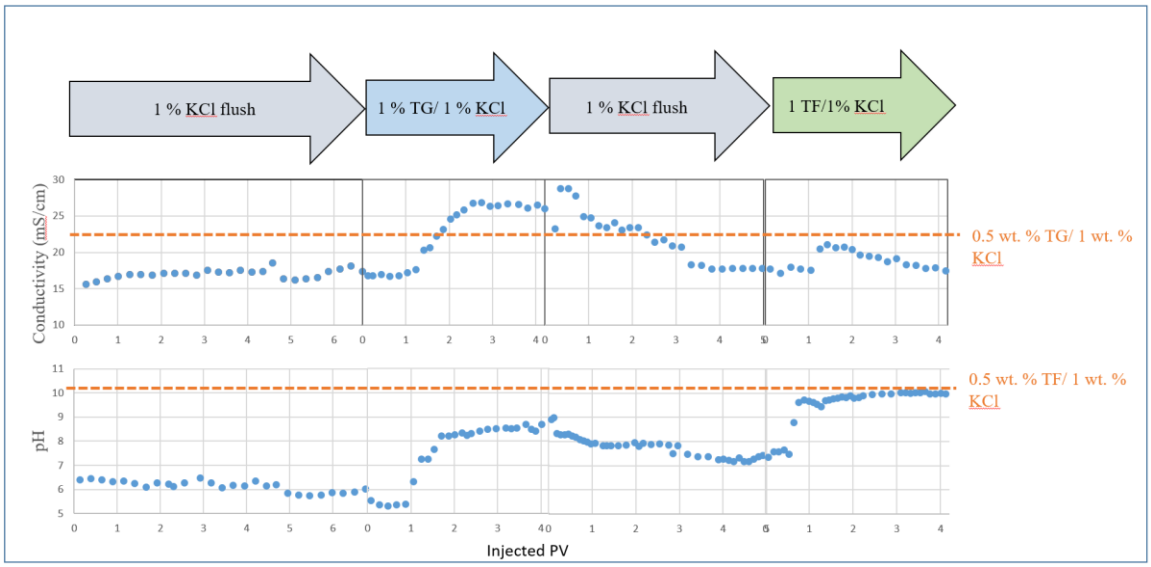

Figure 5.17: Breakthrough curve for dynamic additive retention study.

Since the initial concentration of additives (C_i) in the core was zero, and the concentration of additive in the injection solution (C_j) was 1 wt. %, a C_D value of 0.5 corresponded to 0.5 wt. % additive. The dashed orange lines indicate the conductivity and pH of 0.5 wt. % TG/1 wt. % KCl and 0.5 wt. % TF/1 wt. % KCl solutions respectively. The conductivity graph in Fig. 5.17 shows that TG was detained inside the Idaho Gray core, possibly due to adsorption, diffusion into isolated pore space, or other factors. The 0.5 C_D point was delayed about half a pore volume. Notice that the pH also increased during TG injection since TG is an inorganic alkali; however, the conductivity was used to correlate with additive concentration in the effluent. After the second flush, the conductivity was very close to that of the effluent prior to TG injection, suggesting that almost all the free TG was removed from the core. The pH graph shows that TF seems to also have been detained as well, possibly by adsorption. One thing to keep in mind is that solution pH could decrease by reactions with any calcium ions present from clay, which can react in high pH environments to form $Ca(OH)_2$ precipitates in the core. Such reactions

would delay the s-curve of the pH, but is not indicative of adsorption. The effluent conductivity is also not only affected by the concentration of the injected species. For example, dissolution of core mineral can affect the effluent conductivity. This illustrates one key improvement that can be made to this tool. LC-MS or other analytical techniques can be used to measure additive concentration in the effluent more accurately, but would undoubtedly be more time-consuming compared to a quicker analysis using effluent pH and conductivity. Despite this, this study demonstrates that it is possible to do such a retention study through porous media at high temperature with the given resources available, and provides a working procedure to build upon for future work involving new additives.

Chapter 6 Numerical Simulation Studies on Select Mechanisms

6.1 Overview

The implementation of laboratory-based enhanced oil recovery techniques to the field scale is a very challenging process. In the laboratory scale, complex reservoir geologies, compositions, and conditions are simplified to the size and realm of cores, pipettes, and steel cells. That is why numerical reservoir simulation has been an integral part of petroleum engineering for several decades, and has grown more and more sophisticated over the years. In this study, experimenters built and ran a preliminary SAGD model in CMG STARS to examine the effect of oil-water IFT reduction and reservoir rock wettability alteration on SAGD performance metrics, including the ultimate recovery, oil rate, and cumulative steam-to-oil ratio.

6.2 Model Description

Table 6.1 shows details of the three-dimensional reservoir and SAGD horizontal well pair model. A pair of 800-meter-long horizontal wells ran along the length of the 15-meter-thick producing layer. The injector and producer were placed 3 meters apart in the vertical direction. The injector was the upper well, and the producer was the bottom well. The top of the reservoir was 280 meters deep. A symmetric element was used to reduce computational cost.

Table 6.1: Reservoir Model Description

Well spacing, I-direction (m)	44
Well length, J-direction (m)	800
Reservoir thickness, K-direction (m)	15
Vertical distance between injector and producer, K-direction (m)	3
Grid blocks in I direction	11 (2 m each)
Grid blocks in J direction	10 (300, 100, 100, 100, 100, 100, 100, 100, 100, and 300 m)
Grid blocks in K direction	10 (1, 1, 1, 1, 1, 2, 2, 2, 2, and 2 m)
Topmost depth (m)	280
Horizontal permeability (mD)	2200
Vertical permeability (mD)	1760
k_V/k_H	0.8
Porosity	0.34
Rock compressibility (1/kPa)	7.00E-06
Rock thermal conductivity (J/m-day-°C)	6.60E+05
Rock volumetric heat capacity (J/m^3-°C)	2.35E+06
Overburden and underburden thermal conductivity (J/m-day-°C)	1.73E+05
Overburden and underburden volumetric heat capacity (J/m^3-°C)	2.35E+06
Initial reservoir pressure (kPa)	1340
Initial reservoir temperature (°C)	10
Hydrocarbon composition	95 mole % bitumen, 5 mole % methane
Initial and irreducible water saturation	0.15

Fig. 6.1 shows the viscosity of the model bitumen as a function of temperature. The bitumen viscosity did not vary much with pressure. Table 6.2 lists the operating parameters of the well pair. First, steam was fed through the tubing and recirculated through the annulus of both the injector and the producer for three months to decrease the viscosity of

the bitumen surrounding the well pair. Later, slightly wet steam (90 % quality) was injected at 250 °C into the layer, and fluids were produced from the bottom well.

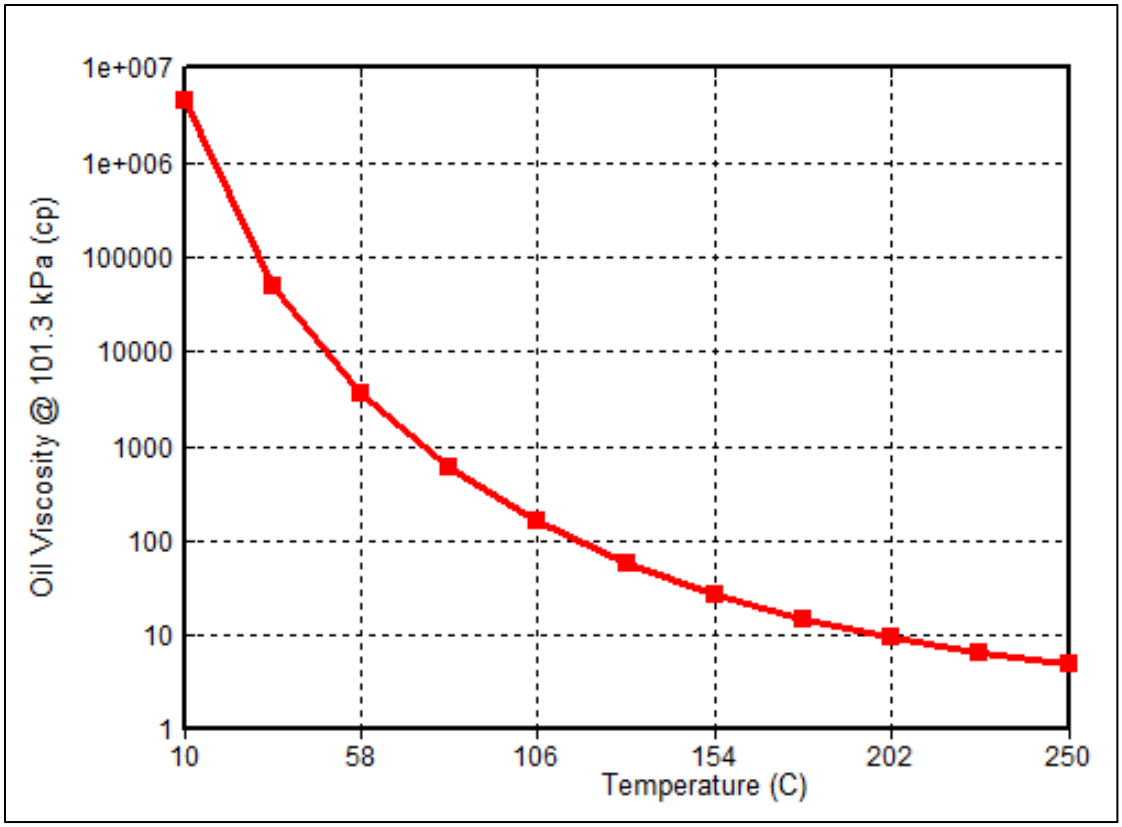

Figure 6.1: Viscosity vs. temperature of model bitumen used in CMG STARS simulation.

Table 6.2: Operating Parameters

Steam Circulation Period (3 months)	
Max Bottom Hole Pressure (kPa)	5500
Max Surface Water Rate/well (m^3/day)	400
Injection Temperature (°C)	250
Steam Quality (kg vapor/(kg vapor + kg liquid)	0.9
Injection & Production Period	
Injector	
Max Bottom Hole Pressure (kPa)	5500
Max Surface Water Rate (m^3/day)	400
Injection Temperature (°C)	250
Steam Quality (kg vapor/(kg vapor + kg liquid))	0.9
Producer	
Min Bottom Hole Pressure (kPa)	2300
Max Surface Liquid Rate (m^3/day)	500
Max Steam Rate (m^3/day)	5

Relative permeability data of SAGD reservoirs were scarce if not non-existent in literature at the time that this work was written. The Underground Test Facility (UTF) project is a large-scale SAGD test drilled near Fort McMurray, Alberta, Canada for the recovery of bitumen (Siu and Nghiem, 1991). Typical relative permeability curves that were used to model early time performance of the UTF project were adopted for this study (Walls et al., 2003).

Eq. 17 through 20 show the equations used to model the water (k_{rw}), gas (k_{rg}), and two-phase oil relative permeabilities (k_{row} and k_{rog}).

$$k_{rw} = k_{rwro}\left(\frac{S_w - S_{wc}}{1 - S_{orw} - S_{wc}}\right)^{Z_w} \tag{17}$$

$$k_{row} = k_{rocw}\left(\frac{1 - S_{orw} - S_w}{1 - S_{orw} - S_{wc}}\right)^{Z_{ow}} \tag{18}$$

$$k_{rg} = k_{rgro}\left(\frac{1 - S_{gc} - S_l}{1 - S_{gc} - S_{wc} - S_{org}}\right)^{Z_g} \tag{19}$$

$$k_{rog} = k_{rocw}\left(\frac{S_l - S_{wc} - S_{org}}{1 - S_{gc} - S_{wc} - S_{org}}\right)^{Z_{og}} \tag{20}$$

In the above equations, k_{rwro}, k_{rocw}, and k_{rgro} represent the endpoints. They are the water relative permeability at residual oil, oil relative permeability at connate water, and gas relative permeability at residual oil respectively. The exponents Z_w, Z_{ow}, Z_g, and Z_{og} control the curvature of the models, while S_w, S_{wc}, S_{orw}, S_{gc}, S_l, and S_{org} are the water saturation, connate water saturation, residual oil saturation to water displacement, connate gas saturation, total liquid (water and oil) saturation, and residual oil saturation to gas displacement.

The effect of altering the wettability to more water-wet and reducing the oil-water IFT on performance metrics was examined by modifying the relative permeability curves. Table 6.3 shows the endpoints and exponent values used for the base case, and Fig. 6.2 displays the two-phase curves. Two-phase water-oil relative permeability tables were generated using Eq. 17 and 18. Similarly, two-phase gas-oil relative permeability tables were generated using Eq. 19 and 20.

Table 6.3: Base Case Relative Permeability Model Values

S_{wc}	0.15	Z_w	2.7
S_{orw}	0.2	Z_{ow}	1.5
S_{gc}	0.05	Z_g	2.2
S_{org}	0	Z_{og}	2
k_{rwro}	0.3		
k_{rocw}	0.8		
k_{rgro}	0.5		

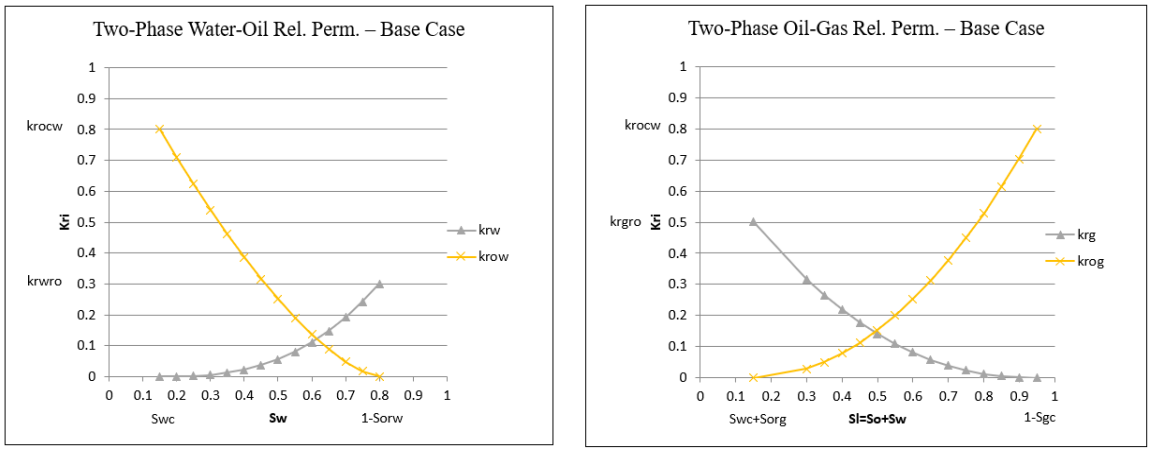

Figure 6.2: Two-phase relative permeability curves for the base case model.

Three-phase relative permeabilities were calculated by CMG STARS as in the following steps below. The three-phase water and gas relative permeabilities were equal to those for two-phase based on a fluid distribution argument, and are functions of only S_w and S_g, respectively. Three-phase oil relative permeability were calculated in step 4) using the Stone's Model II (modified) option.

1. Obtain k_{rw} and k_{row} from two-phase water-oil table as a function of S_w
2. $k_{rocw} = k_{row}(S_w = S_{wc})$

3. Obtain k_{rg} and k_{rog} from liquid-gas relative permeability table as a function of S_g
4. $k_{ro} = k_{rocw}\left(\left(\frac{k_{row}}{k_{rocw}} + k_{rw}\right)\left(\frac{k_{rog}}{k_{rocw}} + k_{rg}\right) - k_{rw} - k_{rg}\right)$
5. k_{rw} and k_{rg} are the same as the two-phase values

Wettability alteration to more water-wet shifts the water-oil relative permeability curves' intersection to the right (Peters, 2012). This was implemented by increasing k_{rocw} from 0.8 to 1 and decreasing k_{rwro} from 0.3 to 0.2. The gas relative permeability k_{rg} was assumed to be unaffected. Fig. 6.3 shows the two-phase curves for the water-wet case compared to the base case.

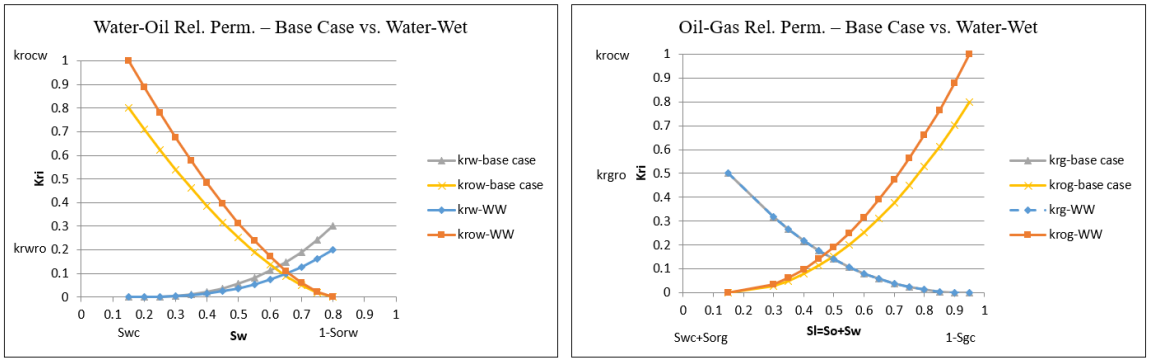

Figure 6.3: Two-phase relative permeability models for the more water-wet case.

Oil-water IFT reduction causes the oil-water relative permeability curves to become more linear (Amaefule and Handy, 1982). This was implemented by lowering Z_w from 2.7 to 2 and Z_{ow} from 1.5 to 1.2. Fig. 6.4 shows the two-phase curves for the lower oil-water IFT case compared to the base case. The gas-oil IFT was not changed.

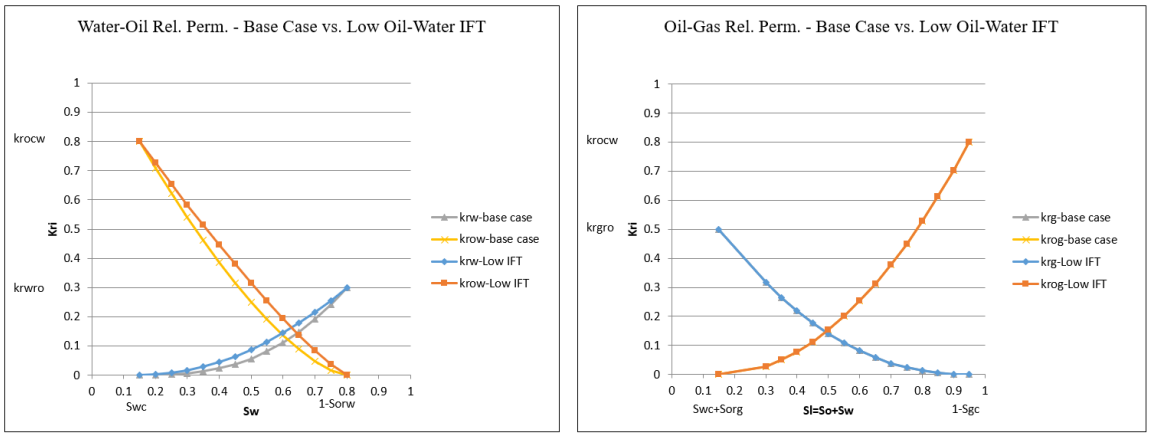

Figure 6.4: Two-phase relative permeability models for the lower oil-water IFT case.

Finally, Fig. 6.5 depicts the two-phase relative permeability curves for a case that was more water-wet and with lower oil-water IFT. The values of parameters k_{rocw}, k_{rwro}, Z_w, and Z_{ow} were 1, 0.2, 2, and 1.2 respectively. All other parameters were the same as those shown in Table 6.3.

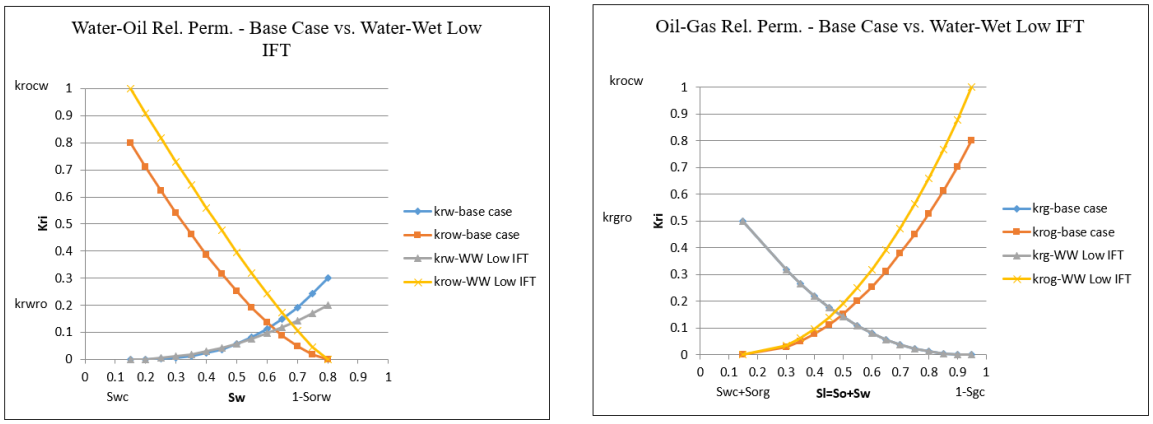

Figure 6.5: Two-phase relative permeability models for the more water-wet and lower oil-water IFT case.

6.3 Results and Discussion

Fig. 6.6 illustrates the temperature profiles inside the reservoir at 6 months and 2 years. The images are cross-sections in the I-K plane at the location of a pair of perforations in the injector and producer. The axis of the horizontal section of the well pair goes into the page. The profiles were very similar for each case tested.

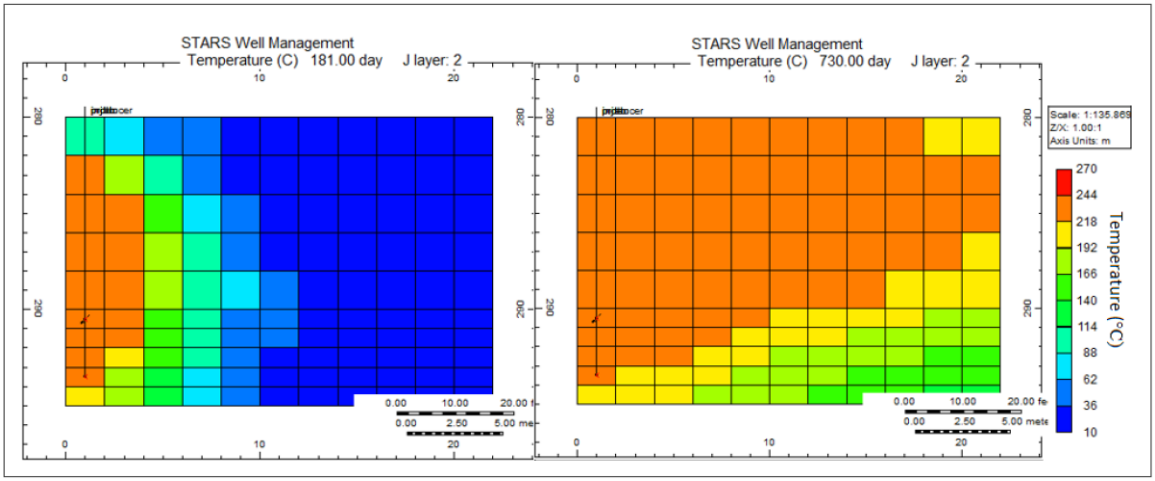

Figure 6.6: Typical temperature profile in an I-K plane at 6 months and 2 years, showing steam chamber growth.

Table 6.4: Fluid Saturations in the Steam Chamber

Case	Time	Steam Chamber Saturation
Base case	0.5 yrs.	S_o = 0.236
		S_w = 0.285
		S_g = 0.479
	2 yrs.	S_o = 0.107
		S_w = 0.195
		S_g = 0.698
More water-wet	0.5 yrs.	S_o = 0.208
		S_w = 0.301
		S_g = 0.491
	2 yrs.	S_o = 0.109
		S_w = 0.202
		S_g = 0.689
Lower oil-water IFT	0.5 yrs.	S_o = 0.256
		S_w = 0.215
		S_g = 0.529
	2 yrs.	S_o = 0.020
		S_w = 0.157
		S_g = 0.823
More water-wet and lower oil-water IFT	0.5 yrs.	S_o = 0.231
		S_w = 0.232
		S_g = 0.536
	2 yrs.	S_o = 0.028
		S_w = 0.160
		S_g = 0.812

Table 6.4 shows saturations of oil, water, and gas in the steam chamber at 6 months and 2 years for the four cases. First, more water-wet decreased oil saturation in the steam chamber at early time. Later, the difference was not as pronounced. During early time the reservoir was filled with more liquid. The improvement in oil saturation at the early time may be attributed to the larger increase in oil relative permeability inside the steam chamber at higher liquid saturations compared to the base case. Further, the oil relative permeability at the condensate zone (edge of the steam chamber) with water and bitumen was also higher. Secondly, lower oil-water IFT led to a lower oil saturation in the steam chamber at the later time. This improvement may be attributed to better drainage at the condensate zone during steam chamber growth, due to the increase in oil relative permeability at the condensate zone at all water saturations.

Fig. 6.7 displays the cumulative steam-to-oil ratio (cSOR). During the first 3 months, no bitumen was produced during steam recirculation. At the late time, the ratio is slightly improved in the lower oil-water IFT case.

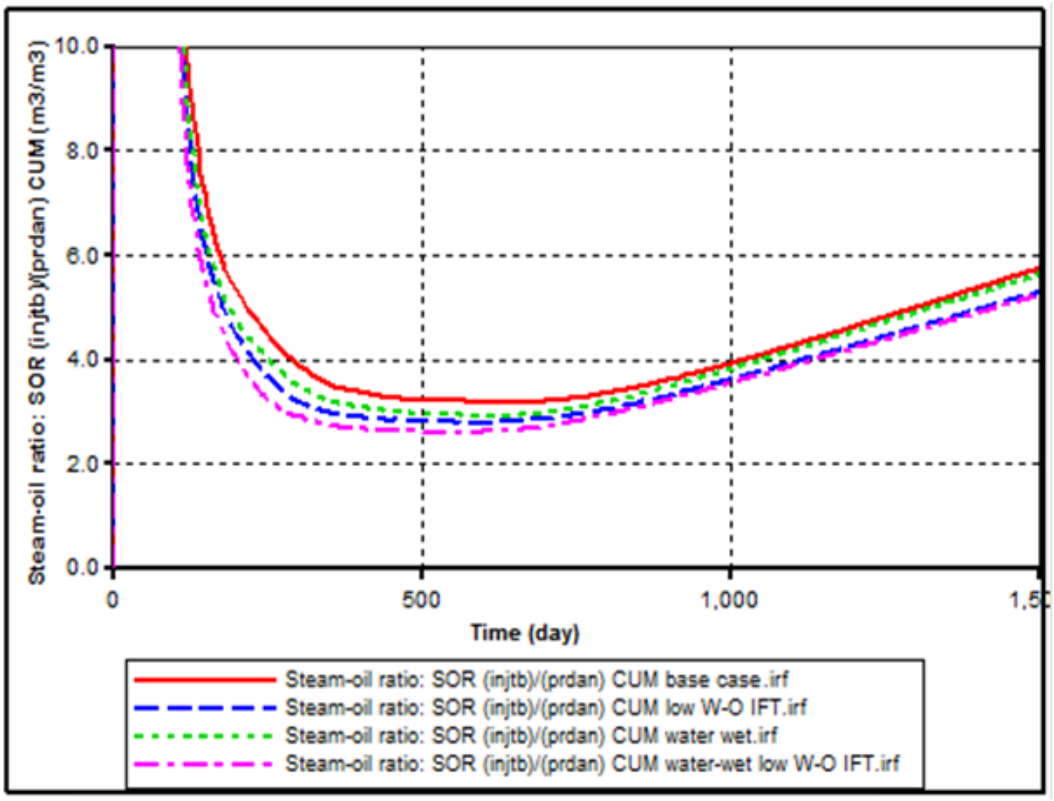

Figure 6.7: Effect of wettability alteration to more water-wet and reduction in oil-water IFT on cSOR.

Fig. 6.8 shows the cumulative oil recovery. Both reduction in oil-water IFT and more water-wet led to an increase in cumulative oil recovery.

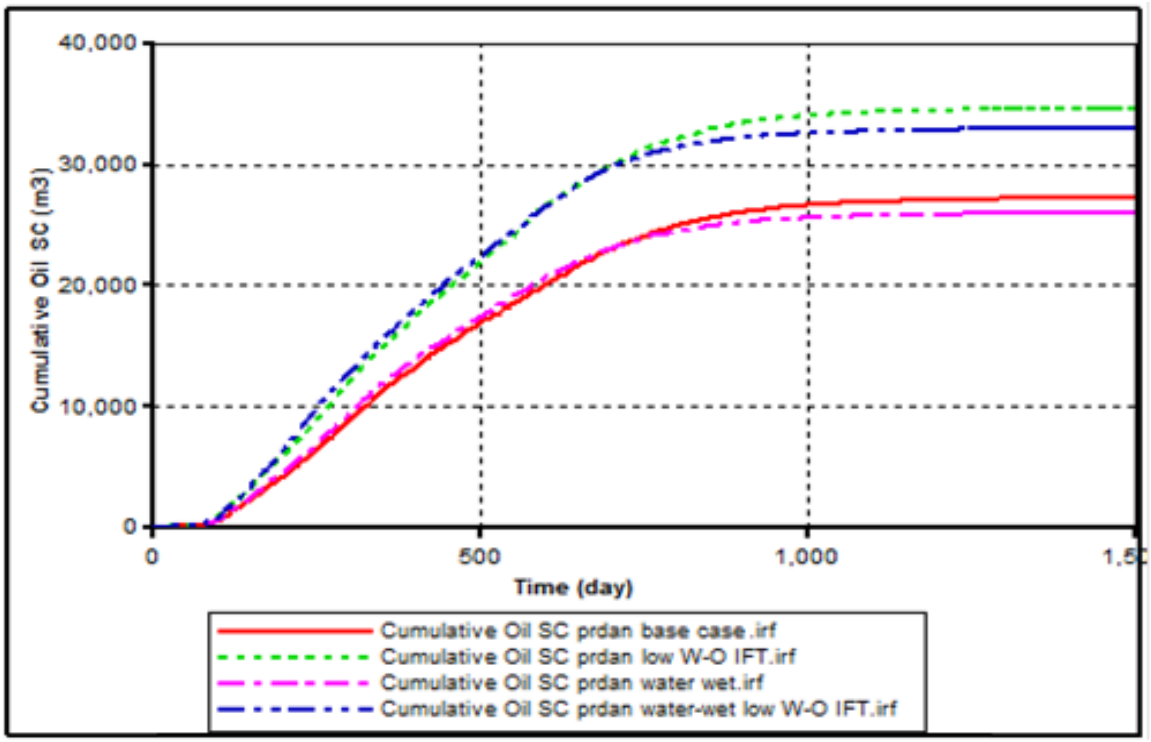

Figure 6.8: Effect of wettability alteration to more water-wet and reduction in oil-water IFT on cumulative oil recovery.

Fig. 6.9 shows the oil rate. The sharp peak at the end of the 3-month-long circulation period is a numerical artifact. The results demonstrate an increase in oil production during the early time for the more water-wet cases, and overall higher drainage rates for reduced oil-water IFT cases.

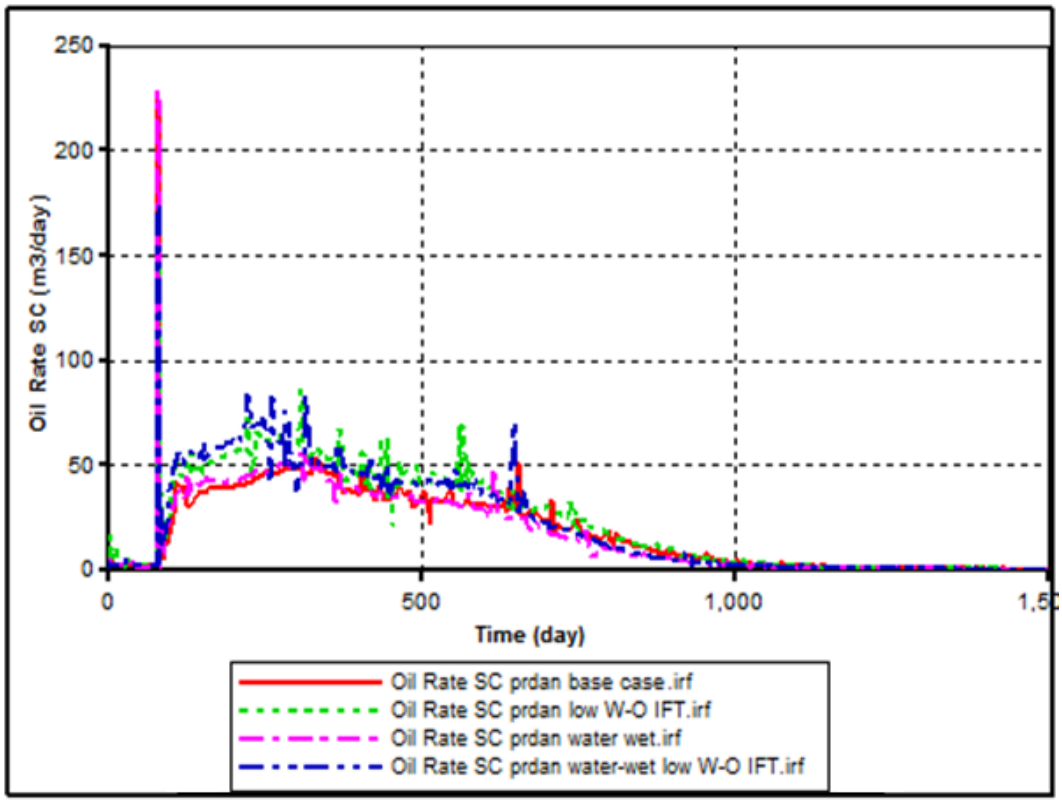

Figure 6.9: Effect of wettability alteration (to more water-wet) and reduction in oil-water IFT on oil rate.

Chapter 7 Conclusions and Recommendations

7.1 Conclusions

The purpose of this work was to study the potential of using chemical additives to improve the performance of SAGD. A list of potential mechanisms for enhanced oil recovery was proposed, which guided the selection of an inventory of potential additives for testing spanning several chemical families. A suite of high-temperature additive characterization tests was developed and executed. Several promising additives were selected to test in corefloods and sandpack floods to determine recovery potential in porous media at the laboratory scale. Finally, a preliminary numerical simulation model of field scale SAGD was developed to test the impact of wettability alteration and oil-water IFT reduction on SAGD performance. The key results and conclusions are summarized as follows.

1. A suite of high-temperature additive characterization tests was developed and successfully executed. Further, these tests can be used for future high-temperature additive characterization studies.
2. TF, Na_2CO_3, and Organic alkali 1 through 11 significantly increased aqueous solution pH.
3. All additives were completely miscible in water at 0.2 wt. % concentration and 150 °C at the salinities tested. However, at 0.5 wt. % concentration TB, TC, Organic alkali 4, Organic alkali 6, and Alcohol 2 all exhibited some phase separation or turbidity due to either cloud point limits or to the higher hydrophobicity of the molecule.
4. TF, Na_2CO_3, and Organic alkali 1 through 11 were able to make oil-in-water emulsions at 150 °C at certain salinities by extracting natural surfactants from bitumen. Organic alkali 7 through 11 were especially effective. The alcohol

solvents were able to increase bitumen miscibility in the aqueous phase at 150 °C. The acids tested did not form any emulsions with the bitumen.

5. Using visual cells, experimenters found that the non-ionic surfactants TB and TC were able to disperse bitumen into much smaller droplets in the aqueous phase. This was indicative of a moderate oil-water IFT reduction, which can be attractive in applications where emulsion breaking cost is prohibitive.
6. Wettability and contact line movement studies at 250 °C on siliceous grains and single quartz crystals proved that 250 °C was too hot. Most of the bitumen was removed from the aged surfaces without any additive, even after 2 months of aging.
7. Capillary action would cause bitumen to imbibe into Berea core plugs during aging, but aging at room temperature significantly slowed down the upward movement of bitumen. None of the additives could noticeably peel bitumen off from the surface of the plugs and move the contact line at 150 °C.
8. Wettability and contact line movement studies were done with single calcite crystals as well. None of the additives tested were effective. Bitumen tends to stick much more on calcite crystals than on quartz. Even when heated to 250 °C, a clean piece of calcite aged in bitumen would not be completely cleaned.
9. High-temperature corefloods and sandpack floods were executed. Setups and procedures were developed and improved successively to the stage that they are currently. Further, these procedures can be used or adapted for future high-temperature additive corefloods and sandpack floods.
10. Coreflood 1 proved TA did not significantly reduce residual oil saturation.
11. Coreflood 2 and 3 demonstrated that TC did not significantly reduce residual oil saturation. TC did not increase the production rate *significantly*, with the caveat that a small increase in production rate may have been possible.

12. Coreflood 4 showed that a TC and Na_2CO_3 mixture was able to increase the oil rate and recovery efficiency after a four-pore volumes delay. The delay was most likely due to adsorption or reactions between the natural surfactants with the Idaho Gray core. This coreflood showed that gravity-stable water flood at 150 °C, though favorable for recovery, does not preclude significant incremental oil recovery by chemical additives.
13. The sandpack floods from top to down showed that an organic alkali was able to moderately improve recovery performance.
14. Oil-water IFT reduction demonstrated the most promise for improving SAGD performance.
15. The additive retention study in Idaho Gray core using effluent conductivity and pH as an indication to additive TG and TF concentration (respectively) showed that both additives were detained to some degree in the core. This study demonstrated the capability to do such a retention study through porous media at high temperature with the available resources, and provided a procedure to involve new additives for future work.
16. A preliminary SAGD model was built in CMG STARS to study the effect of wettability alteration and oil-water IFT reduction on performance metrics. Altering the wettability to more water-wet and lowering the oil-water IFT were shown to improve SAGD performance.

7.2 RECOMMENDATIONS

Based on the rich experiences gained throughout the course of this study and upon reflection of the process, the author suggests these recommendations for improvements and future work.

1. Bitumen-brine IFT measurements may be made using the inverted pendant drop technique and can provide the ability to quantitatively compare surfactant and alkali oil-water IFT reduction capability. Some work has already been done to overcome some of the challenges associated with working with viscous bitumen.
2. Reliable and accurate ways to measure additive concentration in aqueous solution are prerequisites for batch additive adsorption studies and studies on additive mass transfer into the bitumen phase. LC-MS can work. The ideal method will be reliable, accurate, and relatively fast but trade-offs might need to be considered.
3. A liquid-liquid equilibrium experiment between additive solutions and bitumen at various conditions to measure additive partitioning coefficients can provide useful insights on promising additives. For example, one of the ways solvents can improve recovery is by diffusing into the bitumen phase and lowering overall bitumen viscosity. It will be useful to quantify the degree of mass transfer.
4. Batch adsorption studies can be done on promising additives to quantify additive adsorption on rock. This will complement the dynamic additive retention study.
5. A more accurate analytical technique for measuring additive concentration can improve the dynamic additive retention study through cores, since solution conductivity and pH can be affected not just by the additive, but by things such as mineral dissolution and cationic exchange.

6. Gravity-stable steam floods are challenging to design. While corefloods and sandpack floods in the liquid phase simulate what goes on at the condensate zone, gravity-stable steam floods simulate the conditions inside the steam chamber.
7. Core-scale numerical simulation with coreflood and sandpack flood data can be used to quantify the effect of additives on oil-water relative permeability. This can be used to guide relative permeability inputs to the field-scale simulation to better understand field-scale impact.

References

Alberta Energy Regulator. (2015). *Alberta's Energy Reserves 2014 and Supply/Demand Outlook 2015–2024.* Calgary, AB: Alberta Energy Regulator

Allenson, S. J., Yen, A. T., & Lang, F. (2011, January 1). Application of Emulsion Viscosity Reducers to Lower Produced Fluid Viscosity. Offshore Technology Conference. doi:10.4043/22443-MS

Amaefule, J. O., & Handy, L. L. (1982, June 1). The Effect of Interfacial Tensions on Relative Oil/Water Permeabilities of Consolidated Porous Media. Society of Petroleum Engineers. doi:10.2118/9783-PA

Anderson, W. G. (1986, October 1). Wettability literature survey - part 1: rock/oil/brine interactions and the effects of core handling on wettability. *Society of Petroleum Engineers.* http://dx.doi.org/10.2118/13932-PA

Anderson, G. (2006). *Simulation of Chemical Flood Enhanced Oil Recovery Processes Including the Effects of Reservoir Wettability.* MS thesis, The University of Texas at Austin, Austin, Texas (May 2006)

Arsalan, N. (2011). *Surface energy characterization of reservoir rock.* The University of Texas at Austin, Austin, TX.

Babadagli, T., Er, V., Naderi, K., Burkus, Z., & Ozum, B. (2010, November 1). Use of Biodiesel as an Additive in Thermal Recovery of Heavy Oil and Bitumen. Society of Petroleum Engineers. doi:10.2118/141302-PA

Bird, R. B., Stewart, W. E., & Lightfoot, E. N. (2002). *Transport Phenomena* (2nd ed.). New York, NY: John Wiley & Sons, Inc.

Brown, R.J.S., & Fatt. (1956). Measurements of fractional wettability of oil field rocks by the nuclear magnetic relaxation method. *Trans.,207,* 262-64

Butler, R. M. (1994). Steam-assisted gravity drainage: concept, development, performance and future. *The Journal of Canadian Petroleum Technology*, *33*(2), 44-50.

Butler, R. (1998, July 1). SAGD Comes of AGE! Petroleum Society of Canada. doi:10.2118/98-07-DA

Cooke, C. E., Williams, R. E., & Kolodzie, P. A. (1974, December 1). *Oil Recovery by Alkaline Waterflooding*. Society of Petroleum Engineers. doi:10.2118/4739-PA

Craig, F.F. (1971). *The reservoir engineering aspects of waterflooding*, Monograph Series, SPE, Richardson, TX (1971) 3

Dusseault, M. B. (2001, January 1). *Comparing Venezuelan and Canadian Heavy Oil and Tar Sands. Petroleum Society of Canada*. doi:10.2118/2001-061

Eyring, H., Glasstone, S., & Laidler, K. J. (1941). *Theory of Rate Processes.* New York, NY: Wiley

Ghasemi, M., & Whitson, C. H. (2015, October 26). Compositional Variation in SAGD. Society of Petroleum Engineers.

González, G., & Moreira, M. B. (1991). The wettability of mineral surfaces containing adsorbed asphaltene. *Colloids Surf., 58*, 293−302

Haghighat, P., & Maini, B. B. (2013, November 1). Effect of Temperature on VAPEX Performance. Society of Petroleum Engineers. doi:10.2118/157799-PA

Hall, A.C., Collins, S.H., & Melrose, J.C. (1983). Stability of aqueous wetting films in athabasca tar sands. *SPEJ*

James, L. A., Rezaei, N., & Chatzis, I. (2007, January 1). VAPEX, Warm VAPEX, and Hybrid VAPEX-The State of Enhanced Oil Recovery for In Situ Heavy Oils in Canada. Petroleum Society of Canada. doi:10.2118/2007-200

Lake, L.W., Johns, R.T., Rossen, W.R., & Pope, G.A. (2014). *Fundamentals of Enhanced Oil Recovery* (2nd ed.). Richardson, TX: Society of Petroleum Engineers

Lamontagne, J., Dumas, P., Mouillet V., & Kister, J. (2001). *Comparison by Fourier Transform Infrared (FTIR) Spectroscopy of Different Ageing Techniques: Application to Road Bitumens*. Fuel 80, 483-488

Li, R., Etminan, S. R., & Chen, Z. (2015, June 9). Chemical Additives and Foam to Enhance SAGD Performance. Society of Petroleum Engineers. doi:10.2118/174489-MS

Lu, C., Liu, H., Liu, Q., Lu, K., & Wang, L. (2014, June 10). Research on the Effect of Non-condensable Gas and Viscosity Reducer for Better SAGD Performance. Society of Petroleum Engineers. doi:10.2118/170026-MS

Melrose, J.C. (1982). Interpretation of mixed wettability states in reservoir rocks. Paper SPE 10971 presented at the 1982 SPE Annual Technical Conference and Exhibition, New Orleans, Sept. 26-29

Mokrys, I. J., & Butler, R. M. (1993, January 1). In-Situ Upgrading of Heavy Oils and Bitumen by Propane Deasphalting: The Vapex Process. Society of Petroleum Engineers. doi:10.2118/25452-MS

Oldenburg, T. B. P., Yarranton, H. W., & Larter, S. (2010, January 1). The Effect of Low Molecular Weight Multifunctional Additives on Heavy Oil Viscosity. Society of Petroleum Engineers. doi:10.2118/137505-MS

Owens, W.W. and Archer, D.L. (1971). *The Effect of Rock Wettability on the Oil-Water Relative Permeability Relationships.* Journal of Petroleum Technology

Pedersen, K. S., Christensen, P. L., & Shaikh, J. A. (2014*). Phase Behavior of Petroleum Reservoir Fluids* (2nd ed.). Boca Raton, FL: CRC Press

Peters, E. J. (2012). *Advanced Petrophysics* (1st ed.). Austin, TX: Live Oak Book Company

Qi, Zi., Wang, Y., He, H., Li, D., & Xu, X. (2013). Wettability alteration of the quartz surface in the presence of metal cations. *Energy Fuels*, 27, 7354-7359.

Salathiel, R.A. (1973). Oil recovery by surface film drainage in mixed-wettability rocks. *JPT*, 1216-24

Siu, A. L., Nghiem, L. X., Gittins, S. D., Nzekwu, B. I., & Redford, D. A. (1991, January 1). Modelling Steam-Assisted Gravity Drainage Process in the UTF Pilot Project. Society of Petroleum Engineers. doi:10.2118/22895-MS

Svrcek, W. Y., & Mehrotra, A. K. (1989). Properties of Peace River bitumen saturated with field gas mixtures. *The Journal of Canadian Petroleum Technology*, *28*(2), 50-56.

U.S. Energy Information Administration. (2016, May). *International Energy Outlook 2016*. Retrieved from http://www.eia.gov/forecasts/ieo

Walls, E., Palmgren, C., & Kisman, K. (2003, January 1). Residual Oil Saturation Inside the Steam Chamber During SAGD. Petroleum Society of Canada. doi:10.2118/03-01-03